CORA Cork Open Research Archive
Cartlann Taighde Oscailte Chorcaí

Title	Development of monoclonal antibody cell culture processes and antibody characterisation
Authors	Gogia, Shreya
Publication date	2025-11-04
Original Citation	Gogia, S. 2025. Development of monoclonal antibody cell culture processes and antibody characterisation. MRes Thesis, University College Cork.
Type of publication	Masters thesis (Research)
Rights	© 2025, Shreya Gogia. - https://creativecommons.org/licenses/by/4.0/
Download date	2026-10-30 15:48:01
Item downloaded from	https://hdl.handle.net/10468/18814



UCC
University College Cork, Ireland
Coláiste na hOllscoile Corcaigh

Development of Monoclonal Antibody Cell Culture Processes and Antibody Characterisation

Dissertation submitted by

Shreya Gogia

In partial fulfilment of the requirements for the degree of

MRes in Industrial Pharmaceutics

under the supervision of

Dr Evin Allen

and

Dr Alexander Zhdanov

at

School of Pharmacy

University College Cork

Coláiste na hOllscoile Corcaigh

National University of Ireland

Ollscoil na hÉireann

Head of School

Prof Brendan Griffin

Nov 2025

1. Table of Contents

Declaration ..... *III*

Acknowledgement ..... *IV*

List of Abbreviations ..... *V*

Abstract ..... *X*

1. Introduction *1*

1.1. Antibodies **4**

1.1.1 Immunoglobulin Isotypes 4

1.1.2 Polyclonal Antibodies 6

1.1.3 Monoclonal Antibodies 6

1.2 Bioprocessing of Monoclonal Antibodies **11**

1.2.1 Cell Line Development 12

1.2.2 Cell Culture Process 13

1.3 Analytical and Quality Control Strategies for Monoclonal Antibodies **23**

1.3.1 Aggregation 24

1.3.2 Charge Variant Analysis 26

1.3.3 Potency Assessment 27

1.3.4 ELISA 29

1.4 Interleukin-8 and Anti-IL-8 Mabs **31**

1.4.1 Anti-IL-8 Antibodies: Mechanism and Development 33

1.4.2 Anti-IL-8 mAb potency assessment 34

1.5 Thesis Overview **35**

2. Objectives and Hypothesis *36*

3. Methods and Materials *37*

3.1 Materials **37**

3.2 Methods **43**

3.2.1 Cell Culture 43

3.2.2 Purification 47

3.2.3 Protein Concentration 48

3.2.4 Dialysis 48

3.2.5 SDS-PAGE 48

3.2.6 Cell-Based Potency Assays 49

3.2.7 Stability and Forced Degradation Study 55

3.2.8 Size-Exclusion HPLC 56

4. Results – Anti-IL-8 MAb Cell Culture *58*

4.1 Production of Anti-IL-8 mAb **58**

4.1.1 Anti-IL-8 mAb Cell Culture Overview 59

4.1.2 Independent Anti-IL-8 Monoclonal Antibodies Production 59

4.1.3 Media Studies 62

4.1.4 Cell Density Assessment 69
4.2 Anti-IL-8 mAb Stability Study 81
4.2.1 Stability of Anti-IL-8 mAbs at -20°C 81
4.2.2 Stability of Anti-IL-8 mAbs at 4°C 82
4.2.3 Stability of Anti-IL-8 mAbs at 25°C 83
4.2.4 Stability of Anti-IL-8 mAbs at 40°C 84
5. Results - cNIST mAb Cell Culture 86
5.1 Batch 1 86
5.2 Batch 2 90
5.3 cNIST mAb Forced Degradation Study 94
5.3.1 Temperature 95
5.3.2 Light Exposure 98
5.3.3 pH 100
5.3.4 Freeze-Thaw cycles 101
5.3.5 Agitation 102
5.3.6 Summary Analysis of SDS-PAGE AND SEC-HPLC 104
6. Cell-Based Potency Assay Method Development 106
6.1 HL-60 Cell Assay 107
6.2 HCT-116 Cell Assay 111
7. Discussion 123
8. Conclusion 133
9. References 136

Declaration

This dissertation is submitted by the undersigned to University College Cork for examination for the degree of MRes in Industrial Pharmaceutics. It has not been submitted as an exercise for a degree at any other university. All work presented in this dissertation was carried out by me. Certain experimental procedures, including the establishment of a working cell bank and repetition of a specific potency assay, were performed by Dr Alex Zhdanov. This manuscript was written by me with the aid of editorial advice from Dr Evin Allen & Dr Alex Zhdanov. All external references and sources are clearly acknowledged and identified within the contents. I have read and understood the regulations of University College Cork concerning plagiarism.

Student Name: Shreya Gogia Date: November 4, 2025

Acknowledgement

I would like to offer my sincere thanks to my supervisor, Dr Evin Allen, for his guidance throughout the course of this research. His insightful feedback, patience and constant motivation have been pivotal in my growth as a researcher. He not only guided me through challenges but also inspired me to maintain focus and commitment to the objectives of this project. I truly appreciate the time and effort he dedicated to ensuring the successful completion of my work.

I would also like to express my gratitude to Dr Alexander Zhdanov for his continuous support and encouragement during my experimental work. His technical expertise and willingness to help at every stage were invaluable to the progress of this project and greatly contributed to my scientific understanding and research independence.

My heartfelt thanks go to my parents for their unconditional support throughout my academic journey, and for giving me the opportunity to pursue my goals and study abroad. Their unwavering belief in me has been my greatest strength and motivation.

Sincere thanks to University College Cork for allowing me to be part of this esteemed institution, and to the Republic of Ireland for welcoming me with new experiences and learning opportunities.

Finally, I would like to thank all my close friends for always being there for me and making this journey memorable.

List of Abbreviations

AA	Amino Acid
ActD	Actinomycin D
ADCC	Antibody-dependent cellular cytotoxicity
ADCP	Antibody-Dependent Cellular Phagocytosis
ATP	Adenosine Triphosphate
BCA	Bicinchoninic Acid
BSA	Bovine serum albumin
BSE	Bovine Spongiform Encephalopathy
CD	Chemically Defined
CD1, CD2, etc.	Cell Density Condition number
CDC	Complement Dependent Cytotoxicity
CDR	Complementarity Determining Region
CEX	Cation Exchange
CHO	Chinese Hamster Ovary
cNIST mAb	cNational Institute of Standards and Technology Monoclonal antibody
CPP	Critical Process Parameter
CQA	Critical Quality Attribute
CXCR1	C-X-C Motif Chemokine Receptor 1

CXCR2	C-X-C Motif Chemokine Receptor 2
DHFR	Dihydrofolate Reductase
DMEM	Dulbecco's Modified Eagle Medium
DMSO	Dimethyl Sulfoxide
DO	Dissolved Oxygen
DSP	Downstream Processing
DTT	Dithiothreitol
ELISA	Enzyme-Linked Immunosorbent Assay
ERK	Extracellular Signal-Regulated Kinase
Fab	Fragment-antigen binding region
FBS	Fetal Bovine Serum
Fc	Fragment Crystallisable Region
FceR	Fc epsilon receptor
FDA	Food and Drug Administration
FPLC	Fast Protein Liquid Chromatography
GS	Glutamine Synthetase
HCT-116	Human Colorectal Carcinoma Cell Line
HEK	Human Embryonic Kidney
HEPES	4-(2-hydroxyethyl)-1-piperazineethanesulfonic acid
HL-60	Human Promyelocytic Leukaemia Cell Line 60

HMW	High Molecular Weight
HPLC	High Performance Liquid Chromatography
HRP	Horseradish peroxidase
HS	Horse Serum
HT	Hypoxanthine-Thymidine
iCIEF	Imaged Capillary Isoelectric Focusing
IFN	Interferon
Ig	Immunoglobulin
IL-8	Interleukin-8
kDa	Kilodalton
LMW	Low Molecular Weight
mAb	Monoclonal Antibody
mmol	Millimole
MTX	Methotrexate
NS0	Murine Myeloma Cell Line NS0
NK	Natural Killer Cells
OTR	Oxygen Transfer Rate
pAb	Polyclonal Antibody
PBS	Phosphate Buffered Saline
PER.C6	Human Embryonic Retinal Cell Line PER.C6

pERK	Phosphorylated Extracellular Signal-Regulated Kinase
PI3K	Phosphoinositide 3-kinase
pRPS6	Phosphorylated Ribosomal Protein S6
pH	Potential of Hydrogen
PVDF	Polyvinyl difluoride
QC	Quality Control
RA	Retinoic Acid
RPS6	Ribosomal Protein S6
RT	Retention Time
SDS-PAGE	Sodium Dodecyl Sulphate Polyacrylamide Gel Electrophoresis
SEAP	Secreted Embryonic Alkaline Phosphatase
SEC-HPLC	Size Exclusion Chromatography HPLC
Sp2/0	Murine Myeloma Cell Line Sp2/0-Ag14
STR	Stirred Tank Reactor
SUB	Single Use Bioreactor
TBST	Tris-buffered saline containing 0.1% Tween-20
TFF	Tangential Flow Filtration
TNFα	Tumour Necrosis Factor Alpha
TSE	Transmissible Spongiform Encephalopathy
USP	Upstream Processing

WCB	Working Cell Bank
µL	Microlitre
µM	Micromolar

Abstract

Monoclonal antibodies (mAbs) have transformed modern therapeutics due to their high specificity and efficacy for a wide range of diseases. This research project aimed to establish an end-to-end laboratory-scale monoclonal antibody production process, including upstream cell culture, downstream purification and analytical characterisation. A CHO-DP12 cell line engineered for anti-IL-8 mAb expression and a cNIST mAb-producing CHO cell line were employed to investigate key cell culture process parameters.

Upstream studies examined the effects of media formulations and seeding density studies on antibody expression. While serum-supplemented media supported the growth of CHO-DP12 cells, the serum-derived impurities and inconsistent antibody expression limited the production of anti-IL-8 mAbs. In contrast, CHO-NIST cells cultured in manufacturer-recommended, serum-free media successfully produced detectable antibodies.

Analytical characterisation was performed using SDS-PAGE, Western Blotting and SEC-HPLC to assess protein concentration, purity and structural integrity. Stability and forced degradation studies were further conducted to assess the impact of stressful conditions on antibody integrity.

Preliminary cell-based assays were explored using HL-60 and HCT-116 cell lines to study IL-8 signalling and anti-IL-8 mAb activity. These assays generated variable and inconclusive results that highlighted the need for further work using alternative mechanism-specific functional assays.

Overall, while limited in final results, the work advanced the current state of mAb production within the research group and provides a roadmap towards anti-IL-8 mAb production and potency assessment.

1. Introduction

Biopharmaceuticals developed using recombinant DNA technology have revolutionised the treatment of a wide array of diseases, with monoclonal antibodies (mAbs) in particular playing a prominent role. Designed to mimic the immune system's natural responses to infection and inflammation, mAbs possess the unique ability to recognise and target specific molecules (antigens) with high affinity, with lower resulting side effects due to less off-target signalling. (Alejandra et al., 2023).

After Köhler and Milstein's groundbreaking development of hybridoma technology for mAb production in 1975 (Köhler and Milstein, 2005), mAbs have profoundly transformed both scientific research and clinical therapeutics, particularly for cancer, autoimmune disorders, and inflammatory conditions (Alejandra et al., 2023).

Initially derived from murine sources, advances in genetic engineering have facilitated the development of chimeric, humanised, and fully human mAbs, with each successive generation reducing immunogenicity and improving clinical safety profiles (Dhar and Das, 2018), **Figure 1**. Since the approval of adalimumab in 2002, the first fully human mAb approved by the U.S. Food and Drug Administration (FDA), the landscape of mAb development has expanded considerably (Nelson et al., 2010).

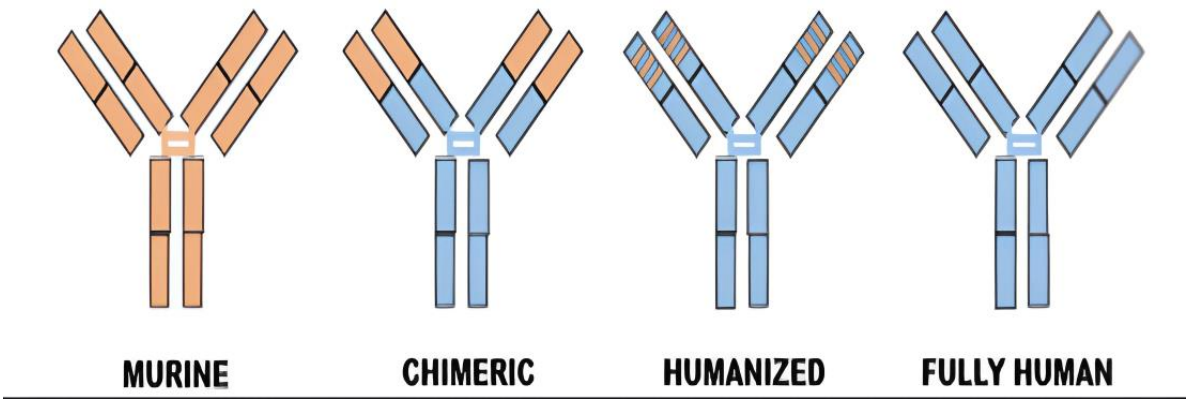


Figure 1: Evolution of mAb products through recombinant engineering advances (Dhar and Das, 2018).

Today, mAbs can be produced and screened using a variety of platforms, including hybridoma technology, recombinant DNA technology, phage and yeast display, and transgenic animals (Singh et al., 2023). Their applications span cancer treatment, where they trigger or inhibit immune responses, block cancer cell division signals, and deliver targeted chemotherapy; autoimmune diseases, where they modulate B-cell activity and reduce inflammatory cytokines such as TNF-Alpha; and infectious diseases, where they neutralise pathogens such as influenza and SARS-CoV-2 (Kothari et al., 2024).

Over the past two decades, mAbs have become one of the fastest-growing sectors within the biopharmaceutical industry, with over one hundred FDA mAb products approved globally and hundreds more in clinical trials (**Figure 2**) (The Antibody Society, n.d.).

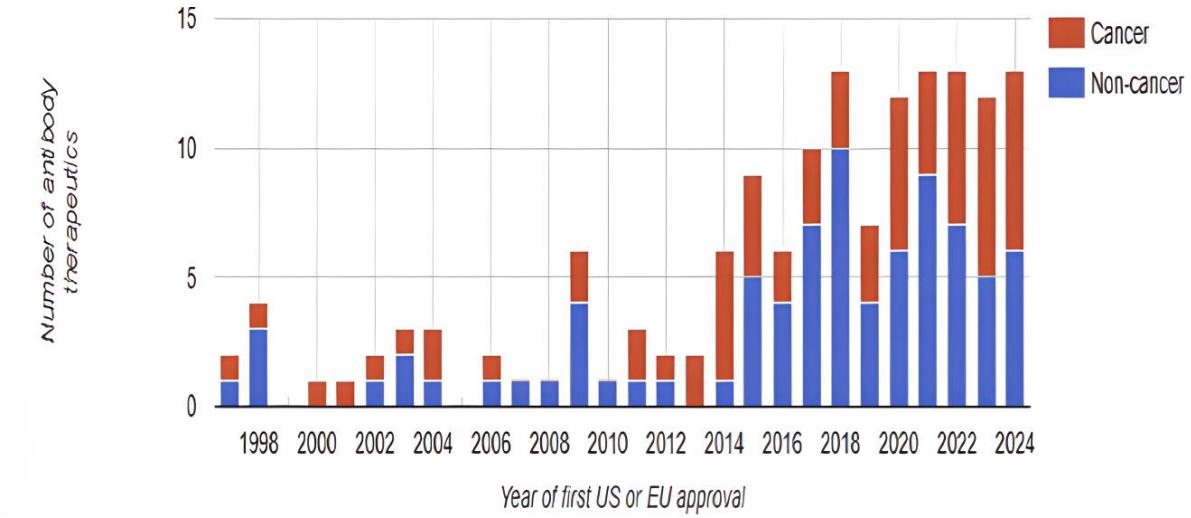


Figure 2: The Antibody Society. Therapeutic monoclonal antibodies approved or in review in the EU or US. (20 September 2025); *www.antibodysociety.org/resources/approved-antibodies*.

This explosion in both clinical and commercial success has been facilitated by advances in both upstream and downstream bioprocessing with improvements in cell-line engineering, culture media optimisation, purification technologies, and analytical methods. Innovations such as continuous processing, single-use bioreactors, and integration of artificial intelligence

and machine learning in antibody design continue to redefine the field's technological frontier (Wilman et al., 2022).

However, despite such success, mAbs face challenges such as high production costs and lengthy cycle times due to complex manufacturing processes relative to small molecules, potential immunogenicity and loss of efficacy over time and the requirement for sterile manufacture to support parenteral administration. These challenges require the field to continue to innovate in bioprocessing and bioanalytical technology and increase the knowledge base.

1.1. Antibodies

Antibodies, also referred to as immunoglobulins (Ig), are glycoproteins secreted by B lymphocytes as a part of the adaptive immune system. They are generated in response to stimulating molecules known as antigens (Atkinson, 2022). Antibodies specifically target the antigen it was generated in response to, and provide high sensitivity. Structurally, they are composed of two identical heavy chains of approximately 50 kDa and light chains of 25 kDa joined by disulfide bonds (Janeway et al., 2001).

Antibodies can be classified in several ways, depending on their structural and functional characteristics. The most fundamental classification is based on the heavy chain, resulting in five major isotopes: IgG, IgA, IgM, IgE, and IgD. Beyond this, antibodies can be grouped according to their light chain type (κ or λ), functional form (membrane-bound B cell receptor and secreted soluble antibody), or whether they are polyclonal or monoclonal (Rawat and Kumar, 2023).

1.1.1 Immunoglobulin Isotypes

1.1.1.1 Immunoglobulin G (IgG)

IgG is the most abundant protein in human serum, making up about 10-20% of plasma protein. There are four subtypes of IgG: IgG1, IgG2, IgG3, and IgG4, each of which displays distinct biological characteristics, including antigen binding capacity, ability to form immune complexes, complement activation, interactions with Fc receptors on effector cells, serum half-life and placental transport (Schroeder and Cavacini, 2010). Among these subclasses, IgG1 is the predominant one and is typically induced in response to soluble protein antigens. IgG2 is essential for immunity against polysaccharide antigens, particularly bacterial capsules. IgG3 is distinguished by its pro-inflammatory properties and is highly effective in activating effector functions. IgG4 is associated with chronic antigen exposure and

contributes to immune tolerance, often seen in allergy or long-term infectious stimulation (Vidarsson et al., 2014).

1.1.1.2 Immunoglobulin A (IgA)

IgA is present as a monomer in blood and as a dimer in mucosal secretions such as saliva, tears, colostrum and intestinal fluids. Secretory IgA plays a critical role in neutralising pathogens at the epithelial barrier and preventing microbial adhesion and invasion without eliciting strong inflammatory responses (de Sousa-Pereira and Woof, 2019). There are two subclasses, IgA1, having a longer hinge region and predominant in serum and IgA2, with a shorter hinge, making it more resistant to bacterial proteases and common at mucosal sites (Schroeder and Cavacini, 2010).

1.1.1.3 Immunoglobulin M (IgM)

IgM is the first antibody produced during a primary immune response to a pathogen. It exists as a membrane-bound monomer on naïve B cells and as a secreted pentamer in plasma, stabilised by a J-chain. It functions by coating the antigen for destruction and fixing the complement (Schroeder and Cavacini, 2010). They are also called natural antibodies, which are essential for the early defence line against infection before affinity maturation occurs(Klimovich, 2011; Schroeder and Cavacini, 2010).

1.1.1.4 Immunoglobulin D (IgD)

Circulating IgD accounts for very low levels in the serum, and its functions are unclear compared to others. IgD is co-expressed with IgM on the membranes of B cells (Schroeder and Cavacini, 2010).

1.1.1.5 Immunoglobulin E (IgE)

IgE is the least abundant isotype in serum but plays a pivotal role in allergic and hypersensitivity reactions. IgE-producing plasma cells are mostly found in the lymphoid tissue associated with the gastrointestinal and respiratory tracts. It is detected either free in the mucosal secretions of these sites or bound to FceR on mast cells (Chung, 2007).

1.1.2 Polyclonal Antibodies

Antibodies can be broadly categorised into polyclonal antibodies (pAbs) and mAbs. Both forms have been widely researched for their therapeutic applications and functional differences.

pAbs are generated by multiple B-cell clones in response to an antigen, resulting in a heterogeneous mixture that recognises multiple epitopes on the same target. This inherent diversity provides several advantages, such as enhanced sensitivity in assays and resilience against antigen conformational changes (Lipman et al., 2005). pAb products are much cheaper to manufacture than Mabs; however, the lack of specificity due to variation in epitope targeting can lead to variation in therapeutic responses (Nelson et al., 2000). Polyclonal pools are generally generated in non-human species against a human antigen; this leads to increased immunogenicity compared to humanised or human mAbs (Lipman et al., 2005).

1.1.3 Monoclonal Antibodies

mAbs are highly specific and lab-engineered symmetrical glycoproteins composed of two heavy chains and two light chains, forming a Y-shaped structure, as shown in **Figure 3**. Commercial and clinical mAbs are almost always IgG, and particularly IgG1 in isotype. Such antibodies are specific to a single antigen and synthetically produced through recombinant engineering and produced in mammalian cells (Liu, 2014)

As such, they are more expensive and complicated to produce than pAbs but provide greater consistency and quality with lower immunogenicity when used for clinical purposes. mAbs often display complex post-translational modifications such as glycosylation and glycation that require production in mammalian cell lines such as Chinese Hamster Ovary (CHO) or

Human Embryonic Kidney (HEK) cells, in contrast to bacterial systems such as *E. coli* (Verma et al., 1998).

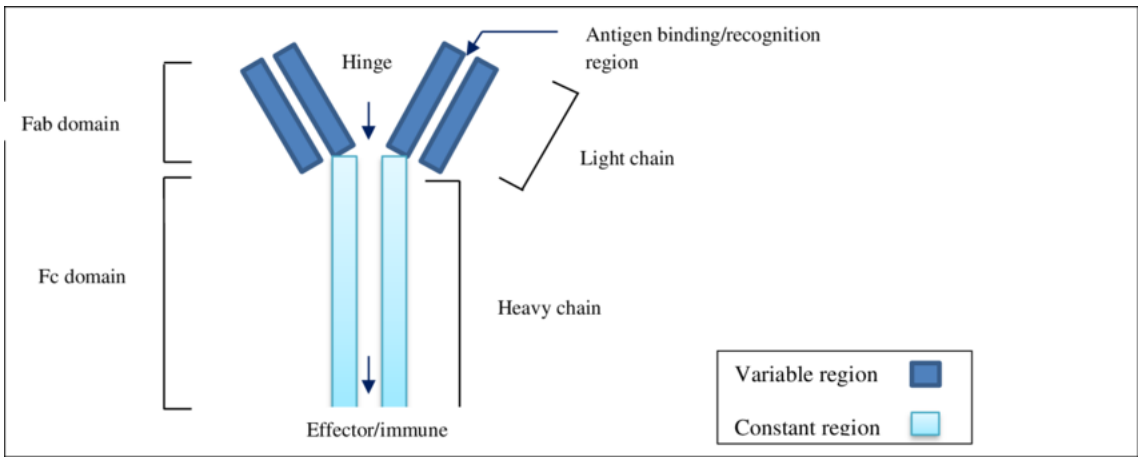


Figure 3: mAb structure demonstrating variable and constant regions (Dabhadkar et al., 2022).

1.1.3.1 Mechanism of Action

While mAbs are highly specific and bind to antigen through the upper arms of the "Y" and antigen-binding region (Fab), where variable domains from both chains come together to form the complementarity-determining regions (CDRs), the effector functions of mAbs are often generated at the Fc region (**Figure 4**) (Kothari et al., 2024)**.** The Fc (fragment crystallizable) region, located at the base of the antibody, mediates interactions with components of the immune system, such as Fc receptors on immune cells and complement proteins. This domain is responsible for downstream immune effects, including ADCC (antibody-dependent cellular cytotoxicity) and complement activation, depending on the antibody isotype—human IgG1, for example, is particularly effective at engaging these pathways (Breedveld, 2000).

mAbs exert therapeutic effects through several mechanisms depending on their target pathology and therapeutic design. The principal modes of action can broadly be classified as immune-effector independent and immune-effector dependent mechanisms (Scott et al., 2012).

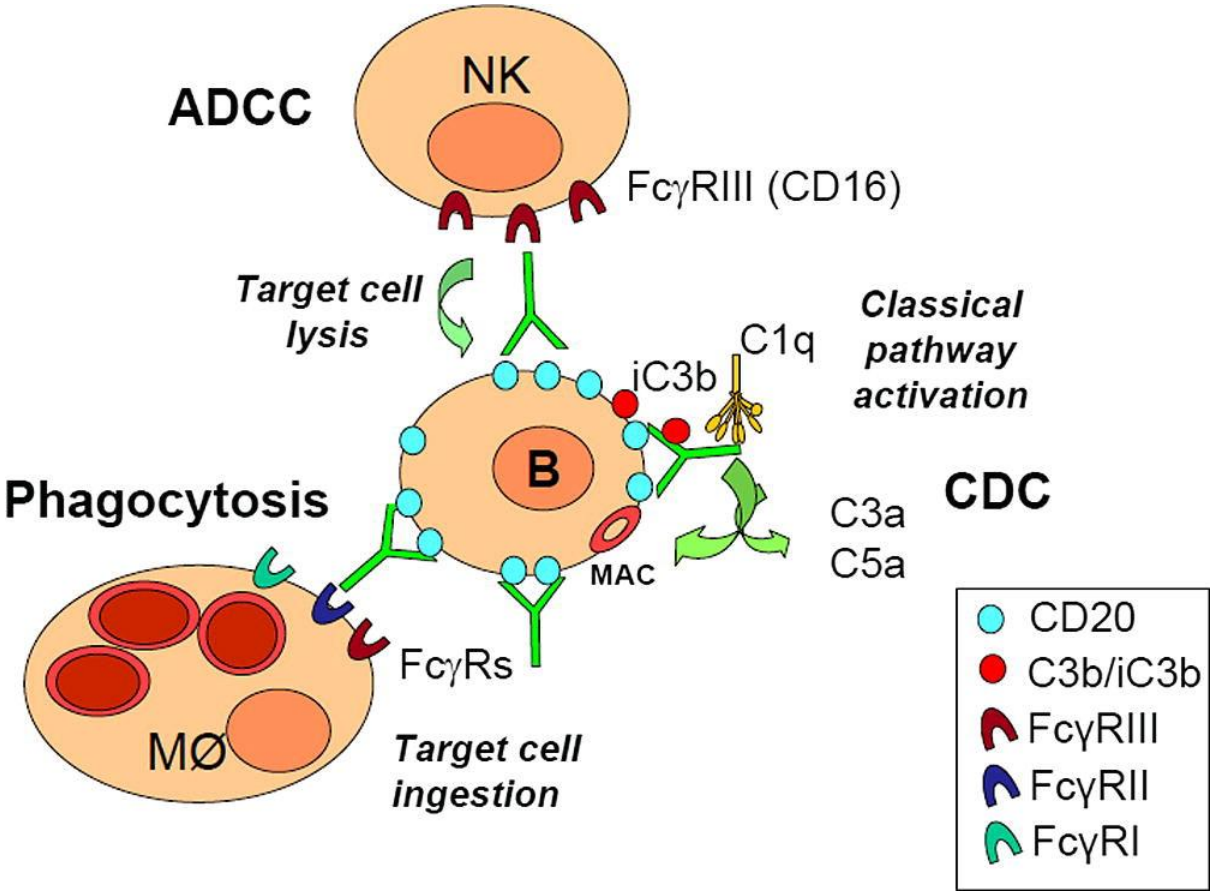


Figure 4: IgG mAb effector function pathways (Golay and Introna, 2012).

1.1.3.2 Mechanisms Independent of Immune Effectors

Signalling-induced apoptosis: Some mAbs can bind to surface receptors on target cells, triggering a signalling cascade that leads to cell death, also known as programmed cell death. This mechanism involves the mAb cross-linking a surface receptor on the cancer cell, which induces a death signal. The ability of a given mAb to mediate signalling-induced apoptosis could be non-specific (Weiner, 2007).

Interfering with ligand-receptor interactions: mAbs can bind to soluble ligands (e.g., IL-8) or surface receptors, thereby blocking interactions essential for disease progression. This is particularly relevant in cytokine-driven diseases and cancer (Weiner, 2007).

This can occur by:

- Removing the ligand from circulation

- Blocking the interaction between the ligand and its receptor
- Inducing modulation of the receptor
- Interfering with ligand-induced dimerisation of the receptor
- Inhibition of proliferation and induction of cell death: The Fab portion of mAbs can have antigen-binding activity that either neutralises the antigen or activates signalling pathways within the target cells, resulting in the inhibition of proliferation or direct cell death (Weiner, 2007) (Adams and Weiner, 2005).

1.1.3.3 Mechanisms Dependent on Immune Effectors:

Antibody-Dependent Cellular Cytotoxicity (ADCC): ADCC is an immune mechanism where the mAb-coated target cell is lysed by effector cells such as NK cells, monocytes, macrophages, and granulocytes. Specific Fc receptors on effector cells bind to the Fc region of the mAb, activating the effector cell and inducing cytotoxicity (Berger et al., 2002).

Complement-dependent Cytotoxicity (CDC): mAbs can induce CDC by activating the complement system, leading to the lysis of the target cell. Human antibodies, including IgM, IgG1, and IgG3, are effective at inducing CDC (Adams and Weiner, 2005).

Antibody-Dependent Cellular Phagocytosis (ADCP): Unconjugated IgG1 antibodies opsonise target cells or pathogens through antigen binding, allowing Fc receptors on phagocytes (macrophages, monocytes) to recognise, engulf and degrade the target (Golay and Introna, 2012).

1.1.3.4 Interacting Mechanisms

In many cases, the mechanisms of action of mAbs often do not function independently but interact with each other. For example, signalling can change the sensitivity of target cells to killing mediated by cellular effectors, and ADCC results in the activation of NK cells that

produce IFN gamma, which can enhance the development of an active immune response. Complement fixation can also influence the movement of mAb-antigen complexes within the membrane, thereby affecting the signal strength (Weiner, 2007)

The overall effectiveness of a mAb depends on factors such as antigen density, tissue distribution, binding affinity, and effector function capability, making structural design a critical aspect of therapeutic development (Breedveld, n.d.).

1.2 Bioprocessing of Monoclonal Antibodies

Unlike small molecule therapeutics, monoclonal antibodies are complex biological glycoproteins which require highly controlled bioprocessing strategies to ensure their production, quality and efficacy. The manufacturing of mAbs is distinguished into two major phases: Upstream Processing (USP), which focuses on media preparation, cell expansion and protein expression, and Downstream Processing (DSP), which includes purification, viral clearance and final formulation of the drug substance (**Figure 5**) (Gronemeyer et al., 2014)**.** For commercial mAb products, a third step is required to formulate and process the drug substance into the final sterile parenteral drug product; this step is known as fill-finish. This can involve the filling of a liquid solution into vials, cartridges or syringes, or in some cases, temperature and moisture-sensitive molecules may need to be lyophilised (Harris et al., 2004).

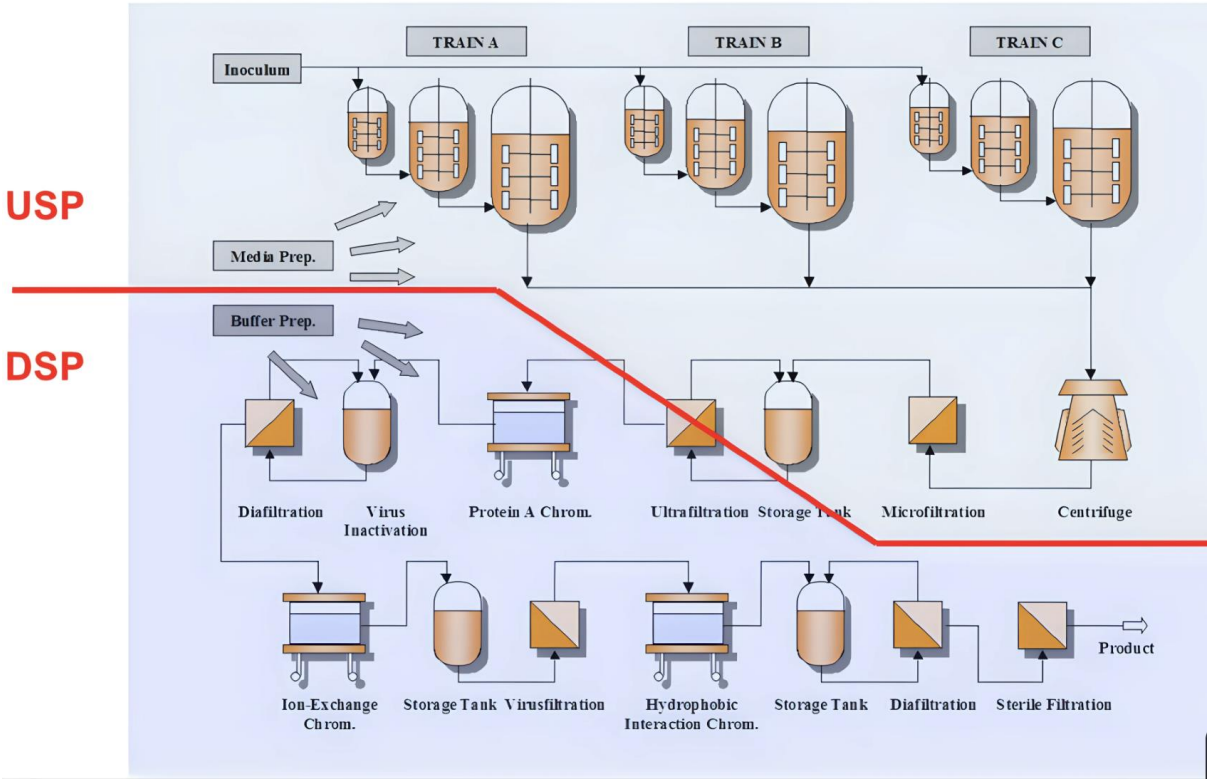


Figure 5: mAb manufacturing process flow diagram (Gronemeyer et al., 2014).

1.2.1 Cell Line Development

The complexity of monoclonal antibodies, including their structure and post-translational modifications, has been previously detailed and requires the use of mammalian expression systems such as CHO, HEK, NSO, Sp2/0, and PER.C6. Initial mAb products were expressed in murine myeloma cell lines such as NSO due to limitations in technology; however, today, the majority of mAbs are expressed in CHO cell lines (Walsh, 2018). Significant research efforts have been invested in the development of high-titre CHO expression systems that produce mAb titres in excess of 10 g/L while maintaining the structural complexity essential to biological function (Kim et al., 2012).

With modern genetic engineering techniques, the DNA sequence of the desired antibody can be inserted into the genome of CHO cells, resulting in subsequent antibody expression when the engineered cells are grown in cell culture. However, the number of copies of DNA inserted into the CHO cell genome varies significantly depending on the gene transfection process and the subsequent screening process (Wurm, 2004).

Efforts have focused on using a variety of metabolic enzyme expression systems such as Dihydrofolate Reductase (DHFR) and Glutamine Synthetase (GS) to screen cells with a high number of gene copies inserted. This has resulted in several distinct CHO cell lines with various selection marker approaches, as shown in Figure 6 (Zhang et al., 2024).

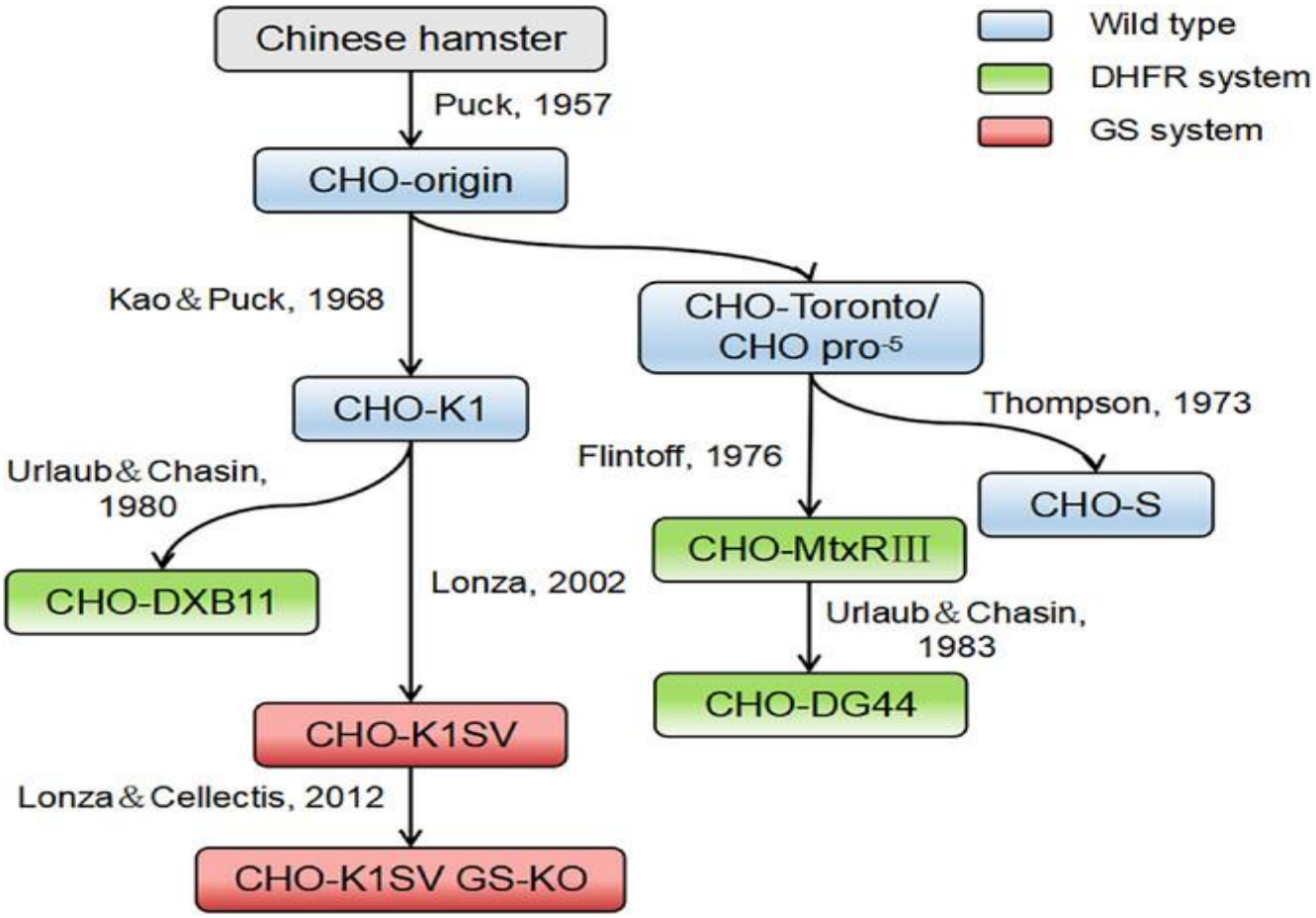


Figure 6: CHO cell lineages (Zhang et al., 2024)

1.2.2 Cell Culture Process

Cell culture in mAb production consists of a lengthy process lasting up to 30 days, depending on the final production bioreactor scale. The process begins with the thawing of a vial taken from a working cell bank (WCB) consisting of many identical vials containing the chosen CHO cell line clone that has been identified as optimal based on titres and genetic stability. There may be multiple WCBs, which are themselves derived from a master cell bank.

WCB and MCB vials are frozen to -180°C in liquid nitrogen with cells stabilised by DMSO and are thawed as required to produce a mAb batch. The thawing process is performed under controlled conditions where cells are warmed up to 37°C (Whaley et al., 2021).

Cells are then incubated in cell culture media in a T-flask with a working volume of 25 or 75 millilitres. Cells are then left to grow until they reach confluency and are added to a larger vessel, and the cell culture process is repeated. This process is repeated at a lab scale until cell volumes and density outgrow the lab scale equipment volume. The cell culture is then expanded in pilot-scale equipment from 50 L and above, the process ends at industrial full scale in bioreactors, which may have a volume of up to 20,000 L (**Figure 5 and Figure 7**).

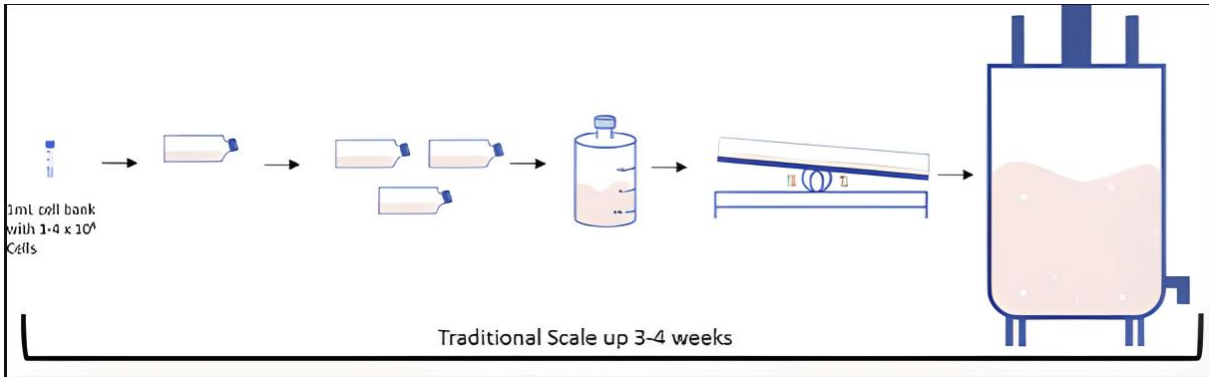


Figure 7: Cell culture Seeding, Expansion and Production Scale-up (Bellani et al., 2020).

Throughout the cell culture process, some critical in-process attributes and parameters require analysis and monitoring (**Table 1**). These attributes and parameters are common at all stages of cell culture scale-up and expansion (Freshney, 2010; Li et al., 2010; Sahoo et al., 2024).

Table 1: Critical Cell Culture Attributes and Parameters

Attribute/Parameter	Definition	Rationale
Cell density	A measure of the number of cells in a given volume of cell culture	Insufficient cell density will result in low titres and/or lengthy process
Cell Viability	A measure of the percentage of cells that are still viable	Low cell viability results in low titres and may be a sign of contamination
Confluence	The percentage of the culture vessel's surface covered by adherent cells	When cells reach confluence, they need to be expanded into a larger vessel
Glucose concentration	Measures the glucose concentration in media	A measure of available energy for cell growth and an indicator of recent cell growth levels

Temperature		CHO cells grow optimally at 37.5C
CO_2	Environmental CO_2 percentage	Controls pH which impacts growth
Dissolved oxygen		Cells require oxygen for growth

In addition to the above parameters and attributes, there are a range of raw materials, equipment, process steps and methodology and measurement technologies that can impact the cell culture process.

1.2.2.1 Materials

The major materials used in cell culture processes are the cell line (section 1.2.1), cell culture media and consumables used, such as T-flasks, shake flasks and single-use wave bags or single-use bioreactors.

Cell culture media traditionally used animal-derived serum, which was nutrient-rich with vitamins, hormones, growth factors and nutrients required to support cell growth in vitro, akin to in vivo cell growth. Examples of such media may include foetal bovine or equine serum (Fan et al., 2024). However, due to risks around the presence of adventitious agents, e.g. Bovine Spongiform Encephalopathy (BSE/TSE) and transmission to humans, the industry has moved to completely removing animal-derived components from the cell culture process. This has resulted in chemically defined media being used in modern cell culture processes or, at a minimum, animal-derived component-free media (van der Valk et al., 2010). Chemically defined media have the advantage of having lower variability in component composition, whereas some media may have naturally occurring components that display variability. In addition, animal serum is likely to contain residual levels of antibodies from the host that may contaminate any batches of mAbs produced (Zhang et al., 2024).

Cell culture media is complex, as it needs to imitate nutrient conditions found in host species, and the list of typical components is provided in **Table 2** (Combe and Sokolenko, 2021; Ritacco et al., 2018).

Table 2: List of materials used in cell culture.

Component	Description	Concentration (Typical)	Rationale
Carbon Source (Glucose)	Primary energy source for cell metabolism.	2–6 g/L	Provides energy for cell growth and mAb production; high levels support high-density cultures but must be controlled to minimize lactate accumulation, which lowers pH and inhibits growth.
Carbon Source (Glutamine)	Key for energy and protein synthesis; often supplemented with analogs like GlutaMAX.	1–4 mM	Supplies nitrogen and carbon for biosynthesis; critical for CHO cell viability, but ammonia buildup from degradation must be managed to prevent toxicity.
Amino Acids	Essential (e.g., leucine, lysine) and non-essential (e.g., proline, asparagine) amino acids.	0.1–1 mM per amino acid	Supports protein synthesis (e.g., mAbs); proline is essential for CHO-K1 derivatives like DP-12 due to auxotrophy, ensuring robust cell growth and productivity.
Vitamins	Biotin, folate, B12, etc., for metabolic pathways.	Trace levels (µM range)	Acts as cofactors for nucleotide synthesis and other metabolic processes, ensuring cell proliferation and mAb expression in high-density cultures.
Inorganic Salts	Sodium, potassium, calcium, magnesium, phosphate.	NaCl: ~120–150 mM; Phosphate: 0.5–1.5 mM	Maintains osmotic balance, supports signaling, and buffers pH; calcium is critical for adherent CHO cells (e.g., DP-12) to promote attachment.
Trace Elements	Iron, zinc, copper, selenium, etc.	Iron: 10–100 µM; Selenium: ~30 nM	Serves as enzyme cofactors; selenium supports antioxidant defense, protecting CHO cells from oxidative stress during bioreactor culture.
Buffering Agents	HEPES, sodium bicarbonate.	Bicarbonate: 15–44 mM	Maintains pH (6.8–7.4), critical for cell health and mAb stability; bicarbonate is essential in CO_2-controlled

			bioreactors for CHO suspension cultures.
Growth Factors/Supplements	Insulin, IGF-1, transferrin, or hydrolysates (in serum-free media).	Insulin: 5–10 mg/L; Transferrin: 5–50 mg/L	Promotes cell survival and proliferation; transferrin aids iron transport, while insulin enhances glucose uptake, boosting mAb yields in CHO cells.
Lipids/Cholesterol	Fatty acids (e.g., linoleic acid) and cholesterol, often in emulsions.	Trace levels	Supports membrane synthesis, essential for CHO cell growth and division, especially in serum-free or chemically defined media.
Osmolality Regulators	NaCl, mannitol.	280–320 mOsm/kg	Maintains osmotic balance to prevent cell swelling or shrinkage, ensuring optimal growth and mAb production in both adherent and suspension CHO cultures.

At laboratory scale, T-flasks are used for cell culture and may be provided in two formats to support adherent or suspension cell culture. As cell culture volumes increase, suspension cell cultures may be transferred to conical shake flasks and onto single-use bags. In contrast, adherent cells will need to be grown on microcarrier systems, fixed-bed bioreactors or roller bottles and multi-layer flasks. These systems, while effective, do not scale as well as bioreactors for suspension cells.

1.2.2.2 Method

Cell culture can be performed in adherent or suspension modes depending on the cell type; some cells, such as CHO cells, may initially be cultured in adherent mode before being adapted to suspension cell culture when scaling up. Other cell lines, particularly cell lines used in bioassays as in vitro cell-based assays for potency assessment, will be grown only as adherent cells and need to attach to the flask surface to grow.

There are two predominant types of cell culture methods used for commercial mAb production: fed batch and continuous methods. Fed-batch relies on the feeding of media to

the cell culture at pre-defined timepoints during the cell culture process. It may be based on a set time frequency or when key nutrients such as glucose are depleted. Process analytical technology (PAT) has significantly aided the optimisation of fed-batch cell culture processes.

In contrast, continuous cell culture relies on the continuous addition of nutrients and the removal of spent media, waste material and antibodies. This process is also known as perfusion cell culture and relies on Tangential Flow Filtration (TFF) to separate waste materials and produced mAbs from cells (**Figure 8**). This allows for extended production and a smaller equipment footprint.

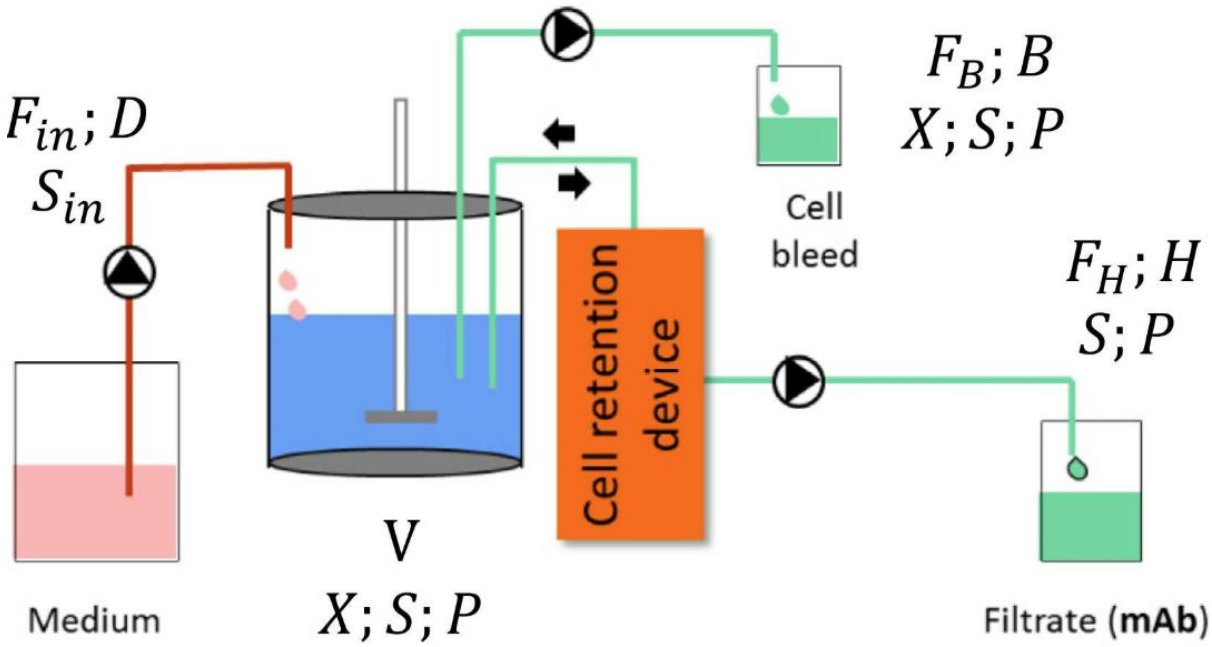


Figure 8: Perfusion Cell Culture Process Flow (Maria et al., 2023).

1.2.2.3 Measurement

As previously mentioned, cell culture is a lengthy process and requires in-process assessments of nutrient conditions, cell performance and process parameters. Historically, cell culture monitoring relied on basic instrumentation to measure fundamental factors such as temperature, pH, dissolved oxygen, airflow, liquid flow, foam accumulation and stirrer speed.

With the advent of PAT, the focus shifted towards the development of in situ and non-invasive analytical tools that enable “real-time release” to better control Critical Process Parameters (CPPs) and Critical Quality Attributes (CQAs) in biopharmaceutical manufacturing processes. This initiative aimed to capture complex metabolic and physiological dynamics of cell cultures, while improving product quality and process robustness (Streefland et al., 2013)

Modern analytical platforms include several spectroscopic techniques. For example, near-infrared (NIR) and mid-infrared (MIR) spectroscopy can generate culture-specific fingerprints that correlate and measure metabolites such as glucose, lactate, ammonia and glutamine. Raman spectroscopy gives detailed chemical information about compounds and is largely useful due to the weaker absorption of water. 2D fluorometry can measure various biomolecules and cofactors with fluorescent properties. It has been previously used to monitor viable cell density and recombinant protein concentration in Baby Hamster Kidney (BHK) cell cultures. Dielectric spectroscopy to measure the permittivity of cells in an electric field, which allows viable cell concentration to be quantified in real time. Electronic nose sensors analyse volatile components in bioreactor exhaust gases, which can be used to detect metabolic shifts or microbial contamination earlier. In addition, on-line HPLC enables direct monitoring of nutrients (Teixeira et al., 2009).

Other approaches include Oxygen Transfer Rate (OTR), which can be monitored online and non-invasively in shake flasks and microtiter plates. It provides valuable information about cell density and metabolic activity, crucial for scale-up studies (Neuss et al., 2025).

Overall, the combination of conventional probes with advanced PAT tools has transformed cell culture monitoring into a multivariate, real-time system enabling comprehensive assessment.

1.2.2.4 Environment

Upstream performance of mammalian cell lines begins with a controlled aseptic environment. Biosafety hoods provide personnel, product and environmental protection. Cell growth and product quality are governed by the surrounding physical, chemical and metabolic milieu, with key variables such as temperature, pH, pCO_2, dissolved oxygen, osmolality, and metabolites (Li et al., 2010).

Most fed-batch CHO runs are operated at a temperature of approximately 37 °C, which is near the physiological temperature. strategies like the mid-run temperature shift to a hypothermic condition have been explored to improve titre and quality (Xu et al., 2023).

The chemical environment required for robust cell growth involves a pH of around 6.8-7.2 and dissolved oxygen levels to be approximately 50%. Elevated pCO_2 levels interact with pH control and can shift cellular lactate metabolism. Hyperosmolality is linked to depressed cell growth and shifts in cell-cycle distribution (Alhuthali et al., 2021).

Glucose, glutamine and amino acids are essential to supply energy for cells and maintain their metabolic environment. High levels of lactate lower pH, cause stress to the cells and impair productivity. For CHO cells, a concentration of lactate above ~20mM is considered toxic, leading to poorer growth and quality. Ammonium ions can contribute to growth inhibition even at modest levels (2-10 mM) due to changes in glycosylation (Freund and Croughan, 2018).

PAT tools can also be used to measure and control the environment in real time. It can enable tracking of viable biomass and allow feedback control that reduces manual sampling, stabilises the cell culture (Kornecki and Strube, 2018).

1.2.2.5 Machine

On a laboratory scale, a Class II Biological Safety Cabinet (BSC) are used to maintain an aseptic area of cell culture work. This ventilated hood has an open front with inward airflow and downward High Efficiency Particulate Air (HEPA) filtered laminar airflow over the workspace (National Institutes of Health, 2019). Incubation chambers used for tissue culture hold a temperature of 37°C, 5% CO_2 and 95% relative humidity (van der Valk et al., 2010).

Historically, cultures progress through T-flasks and shake flasks for small-scale production before moving on to industry standards. In the late 1990s, rocking single-use "wave" bioreactors emerged, using wave-agitated, pre-sterilised plastic bags as a cultivation chamber for small to pilot runs (Singh, 2002). These single-use bioreactors (SUBs) reduce the risk of cross-contamination and shorten the turnaround time between batches (Shukla and Gottschalk, 2013).

In current times, industries commonly combine SUBs and stainless steel Stirred-tank bioreactors (STRs) assets. STRs, primarily made of stainless steel, are one of the most common types of vessels, providing robustness for very large-scale production. They can also be utilised as a Single-Use STR, having a disposable bag with an internal impeller mounted in a rigid support frame (Eibl et al., 2010; Wilde et al., 2009)



Figure 9: Single-use wave bioreactor bags for cell culture (Cytiva, n.d.).

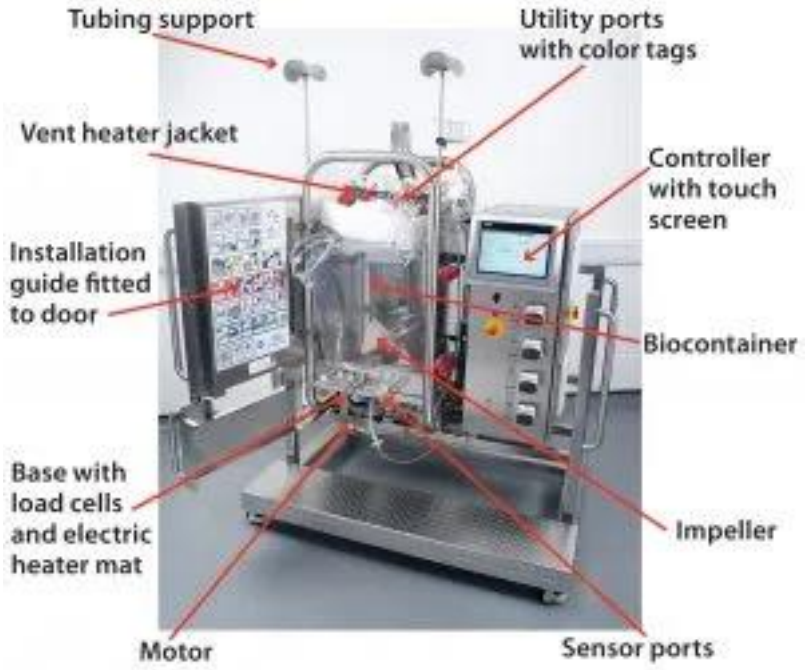


Figure 10: Single-use stirred-tank (Nienow et al., 2016).

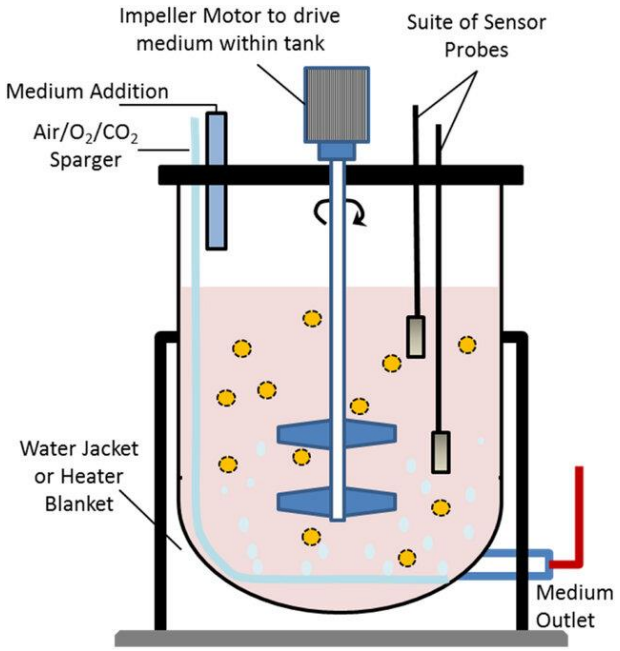


Figure 11: Stirred tank bioreactor with marine impeller-type blades (Kumar and Starly, 2015)

1.3 Analytical and Quality Control Strategies for Monoclonal Antibodies

Robust analytical and quality control (QC) frameworks are essential in the biomanufacturing of monoclonal antibodies to ensure product identity, purity, potency, and structural consistency as detailed in ICH Q6B. In addition, characterisation, in-process controls and QC testing are part of the broader process control strategy defined in ICH Q8, with product stability requirements defined in ICH Q1.

A typical mAb control strategy defines standard critical quality attributes and associated quality control tests as per **Table 3**.

Table 3: Typical monoclonal antibody CQAs and Test Methods

CQA Group	Attribute	Test Method(s)
Purity	Size-related variants	SEC-HPLC CE-SDS
	Charge-related variants	CEX-HPLC iCIEF
Potency	Binding affinity	ELISA SPR
	Activity	Cell based potency assay
	Particulate	Light Scattering/Microscopy
Contamination	Sterility	Sterility Test
	Bioburden	Bioburden count
	Endotoxin	LAL test
Process related Impurity	Host-cell protein	ELISA
	Viral contamination	PCR/Cell based etc
	Residual DNA	PCR
	Leachable & Extractable	LC-MS, GC-MS, TOC
Obligatory	Concentration	Nanodrop
	Expellable volume	USP
	Container closure integrity	Dye-ingress, Headspace, Helium leak, vacuum decay
	pH	USP
	Conductivity	USP
	Osmolality	USP
	Identity	ELISA, Peptide mapping

1.3.1 Aggregation

In mAb processing, a major product quality risk is the generation of aggregates due to common manufacturing hazards such as interfacial stress, phase changes, light, heat and pH. These hazards can lead to partial unfolding, dimer formation, followed by the generation of clusters, nuclei and ultimately fibrils, aggregates and phase separation (**Figure 12**).

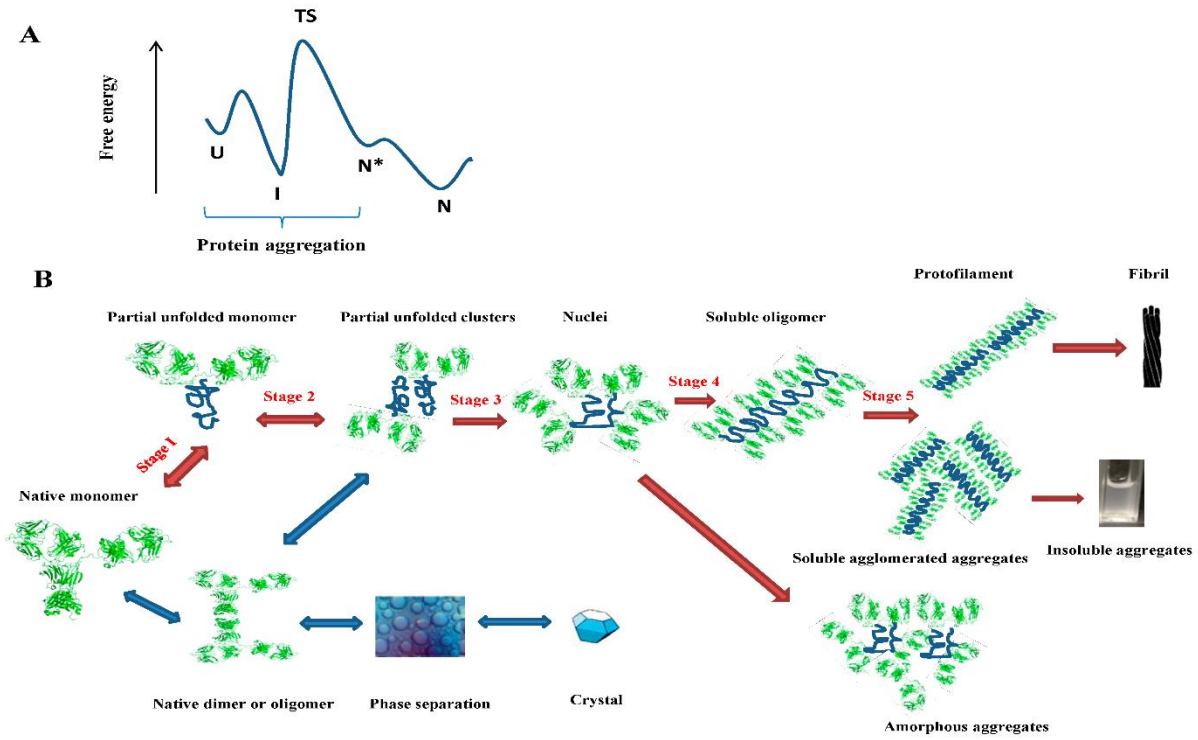


Figure 12: mAb aggregation, including (a) free energy kinetics behind aggregation and (b) aggregation pathways (Li et al., 2016).

SEC-HPLC is a key analytical method in the analysis of aggregates, employing standard HPLC equipment with a porous column as a stationary phase and phosphate buffer as a typical mobile phase. The technique works on the principle that larger molecules have a shorter residency time in the porous beads making up the stationary phase and elute first compared to relatively smaller molecules that tend to reside in the pores of the beads for longer. The technique benefits from a short run time of <15 minutes and a low sample volume requirement of ~50 µL when using vial inserts. A large number of samples can be run

in one analysis session due to the autosampler function of HPLC. A typical chromatogram for SEC-HPLC is shown below in **Figure 13**. The various fractions are detected by UV at 280 nm. mAb fragments or low molecular weight species can also be detected.

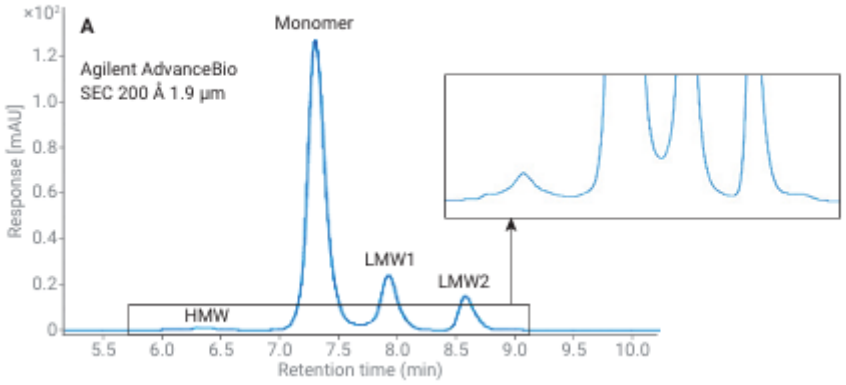


Figure 13: Typical mAb SEC-HPLC Chromatogram with aggregates (HMW) as well as fragments (LMW) and monomer detail (Qin, 2019).

A widely used bio-analytical technique used to characterise aggregates and fragments in academic environments is SDS-PAGE, which separates sample components based on size alone. Samples are denatured and then coated with a negative charge, which ensures that separation is based on size alone. Samples are then separated across a gel, which acts as a mesh with larger particles moving at slower rates than small particles. The technique allows for between 10-15 samples to be tested, with a molecular weight ladder added to the first lane to allow molecular weights to be assigned to bands.

The technique requires little equipment and has low consumable costs; however, the assay suffers from a lack of sensitivity and reproducibility compared to size exclusion HPLC. This has resulted in the development and implementation of CE-SDS, a miniaturised and automated version of SDS-PAGE that is performed in capillaries and complements SEC-HPLC in GMP laboratories (Gahoual et al., 2016; Rustandi et al., 2008).

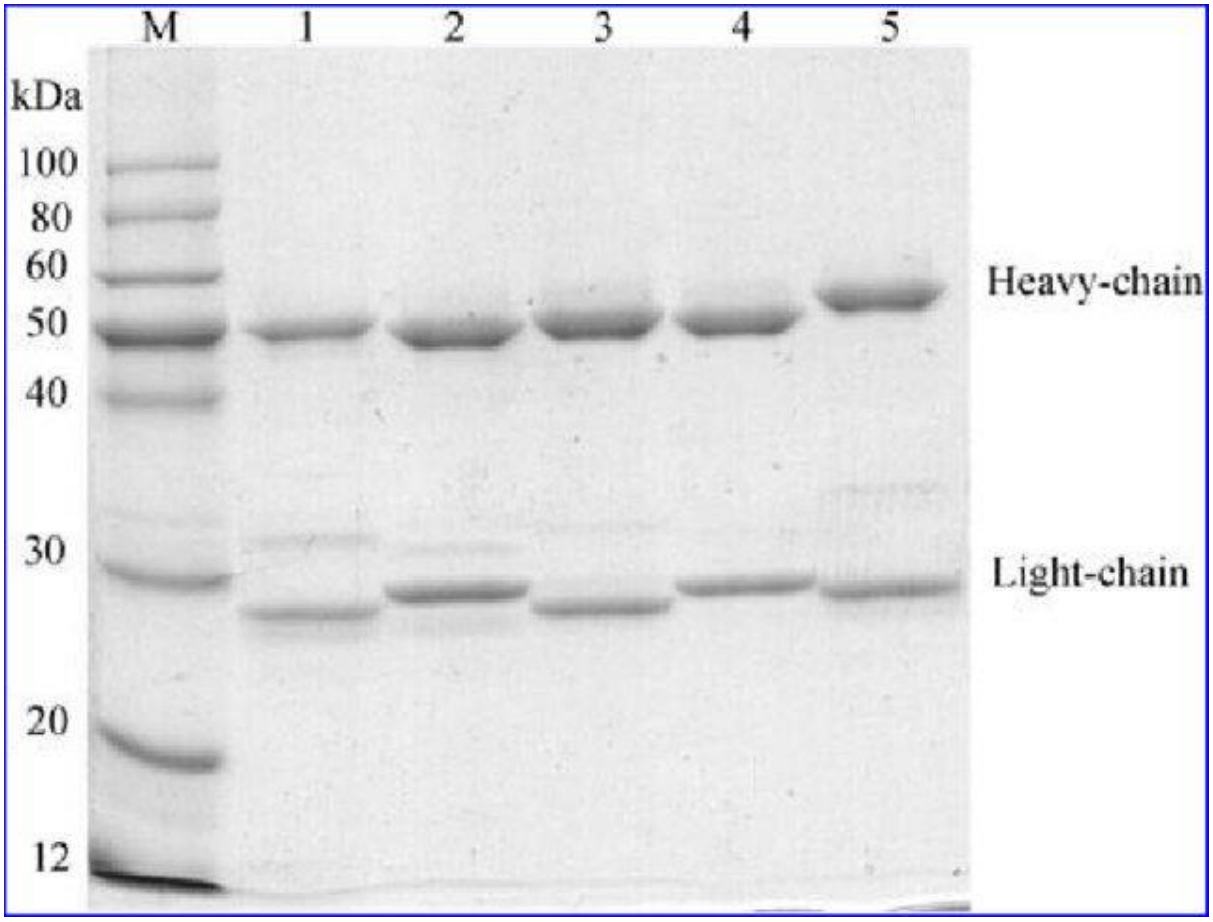


Figure 14: A typical SDS-PAGE gel of purified monoclonal antibodies (Li et al., 2011)

1.3.2 Charge Variant Analysis

Purity of monoclonal antibodies is also assessed in terms of charge heterogeneity, with a variety of post-translational modifications resulting in charge heterogeneity. The specific PTMs resulting in acidic or basic charge variants are described in **Table 4** (Alt et al., 2016).

Table 4: Post-translational modifications leading to charge variants in monoclonal antibodies (Alt et al., 2016).

Charge-related Variants (Acidic)	Deamidation in CDR
	Deamidation in Non-CDR
	Glycation in CDR
	Glycation in Non-CDR
Charge-related Variants (Basic)	Aspartic Acid Isomerization in CDR
	Aspartic Acid Isomerization in Non-CDR
	N-Terminal Leader Sequence (may be molecule specific)
	N-Terminal Pyroglutamic Acid
	C-Terminal Lysine
	C-Terminal Proline (IgG1) or Leu (IgG4) Amidation

There are two common methods used in industry to quantify charge variants: cation exchange (CEX) HPLC and imaged capillary isoelectric focusing (iCIEF). CEX-HPLC relies on antibodies being below their isoelectric point and being positively charged, allowing for an interaction with the weakly charged negative column. An increase in salt concentration or pH is used to elute the bound mAb based on relative charge, with the most positively charged basic species eluting last (Fekete et al., 2015). Isoelectric focusing is another technique that resolves mAb charge variants in a gel with a pH gradient. The traditional gel IEF technique has been superseded by a miniaturized capillary system with imaging capability e.g. iCIEF (Ghizzani et al., 2025).

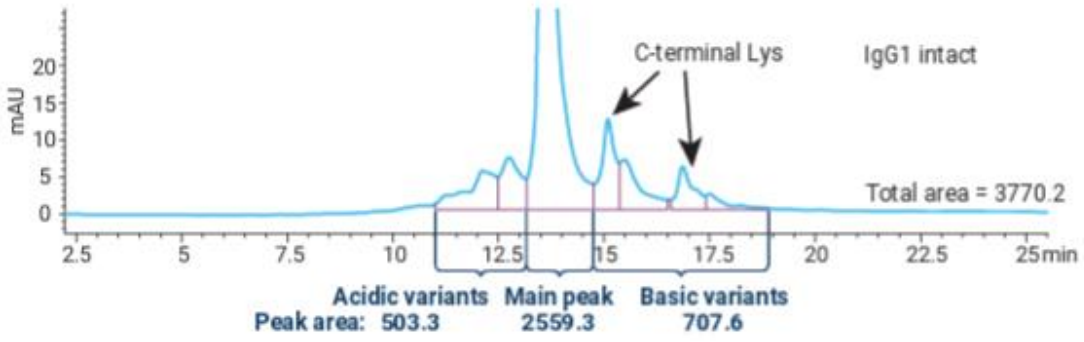


Figure 15: Charge variant HPLC (Agilent, n.d.)

1.3.3 Potency Assessment

A critical regulatory requirement in the development and production of mAbs is to demonstrate bioactivity, which can be through animal-based models, cell-based assays or bioassays such as Enzyme-Linked Immunosorbent Assay (ELISA). Animal-based assays are expensive, impractical and unethical in modern science when many alternatives exist. Cell-based potency assays are used widely in the industry and can be developed with assays reflective of the disease pathogenesis and the intended therapeutic mode of action (Abraham, 2010; Salmikangas et al., 2023). In practice, this can involve the use of cells that are targeted

in vivo or involve the use of cells engineered to mimic the biological targets e.g. reporter cell lines. An example of engineered cells used in potency assays are HEK Blue Tumour Necrosis Factor Alpha (TNF-α).

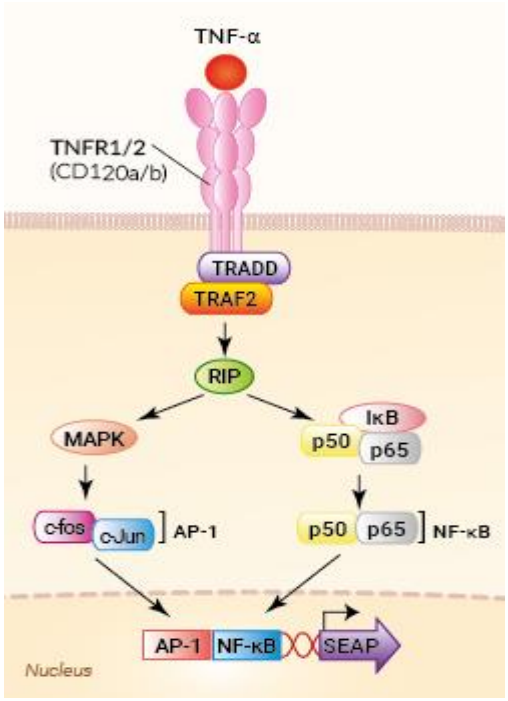


Figure 16: HEK BLUE Cells engineered to act as a reporter cell line for anti-TNF alpha mAbs (InvivoGen, n.d.)

HEK-Blue TNF-α cells were created by stable transfection with the genes encoding for the human TNF-α receptor (TNFR1 and TNFR2 chains), as well as an NF-κB/AP-1-inducible Secreted Embryonic Alkaline Phosphatase (SEAP) reporter (InvivoGen, n.d.; Pradeep et al., 2026). The binding of TNF-α to the receptor triggers a signalling cascade leading to NF-κB/AP1 activation and the subsequent production of SEAP. The addition of an antibody to such a cell system should block TNF receptor activation and reduce signalling. This is the basis of using such a cell line as a potency assay (InvivoGen, n.d.).

An alternative cell line that can be used as a potency assay for anti-TNF alpha mAbs is L929 cells. TNF-α binds to TNF receptors (TNFR1 and TNFR2) on L929 cells, triggering signalling cascades that lead to cell death via apoptosis or necroptosis (Humphreys and

Wilson, 1999). L929 cells are highly susceptible to this cytotoxicity, especially when pretreated with a protein synthesis inhibitor like actinomycin D (ActD), which sensitises them by blocking protective gene expression (Pradeep et al., 2026). In the presence of an anti-TNF-α mAb, the antibody binds to TNF-α, preventing receptor activation and cell killing.

Instead of measuring SEAP, cell counts, or Adenosine Triphosphate (ATP) analysis can be performed to measure cell death and provide an orthogonal, distinct assessment of antibody potency. As previously mentioned, both assays could be proposed as part of a control strategy, with each assay type having advantages and disadvantages in terms of knowledge provided, ease of use, sensitivity, etc. In development, the use of two or more orthogonal bioassays can be helpful, particularly if the mAb is stated to have multiple modes of action (Pradeep et al., 2026).

1.3.4 ELISA

Enzyme-Linked Immunosorbent Assay (ELISA) is a sensitive and versatile technique used to evaluate mAbs, for binding affinity, specificity, and quantification (Crowther, 2001). In a typical ELISA for mAbs, the antigen is coated onto a microplate, followed by incubation with the mAb, which binds specifically to the target antigen. A secondary enzyme-conjugated antibody detects the bound mAb, and a substrate reaction produces a measurable colourimetric signal, quantified by absorbance. This method supports potency assessment, pharmacokinetic studies, and quality control of mAbs (Aydin, 2015; Crowther, 2001). There are 4 different types of ELISA methods used in the industry (**Figure 17**).

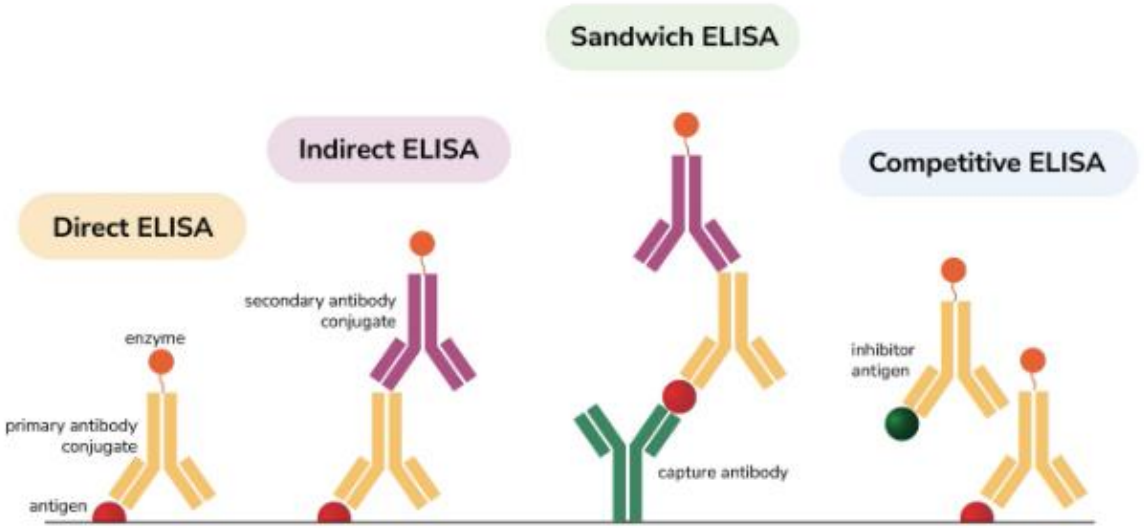


Figure 17: ELISA methods used in the biopharma industry (Supermodics, n.d.).

1.4 Interleukin-8 and Anti-IL-8 Mabs

IL-8, also known as CXCL8, is a pro-inflammatory Cysteine-X-Cysteine (CXC) chemokine that plays a significant role in cancer and inflammation. It exerts its biological effects by binding to cell-surface G protein-coupled receptors, IL-8RA (CXCR1) and IL-8RB (CXCR2), which are expressed on various cells, including neutrophils, monocytes, endothelial cells, and cancer cells (David et al., 2016). Structurally, IL-8 is a 72-amino acid peptide with an N-terminal ELR motif (Glu-Leu-Arg) critical for receptor activation (Murdoch and Finn, 2000). Upon binding to its receptors CXCR1 and CXCR2, IL-8 triggers intracellular signalling cascades (**Figure 18**), most notably the:

- Phosphoinositide 3-kinase/Akt (PI3/Akt) pathway, which promotes cell survival, migration and proliferation.
- Mitogen-activated protein kinase (MAPK) pathway, particularly through the ERK branch, which regulates gene expression, chemotaxis and cellular growth.
- Phospholipase C pathway, which modulates calcium signalling and contributes to cytoskeletal rearrangement (Li et al., 2020).

These downstream signals collectively result in a variety of biological effects, including:

- Neutrophil chemotaxis and activation
- Angiogenesis
- Proliferation and migration of endothelial and tumour cells (Li et al., 2020).

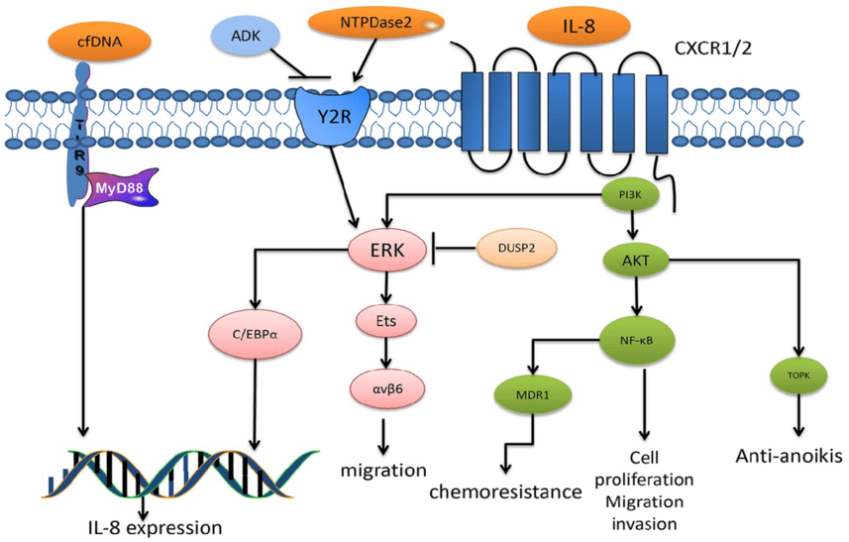


Figure 18: IL-8 signalling cascade (Li et al., 2020).

IL-8 plays a dual role in physiology and pathology. In normal immune responses, it coordinates acute inflammation and host defence responses. However, dysregulated IL-8 expression contributes to chronic inflammation, tissue damage, and tumour progression.

Elevated IL-8 levels are found in a range of pathological conditions:

- **Cancer**: Promotes tumour angiogenesis, epithelial-mesenchymal transition (EMT), metastasis, and immune evasion in colorectal, pancreatic, lung, breast and ovarian cancer (David et al., 2016).
- **Chronic inflammatory diseases**: IL-8 drives disease activity in rheumatoid arthritis, psoriasis, and cystic fibrosis (Murdoch and Finn, 2000).
- **Infectious diseases**: It is upregulated in bacterial and viral infections, contributing to cytokine storms (Harada et al., 1994).

Accordingly, the inhibition of IL-8 signalling carries significant potential therapeutic impact for targeting the tumour microenvironment and sensitising cancer cells to chemotherapeutic and biological agents. In addition, autoimmune inflammatory conditions such as Crohn's disease, rheumatoid arthritis may benefit from the targeting of IL-8.

1.4.1 Anti-IL-8 Antibodies: Mechanism and Development

Anti-IL-8 monoclonal antibodies (mAbs) are designed to neutralise circulating IL-8, thereby preventing its interaction with CXCR1 and CXCR2 receptors (Gabellini et al., 2009). This interrupts downstream signalling and mitigates neutrophil recruitment, inflammation, and tumour-promoting effects. These antibodies are excellent candidates for precision immunotherapy, especially when paired with biomarker-driven patient selection (e.g., IL-8 overexpression) (Waugh and Wilson, 2008). The success of anti-IL-8 mAbs will depend on their manufacturability, pharmacokinetics, and ability to integrate into existing cancer or inflammation treatment regimens (Chames et al., 2009).

Several strategies have been developed to target IL-8, including fully human monoclonal antibodies (e.g., ABX-IL-8, HuMax-IL-8) and small molecule inhibitors of CXCR1/2 signalling.

ABX-IL-8, a fully human anti-IL-8 antibody, inhibits angiogenesis, tumour growth, and metastasis of human melanoma in preclinical studies (Huang et al., 2002). ABX-IL-8 suppresses MMP-2 activity in melanoma cells and inhibits tumour cell invasion through the basement membrane in vitro (Huang et al., 2002; Luca et al., 1997). ABX-IL-8 treatment decreases vascularisation and increases apoptosis of tumour cells in vivo and directly interferes with tubule formation by human umbilical vein endothelial cells in vitro (Huang et al., 2002).

In a phase I/II clinical trial, HuMax-IL-8 (BMS-986253), a fully human IgG1 kappa mAb that binds to free IL-8, was well tolerated and effective in reducing disease activity in patients with palmoplantar pustulosis, a rare chronic inflammatory skin disorder (Bilusic et al., 2019; Gabellini et al., 2009). HuMax-IL-8 monotherapy was associated with significant decreases in serum IL-8 across all doses tested. Prolonged decreases of serum IL-8 levels were

observed at higher doses of HuMax-IL-8 and were associated with a longer study duration, informing subsequent exploration of combination treatment approaches (Bilusic et al., 2019).

1.4.2 Anti-IL-8 mAb potency assessment

The physiological mechanism of action of IL-8 provides several potential modes of assessing the potency of any anti-IL-8 mAb. The cell signalling cascade generates the upregulation of a number of proteins, such as PI3/Akt, ERK, that could be detected qualitatively and potentially quantified using western blotting after SDS-PAGE. Alternatively, the ability of IL-8 to cause chemotaxis could be leveraged in migration assays where an anti-IL-8 mAb should diminish or prevent chemotaxis. The tumour progression properties could also be assessed with anti-IL-8 Mabs, potentially reducing or preventing tumour cell line growth by removal of IL-8 stimulation.

1.5 Thesis Overview

This thesis focused on the cell culture and subsequent downstream processing of an anti-IL-8 mAb-producing CHO cell line, namely CHO DP-12 clone#1934. This cell line was donated to the ATCC by Genentech and is intended to be a publicly available, industrially relevant CHO cell line with titres representative of industrial titres. The reported titre of the cell line is 250mg/L.

Upstream processing studies were conducted using the CHO DP-12 Anti-IL-8 cell line initially, followed by a CHO NIST cell line to evaluate parameters influencing antibody production. The experiments focused on evaluating different media compositions and cell seeding density on antibody titre. Cell growth, viability, glucose consumption and antibody titre were assessed to identify trends affecting culture performance and productivity.

Downstream processing and analytical characterisation were performed using SDS-PAGE and SEC-HPLC to assess antibody stability, aggregation and fragmentation under stress-induced conditions.

In addition, the thesis focused on developing in vitro cell-based potency assays to assess the biological activity of anti-IL-8 mAbs produced during cell culture experiments. Two cellular models were investigated: HL60 cells due to their neutrophil-like response to IL-8 and HCT-116 cells, a carcinoma cell line sensitive to IL-8 mediated proliferative signalling. This enabled comparative assessment of the IL-8 signalling cascade and anti-IL-8 mAb-mediated inhibition.

2. Objectives and Hypothesis

The specific objectives of this thesis were as follows:

- **To develop an end-to-end mAbs production process**, from upstream cell culture to downstream purification and formulation, using a CHO-DP12 cell line engineered for anti-IL-8 mAb production and a cNIST mAb-producing CHO cell line.
- **To characterise the purified mAbs** using analytical and bioanalytical techniques such as ELISA, SDS-PAGE, and HPLC to evaluate concentration, purity, and integrity.
- **To develop cell-based bioassays** using HL-60 and HCT116 cell lines to assess the biological activity of IL-8 and determine the neutralising potency of commercial and in-house produced anti-IL-8 mAbs.
- **To assess the functional stability and potency of anti-IL-8 mAbs** under various storage conditions, focusing on refrigerated and ambient temperature stability over time.

3. Methods and Materials

3.1 Materials

Material	Grade	Supplier	Part Number	Application
Cell Culture				
CHO DP-12 clone#1934	Research Grade Test Material	ATCC	CRL-3614	CHO Cell Line
CNISTmAb CHO cell Line	Research Grade Test Material	NIST	RM 8675	CHO Cell Line
DMEM - High Glucose	Cell Culture	Sigma Aldrich	D6429-6X500ML	Media
Fetal Bovine Serum (FBS) Heat Inactivated	Cell Culture	Sigma Aldrich	F9665-500ML	Cell Resuscitation & Media
Penicillin-Streptomycin	Cell Culture	Sigma Aldrich	P4333	Prevention of microbial contamination
HEPES SOLUTION 1 M, PH 7.0-7.6	Cell Culture	Sigma Aldrich	H0887-100ML	Media
MEM Amino Acids (50x) Solution	Cell Culture	Sigma Aldrich	M5550-100ML	Media
Glucose	Cell Culture	Sigma Aldrich	G7528-250G	Media
L-Glutamine Solution 200mm	Cell Culture	Sigma Aldrich	59202C-100ML	Media
Milli Disposable Hemocytometer	N/A	Millipore	MDH-2N1-50PK	Cell counting
Nutrient Mix F12 Ham	Cell Culture	Sigma Aldrich	N6658-500ML	Media
Dulbecco's Phosphate	Cell Culture	Sigma Aldrich	D8537-500ML	Washing of Cells

Buffered Saline				
Trypsin-EDTA Solution 0.25%	Cell culture	Sigma Aldrich	T4049-100ML	Detachment of adhered cells
Erythrosin B	Cell culture	Sigma Aldrich	198269-25G	Staining of cells
EX-CELL® CD CHO	Cell Culture	Sigma Aldrich	14360C-1000ML	Media
CD CHO Medium	Cell Culture	Gibco	10743-029-1000ML	Media

Material	**Grade**	**Supplier**	**Part Number**	**Application**
HL-60 Cell Based Potency Assay				
HL-60 Cell Line	N/A	ATCC	N/A	Reporter Cell Line
RPMI 1640-1640 Medium	Cell Culture	Sigma Aldrich	R8758	Expansion Media
Dulbecco's Phosphate Buffered Saline	Cell Culture	Sigma Aldrich	D8537-500ML	Washing of Cells
Trypsin-EDTA Solution 0.25%	Cell culture	Sigma Aldrich	T4049-100ML	Detachment of adhered cells
Collagen From Human Placenta	Cell culture	Sigma Aldrich	C5533-5MG	Cell adherence
Bovine Serum Albumin, Lyophilized	>96% Pure	Sigma Aldrich	A2153-50G	Increase antigen stability
BCA Assay Kit	N/A	ThermoFisher Scientific	A55860-500ML	Protein concentration
HCT116 Cell Potency Assay				
HCT116 cell line	NCTC	ATCC	N/A	Reporter Cell Line

Cell Titer-Glo® 2.0 Cell Viability Assay	N/A	Promega	G9241	ATP detection
Human Interleukin-8	N/A	MedChem Express	N/A	Antigen for potency assays
RIPA Buffer	N/A	ThermoFisher Scientific	89901-250ML	Cell lysis
Protease inhibitor cocktail tablets	N/A	Roche Diagnostics	11836170001	Protect protein structure
Phosphatase inhibitor cocktail tablets	N/A	Roche Diagnostics	04906845001	Protect phosphorylation
p44/42 MAPK (Erk1/2) (137F5) Rabbit mAb	N/A	Cell Signaling Technology	4695	Primary antibody for western blot
Phospho-p44/42 MAPK (Erk1/2) (Thr202/Tyr204) Rabbit mAb	N/A	Cell Signaling Technology	4370	Primary antibody for western blot
S6 Ribosomal Protein (5G10) Rabbit mAb	N/A	Cell Signaling Technology	2217	Primary antibody for western blot
Phospho-S6 Ribosomal Protein (Ser235/236) (D57.2.2E) Rabbit mAb	N/A	Cell Signaling Technology	4858	Primary antibody for western blot
Secondary-anti-rabbit HRP conjugated	N/A	Sigma Aldrich	N/A	Antibody for western blot
Anti-IL-8 monoclonal antibodies	N/A	Thermo Fisher	N/A	Commercial antibody for potency assays
Cell Banking				
Dimethyl Sulfoxide Hybri-Max Sterile	Cell culture	Sigma Aldrich	D2650-5X5ML	Cell Banking/ Cryopreservation

Material	Grade	Supplier	Part Number	Application
Purification, Dialysis & TFF				
NeoTrap Protein G FLPC Column	Research	Neo Biotech	NB-19-0074-1mL	Affinity Chromatography
NeoTrap Protein G FLPC Column	Research	Neo Biotech	NB-19-0074-5mL	Affinity Chromatography
Sodium Phosphate Monobasic Dihydrate	Reagent	Sigma Aldrich	71505-1KG	Buffer A
Sodium Phosphate Dibasic Dihydrate	Reagent	Sigma Aldrich	71643-1KG	Buffer A
Glycine	>= 99% (HPLC)	Sigma Aldrich	T6066-1KG	Buffer B
Hydrochloric Acid 36%	Suprapur	Sigma Aldrich	1151861000	Buffer B
Tris-HCL	N/A	Internal	N/A	Buffer C
Ethanol	N/A	Internal	N/A	Column Storage & Wash
Tube-O-Dialyzer (Tm) Mini Dialysis System (4 KDa MWCO)	N/A	Geno Technology	Z742631-20EA	Dialysis
Tube-O-Dialyzer (Tm) Medi Dialysis System	N/A	Geno Technology		Dialysis
Sucrose	99%	Thermo Scientific Chemicals	A15583.0C	Drug Product Formulation
L-Histidine	98%	Thermo Scientific Chemicals:	166155000	Drug Product Formulation
Polysorbate 80	Chemical	Thermo Scientific Alfa Aesar	L13315.AP	Drug Product Formulation
Sodium Hydroxide	Reagent Grade,	Sigma Aldrich	S5881-1KG	TFF Membrane Storage

	>=98%			

Equipment	Make	Model
Centrifuge	Thermo Scientific	Heraeus Megafuge 8
Vacuum Pump	Thermo Scientific	Aspiration Advantage System with 4L polypropylene
Incubator	Thermo Scientific	VIOS 160i CO_2 SS IR 230V LK
Biosafety Cabinet	Thermo Scientific	MSC-Advantage Class II BSC
Microscope		
Purification Skid	Cytiva	AKTA START
UV Plate Reader	BMG	Spectro Star Nano
Visible Plate Reader	Revvity	Victor
SDS-PAGE Chamber & Power Pack	Bio-Rad	Mini-Protean Tetra Cell
UV Protein Concentration	Thermofisher Scientific	Nanodrop
Gel Scanner	Thermofisher Scientific	iBright 1500
TFF	Pall	Minimate EVO Tangential Flow Filtration (TFF) System

Consumable	Make	Model
T-25 Flask (non-adherent)	Sarstedt	83.3910.502
T-25 Flask (adherent)	Sarstedt	83.3910.002
T-75 Flask (non-adherent)	Sarstedt	83.3911.502
T-75 Flask (adherent)	Sarstedt	83.3911.002
T-175 Flask (non-adherent)	Sarstedt	83.3912.502
T-175 Flask (adherent)	Sarstedt	83.3912.002
Baffled flask, GL 45, with 4 bottom baffles, complete with membrane screw cap, 500ML	Duran	11736278

Flask, conical, baffled, membrane screwcap, 1000mL	Pyrex	15272816
S-Pak® Membrane Filter (0.22 Micron)	Millipore	GSWG047S6
Filtropur V100, Vacuum filtration unit, 1,000 mL, PES, 0.22 µm	Sarstedt	83.3942.001
10K Minimate Tangential Flow Filtration (TFF) capsule with Omega membrane	Pall	17194761

3.2 Methods

3.2.1 Cell Culture

3.2.1.1 Anti-IL-8 CHO DP12 cell culture

3.2.1.1.1 Generation of a working cell bank

A WCB was established from a Master Cell Bank (MCB) donated from an internal collaborator by Dr Alex Zhdanov. The MCB vial, containing cells frozen in 10% DMSO, was transported on dry ice and promptly thawed upon arrival. Thawed cells were centrifuged, resuspended in resuscitation medium consisting of DMEM supplemented with 10% FBS, 1% HEPES and 1% penicillin-streptomycin, and incubated for 2 days at 37 °C in 5% CO_2. Following initial recovery, cells were expanded in T-75 cm^2 flasks and subcultured routinely until passage 7, achieving consistent high viability of cells.

There were 15 vials of stock, each containing 700 µL of cells at a concentration of 2 x 10^6 cells per mL and were kept in a liquid nitrogen tank for long-term storage. All experimental batches conducted as part of this thesis were produced from this WCB.

The media composition of DMEM, 10% FBS, 1% HEPES buffer and 1% penicillin-streptomycin is hereafter defined as DMEM-complete media for the anti-IL-8 mAb CHO DP12 cell line cell culture.

3.2.1.1.2 Cell Thawing:

A vial of CHO DP12 Anti-IL-8 cells was retrieved from liquid nitrogen and rapidly thawed in a water bath at 37°C. Under aseptic conditions within a biosafety cabinet, the fully thawed cell suspension was transferred to a 50 mL conical tube containing 20 mL of prewarmed DMEM-complete media. The 50 mL conical tube was then centrifuged at 220 x g for 5 minutes at room temperature. Using a vacuum pump, the supernatant was aspirated and discarded as waste. The resulting cell pellet was resuspended in 15 mL of the same supplemented DMEM medium and transferred to a T-75 cm^2 cell culture flask. The cells

were cultured in adherent conditions and incubated at 37 °C in a humidified atmosphere with 5% CO_2 for 2 days.

3.2.1.1.3 Cell Expansion:

After 48 hours of initial incubation, the cell culture was passaged to facilitate expansion. The culture medium was aspirated, and the cells were gently washed with 10mL of DPBS to remove residual media components. The DPBS was discarded, and 1mL of trypsin was added to the flask to detach the adherent cells. The flask was then incubated at 37°C for approximately 2 minutes to allow for complete detachment. To neutralise the trypsin, 5 mL of DMEM-complete medium was added. The cell suspension was gently resuspended and transferred to a T-175 cm^2 culture flask containing 50 mL of the same supplemented medium. This expansion process was repeated until a total of six T-175 cm^2 flasks, each containing 100 mL of medium, were established. Confluence was regularly assessed during the expansion process.

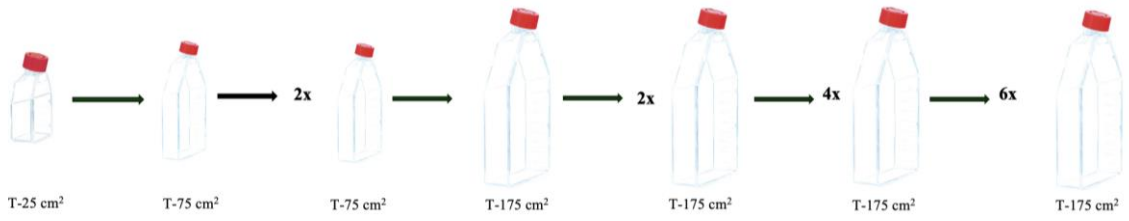


Figure 19: Expansion of CHO-DP12 Anti-IL-8 cell culture from T-25 cm^2 to T-175 cm^2 flasks.

3.2.1.1.4 Cell Production:

The T-175 cm^2 culture flasks were passaged to prepare cells for production experiments. All cells were pooled and collected into a 50 mL conical centrifuge tube. Cell viability and concentration were assessed using erythrosin B staining and manual counting with a hemacytometer. The resulting cell count was used to calculate seeding densities for subsequent experiments involving different culture media and varying cell densities. Cell viability and glucose levels were measured at regular intervals following the initiation of the production phase, using erythrosin B staining and a glucometer and test strips. Glucose was

added when levels dropped below 5 mmol glucose or regularly to maintain nutrient intake. After 10 days of the production phase, the conditioned media were carefully collected into 50 mL conical centrifuge tubes and centrifuged at 3000 G for 15 minutes to pellet the cells. The supernatant containing the secreted antibodies was collected, while the cell pellets were disposed of as biological waste. To eliminate any remaining cellular debris or particulate matter, the supernatant was filtered through a 0.22 µm sterile membrane. The clarified medium was then stored at 4°C until further use for downstream purification.

Batch-specific variations in anti-IL-8 mAb production

All production batches were based on the general workflow described above; however, batch-specific methodological variations were introduced. For Independent Anti-IL-8 mAb Production in CHO-DP12 cells, Batch 1 was conducted using adherent CHO-DP12 cultures expanded and produced in T-175 cm^2 flasks in DMEM-complete medium. In contrast, Batch 2 employed a suspension-based culture for production in a single 1 L shaking bottle using Ex-Cell CD CHO medium. For Media Studies and Cell Density Studies, variations in culture media and seeding density are mentioned specifically in the corresponding results sections for each batch.

3.2.1.2 cNISTmAb Cell Culture:

3.2.1.2.1 Cell line source:

The CHO NIST mAb-producing cell line (cNISTmAb) was obtained from the National Institute of Standards and Technology (NIST). Cells were provided as cryopreserved vials at a density of approximately 1 x 10^7 cells in liquid nitrogen storage. Gibco CD CHO medium supplemented with 8mM L-glutamine, 1% HEPES buffer, and 1% Penicillin-Streptomycin solution was used for the cell line's growth and expansion.

3.2.1.2.2 Cell Thawing:

A vial of CHO NIST cells was retrieved from liquid nitrogen storage and rapidly thawed in a 37°C water bath. Under aseptic conditions in a biosafety cabinet, the thawed cell suspension

was transferred to a 50 mL conical tube, containing 20mL of pre-warmed Gibco CD CHO medium supplemented with 8mM L-glutamine, 1% HEPES buffer, and 1% Penicillin-Streptomycin solution. The tube was then centrifuged at 220 × g for 5 minutes at room temperature. The supernatant was aspirated and discarded using a vacuum pump, and the resulting cell pellet was resuspended in 10 mL of the same media. The suspension was then transferred to a T-25 cm^2 cell culture flask and incubated under suspension culture conditions at 37°C in a humidified atmosphere with 5% CO_2 for 2 days.

3.2.1.2.3 Cell Expansion:

Following initial recovery in the T-25 cm^2 flask, the cells were successively expanded to larger flasks. After sufficient growth, the culture was transferred to a T-75 cm^2 flask, then expanded further into two T-75 cm^2 flasks. Once adequate cell density was achieved, the culture was scaled up into a T-175 cm^2 flask. At each step, cells were centrifuged at 220 × g for 5 minutes and resuspended in fresh Gibco CD CHO medium supplemented with 8 mM L-glutamine, 1% HEPES, and 1% Penicillin-Streptomycin. Expansion continued until a total of six T-175 flasks, each containing 100 mL of supplemented medium, were established.

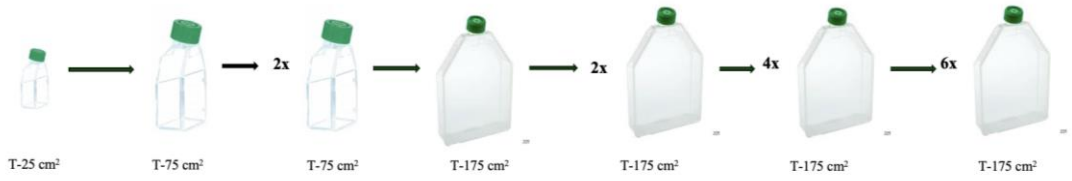


Figure 20: Cell culture expansion of CHO-NIST cells for each batch.

3.2.1.2.4 Cell Production:

The T-175 culture flasks were passaged to prepare cells for production experiments. All cells were pooled and collected into a 50 mL conical centrifuge tube. Cell viability and concentration were assessed using erythrosin B staining and manual counting with a hemacytometer. The resulting cell count was used to calculate seeding densities for subsequent experiments under varying cell densities.

CHO NIST cells were divided into 4 conditions of cell densities, 100 mL per condition in a T-175 flask with the Gibco CD CHO medium supplemented with 8mM L-glutamine, 1% HEPES buffer, and 1% Penicillin-Streptomycin solution. Glucose and viable cell density were measured every other day.

After 10 days of antibody production, the conditioned media from each culture flask were carefully collected into 50 mL conical centrifuge tubes. The tubes were centrifuged at 3000 G for 15 minutes to pellet the cells. The resulting supernatant, containing the secreted antibody, was collected while the cell pellets were discarded as biological waste. To ensure removal of residual cells and debris, the supernatant was passed through a 0.22 µm sterile filter. The clarified media were then stored at 4°C until further use for downstream purification.

3.2.2 Purification

The anti-IL-8 mAb 8 and cNIST mAb were purified using protein G affinity chromatography on an AKTA Fast Protein Liquid Chromatography (FPLC) system. Following harvesting, the conditioned media with secreted antibodies were directly connected to the FPLC setup for purification. A 1mL HiTrap Protein G column was used to bind IgG antibodies from the supernatant. The purification process involved binding, elution and neutralisation steps using three different buffers namely Buffer A (sodium phosphate buffer, pH 7.0), Buffer B (glycine buffer, pH 2.7) and Buffer C (Tris-HCl buffer, pH 9.0), respectively. All the buffers and conditioned media were equilibrated to room temperature and degassed using vacuum filtration through a 0.22 µm pore membrane prior to use. 200 µL of neutralisation buffer was pre-aliquoted into Eppendorf tubes before the start of purification. A flow rate of 1 mL/min was selected with a maximum pressure of 0.3 psi. Antibody elution was observed by in-line UV absorbance at 280 nm on the AKTA FPLC system. The 1 mL fractions of eluted

antibodies were collected into the same Eppendorf tubes to prevent denaturation and stored at 4°C until further use.

3.2.3 Protein Concentration

The protein concentration of the purified antibody fractions was determined using a Nanodrop spectrophotometer at 280 nm, and an absorbance of 1.0 corresponding to 1 mg/mL for IgG. A mixture of 1mL Buffer B and 200 µL Buffer C was used as the blank for baseline correction. For each measurement, 2 microliters of each fraction was placed on the pedestal, which was cleaned with milliQ water before and after use. Based on the concentration results, selected samples were subjected to dialysis for buffer exchange. Protein concentrations were reassessed post-dialysis to confirm the yield.

3.2.4 Dialysis

Purified antibody samples were subjected to dialysis to remove low-molecular-weight impurities and perform buffer exchange. Samples were placed in pre-treated Tube-O-Dialyser Mini and Medi Dialysis systems against sucrose-histidine buffer at 4°C. The external buffer was replaced three times over 24 hours to ensure removal of contaminants and complete equilibration. Post-dialysis, the samples were collected and stored at 4°C until further analysis.

3.2.5 SDS-PAGE

Sodium dodecyl sulphate-polyacrylamide gel electrophoresis (SDS-PAGE) was performed under reducing and denaturing conditions using a 10-well or 15-well ExpressPlus™ PAGE Gel (4-20% gradient), depending on experimental requirements. Protein concentrations were first measured using a Nanodrop spectrophotometer as mentioned above (Section 3.2.3). SDS-PAGE samples were prepared in 1x Laemmli sample buffer containing SDS and

dithiothreitol (DTT) to obtain a concentration of 0.25 μg/μL. Samples were subsequently heated at 95°C for 4-5 minutes and immediately put on ice and stored at -20°C until the day of analysis. SDS-PAGE running buffer was prepared using Running Buffer Powder dissolved in milliQ water. A pre-stained protein ladder was used in the gel as a molecular weight standard. Electrophoresis was conducted at a constant voltage of 50 V initially until the samples migrated through the stacking gel, followed by 100 V for 2 hours till the dye front reached the bottom of the gel. The gel was then taken out from the cast and placed in a petri dish containing Coomassie blue stain and kept at 4°C overnight. The next day, the gel was washed 5 times with milliQ water, and the gel image was captured using an iBright 1500 imaging system. Quantitative analysis of band intensity was not performed.

3.2.6 Cell-Based Potency Assays

3.2.6.1 HL-60 Cell Assay

Cell Culture

Human Promyelocytic leukaemia cells (HL-60) were cultured in RPMI-1640 medium initially supplemented with 20% FBS and further shifted into 10% FBS, 1% HEPES and 1% penicillin-streptomycin after 1 week, under suspension conditions. Cells were incubated at 37°C with a 5% CO_2 environment and passaged every 2 days to maintain and expand their growth. Cell density and viability were measured using a hemacytometer and erythrosin B stain.

Retinoic Acid Differentiation

In the first experimental batch, HL-60 cells were treated with increasing concentrations of all-trans retinoic acid (RA) at concentrations of 0, 0.25, 0.5 and 1 μM for 7 days to induce neutrophil-like differentiation. Each RA condition was evaluated in the presence and absence of 10 ng/mL IL-8, to identify the optimal RA concentration for differentiation. After treatment, cells were harvested, lysed, and analysed by western blotting for phosphorylation

of ERK (pERK) and RPS6 (pRPS6) as biomarkers for IL-8 signalling. Based on these results, 0.5 µM RA was selected for subsequent experiments for optimal differentiation of HL-60 cells.

Following RA optimisation, HL-60 cells were treated with 0.5 µM all-trans retinoic acid for 1 week to mimic neutrophil-like differentiation and then stimulated with 50 ng/mL IL-8 as supported by the literature (Bernhard et al., 2021). As cell proliferation decreases in the presence of retinoic acid, a larger number of cells were treated to ensure sufficient numbers, and they were monitored microscopically for changes indicative of differentiation.

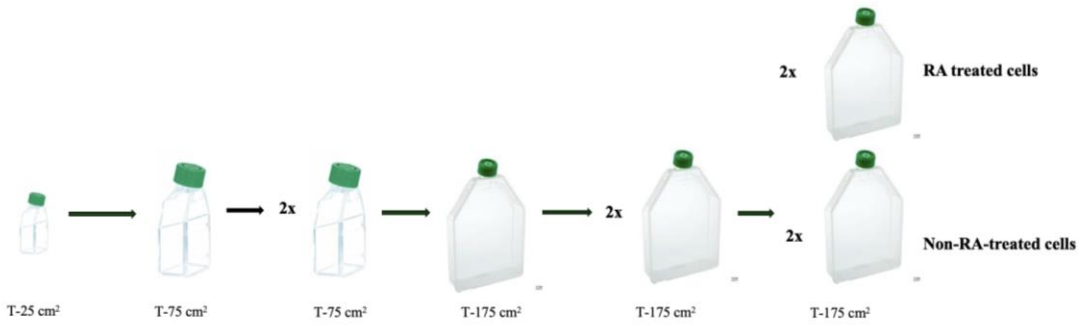


Figure 21: Cell culture expansion of HL-60 cells into differentiated and undifferentiated cells.

IL-8 Stimulation with Differentiated and Undifferentiated HL-60 Cells

Both retinoic acid-treated cells (differentiated) and non-retinoic acid-treated cells (undifferentiated) were stimulated with human IL-8 antigen at different time points to evaluate their cellular response to IL-8 antigen. Cells were seeded at a density of $2x10^6$ cells/mL in 6-well plates with 50 ng/mL IL-8 for 0 min, 15 min, 20 min, 1 hour, 2 hours and 4 hours. After the completion of the time limit exposure, the cells were collected and centrifuged at 220 x g for 5 minutes at room temperature and washed with PBS.

Cell Lysis and Protein Extraction

The resulting cell pellets were lysed using Radio-ImmunoPrecipitation Assay (RIPA) buffer supplemented with protease and phosphatase inhibitors and kept on ice for 20 minutes. Lysates were then centrifuged at 14,000 x g for 15 minutes at 4°C, and the supernatants were

collected for protein quantification using the BCA assay. The samples were stored at -20°C until further analysis.

BCA Assay for Protein Quantification

Protein concentration of all the samples was determined using the BCA Protein Assay Kit, according to the protocol detailed in the Appendix. Briefly, absorbance was measured at 562 nm using a microplate reader. Based on the results, the samples were diluted with 5x Laemmli SDS buffer and lysis buffer, heated at 95°C for denaturation, for Western Blotting.

Western Blotting

Western blotting was performed to assess the effect of IL-8-mediated signalling in HL-60 cells. Uniform concentrations of protein, as determined by the BCA Assay, were used for SDS-PAGE gels under reducing conditions as described in section 3.2.5. Proteins were then transferred using a Tris-glycine-based transfer buffer supplemented with methanol onto polyvinylidene difluoride (PVDF) membranes, using a wet transfer system. The transfer sandwich was assembled using fibre pads and filter papers saturated in transfer buffer, with the gel positioned toward the cathode and PVDF membrane towards anode to ensure efficient protein transfer, while care was taken to avoid air bubbles. Following this, these membranes were washed briefly in Tris-buffered saline containing 0.1% Tween-20 (TBST) and blocked for 1-2 hours at room temperature. For phosphorylated proteins, membranes were blocked in 5% bovine serum albumin (BSA) in TBST, while 5% non-fat milk in TBST was used for non-phosphorylated proteins. Membranes were then incubated overnight at 4°C with primary antibodies against pERK, ERK, pRPS6 and RPS6.

The next day, membranes were washed thoroughly with TBST and incubated for 2 hours at room temperature with anti-rabbit horseradish peroxidase (HRP) secondary antibodies. Protein bands were visualised using enhanced chemiluminescence (ECL) detection. Where

applicable, membranes were reprobed with antibodies against housekeeping proteins to confirm equal protein loading.

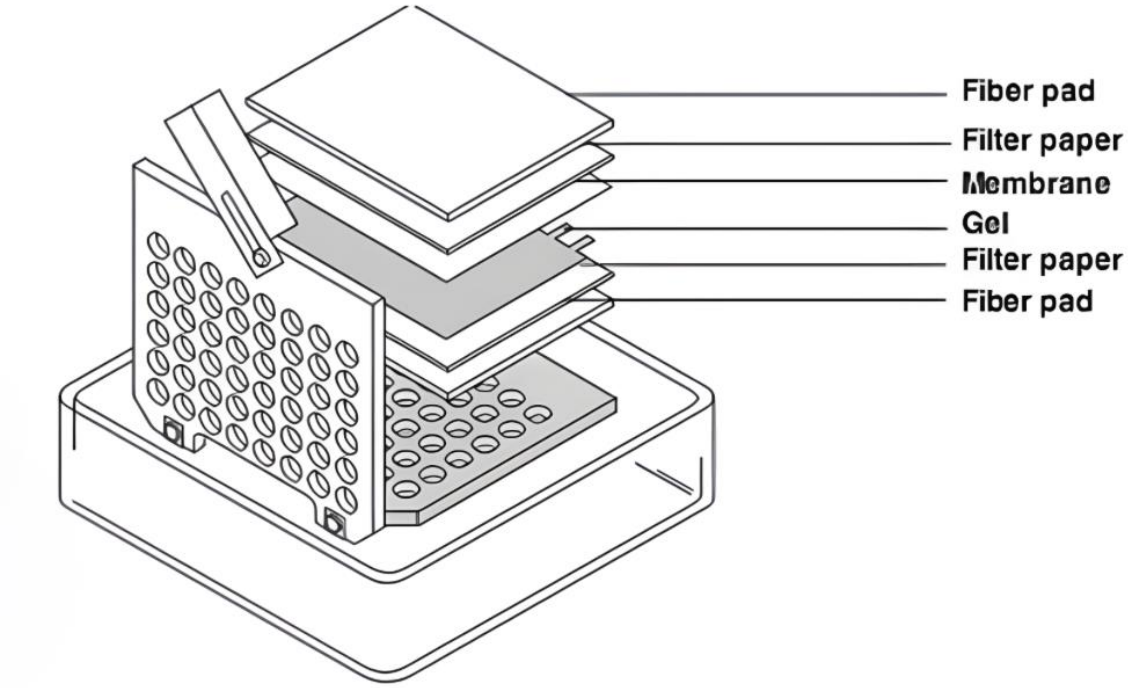


Figure 22: Schematic representation of the wet transfer sandwich assembly used for Western Blotting.

3.2.6.2 HCT-116 Cell Assay

Cell Culture

HCT-116 cells were taken from liquid nitrogen and cultured in McCoy's medium supplemented with 10% FBS, 1% HEPES and 1% penicillin-streptomycin. The cells were maintained as adherent cells in T-75 flasks at 37°C in a humidified incubator with 5% CO_2. Medium was replaced every 2-3 days, and cells were passaged upon reaching 80-90% confluency.

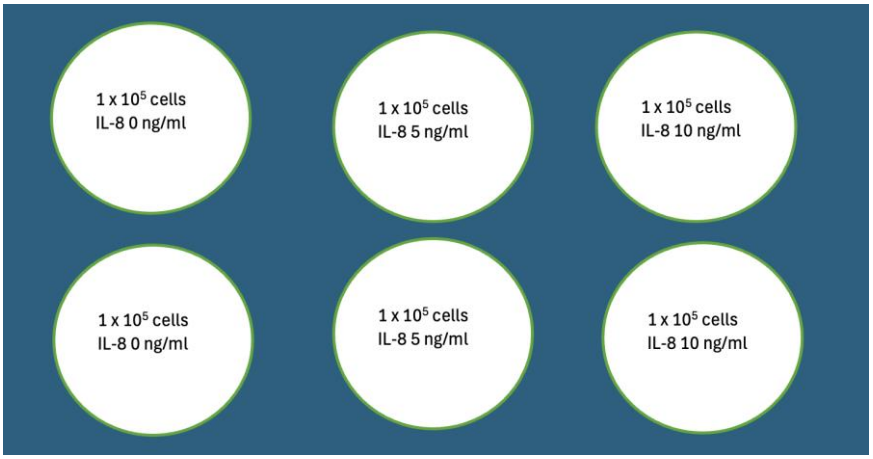
Western Blot:

HCT116 cells were treated with 50 ng/mL recombinant human IL-8 for short-term stimulation investigation. Cells were seeded at $1x10^6$ cells per well in 6-well plates and

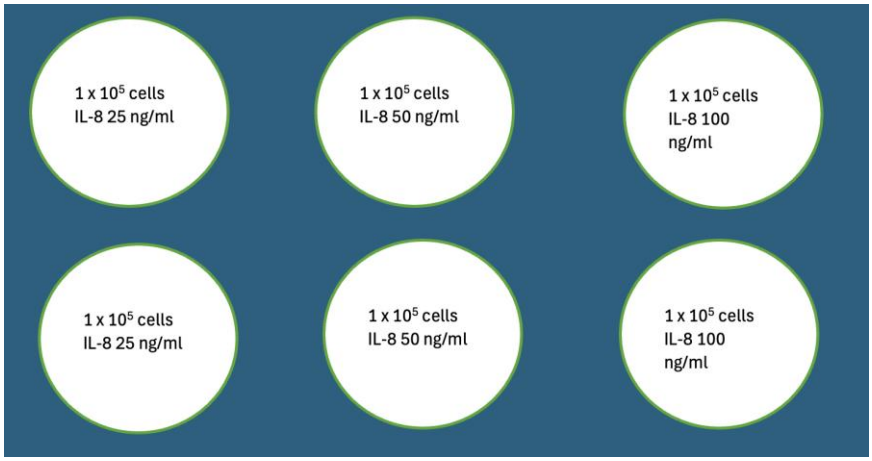
treated with IL-8 at 0 min, 30 minutes, 1 hour, 2 hours, 3 hours and 4 hours' time points. These cells were then lysed, and protein concentrations were determined using the BCA assay. Based on the results, samples were prepared with equal amounts of total protein and analysed by Western Blotting to assess changes in protein expression. A detailed Western Blot protocol is described above.

Cell Proliferation Assay

To evaluate the effect of IL-8 on cell proliferation, HCT-116 cells were seeded in 6-well plates at a density of 1 x 10^5 cells per well. The cells were cultured in McCoy's 5A medium supplemented with 2% FBS and treated with increasing concentrations of recombinant human IL-8: 0,5,10,25,50, and 100 ng/mL. Each concentration was tested in duplicate wells. The cells were incubated for 72 hours under standard conditions. After 72 hours, the cells were trypsinized and manually counted using a hemacytometer with erythrosin B stain. Viable and non-viable cell numbers were recorded, and average cell counts were calculated for each IL-8 concentration. The experiment was conducted across 3 different batches, with randomisation of IL-8 concentrations to minimise positional bias on the well plates.



(a)



(b)

Figure 23: Representative 6-well plate layout for IL-8 stimulation of HCT-116 cells. (a) Example layout for IL-8 concentrations 0, 5, 10 ng/mL (duplicates per well). (b) Example layout for IL-8 concentrations 25, 50, 100 ng/mL (duplicates per well)

ATP Assay

In parallel to cell counting, HCT116 cells were also assessed for their ATP activity with IL-8. Cellular ATP levels were analysed using the Cell Titer Glo Assay, which relies on luciferase-catalysed oxidation of luciferin in the presence of ATP, producing light. The luminescence signal generated is directly proportional to the amount of ATP present reflecting on the measure of metabolically active, viable cells.

For IL-8 stimulation experiments, the cells were seeded in 96-well plates at a density of 1 × 10^4 cells per well with McCoy's medium supplemented with 2% FBS. They were treated with IL-8 concentrations at 0,5,10,25,50, and 100 ng/mL, with 3 replicates per concentration. Following a 72-hour incubation, an equal volume (100 µL) of CellTiter-Glo reagent was added directly to each well. Plates were mixed on an orbital shaker for 5-7 minutes, after which the total 200 µL lysate from each well was transferred to a white-walled 96-well plate for measurement of luminescence on a microplate reader. The assay was repeated across 3 batches, including a randomised layout of IL-8 concentrations across the plate.

For anti-IL-8 mAb experiments, 1x10^4 HCT-116 cells were seeded in a 96-well plate with McCoy's medium supplemented with 2% FBS. They were stimulated with a commercially

available anti-IL-8 mAb at concentrations of 0, 0.5, 1, 2, 5 and 10 µg/mL , both in the presence and absence of 10 ng/mL IL-8 antigen. Appropriate controls were included, consisting of untreated cells stimulated with IL-8 alone and cells treated with antibody alone. Following a 72-hour incubation, ATP content was analysed using the Cell Titer Glo Substrate kit as described above. Each condition was tested in duplicate for Batch 1 and in quadruplicate for Batch 2 to ensure reproducibility.

3.2.7 Stability and Forced Degradation Study

3.2.7.1 Anti-IL-8 mAb stability study

A stability study was performed for anti-IL-8 mAbs derived from CHO DP12 cells from Independent Batch 1. Samples containing 100 µL each at a concentration of 1.14 mg/mL were taken into Eppendorf tubes and kept at different temperature conditions for predefined time points as per **Table 5**. These samples were withdrawn after completion of the period and transferred to -80°C storage until further analysis. In addition, one aliquot was kept frozen at -80 °C from the start of the study and served as the time zero control for comparison. All samples were assessed for protein integrity using SDS-PAGE.

The temperature conditions for the samples were as follows:

Table 5: Stability study protocol of anti-IL-8 monoclonal antibodies over 2 months under different temperature storage conditions (-20°C, 4°C, 25°C and 40°C); n=1 per condition.

Temperature	Time Points					
-20 ºC	4 days	1 week	2 weeks	3 weeks	1 month	2 months
+4 ºC	4 days	1 week	2 weeks	3 weeks	1 month	2 months
+25 ºC	4 days	1 week	2 weeks	3 weeks	1 month	2 months
+40 ºC	4 days	1 week	2 weeks	3 weeks	1 month	2 months

3.2.7.2 cNIST mAb stability study

A forced degradation study was carried out using cNIST mAb samples from Batch 1 of the cell density study, pooled together to assess their stability under stress-inducing conditions. 200 µL aliquots of the antibodies at a concentration of 1.822 mg/mL were dispensed in

Eppendorf tubes and subjected to various physical and chemical stress conditions for predefined time periods to stimulate accelerated degradation. After the specified period, all samples were collected and stored at -80°C until analysis, using SDS-PAGE and size exclusion HPLC. The following conditions were used as per **Table 6**.

Table 6: Forced degradation study protocol of cNIST monoclonal antibodies under different stress conditions, including temperature, light, pH, freeze-thaw and agitation; n=1 per condition. An overall stability control sample was kept at -80°C since the beginning of the study.

Condition	Control	Test 1	Test 2
Temperature	4°C	40°C 1 week	40°C 2-weeks
Light	Tinfoil wrapped at 25°C in chamber	Unwrapped 1 week at 100% UV & Light	Unwrapped 2 week at 100% UV & Light
pH	4°C	pH3 Glycine HCL buffer B 24 hours	pH11 Tris buffer not neutralized 24 hours
Freeze-Thaw	4°C	Freeze -80°C for 24 hours thaw to room temperature for 24 hours x 3 times	-
Agitation	25 °C no mixing 48 hours	Mixing for 24 hours	Mixing for 48 hours

3.2.8 Size-Exclusion HPLC

Size-exclusion chromatography (SEC) was performed using an AdvanceBio SEC 300 A column (2.7 µm, 4.6 x 150 mm; Agilent Technologies) connected to an Agilent 1200 Series HPLC system. This setup was selected for its high analytical precision, reproducibility and operational flexibility. The mobile phase consisted of 150 mM sodium phosphate buffer, adjusted to pH 7.0, prepared using milliQ water and filtered through a 0.22 µm membrane prior to use.

Chromatographic separations were conducted at a constant flow rate of 0.35 mL/min, with the column maintained at 25°C to ensure stable retention time and optimal peak resolution.

Samples from the forced degradation study of cNIST mAb, stored in sucrose-histidine buffer, were injected at a volume of 5 µL, and elution was monitored by UV absorbance at 280 nm. Each analytical cycle was completed within approximately 12 minutes, including column re-equilibration to the initial conditions before subsequent injections.

This method was optimised to resolve monomeric and high molecular weight species (HMWS) within a short runtime, enabling assessment of aggregation and degradation behaviour of the cNIST mAb under various stress conditions.

4. Results – Anti-IL-8 MAb Cell Culture

4.1 Production of Anti-IL-8 mAb

A range of cell culture experiments were performed with the Anti-IL-8 mAb CHO cell line, investigating the impact of media and cell density primarily on titre. A brief overview of each experimental batch and key observations is shown below in **Table 7**.

Table 7: Summary of experiments conducted with CHO-DP12 Anti-IL-8 cell line.

Experiment Type	Objective	Production Conditions	Key Observations
Independent Anti-IL-8 mAbs Production	Produce Anti-IL-8 mAbs	DMEM, 10% FBS, grown as adherent cell culture	1.144 mg/mL of antibodies produced, but with impurities due to FBS
Independent Anti-IL-8 mAbs Production	Produce Anti-IL-8 mAbs	Ex-Cell CD CHO medium under shaking conditions; grown as suspension cell culture	No antibodies expressed
Media Study 1	Compare protein expression across 8 different media cultures	8 media conditions, with different combinations of FBS and AA/L-Glu; grown in adherent cell culture	Low and variable protein expression. Highest protein yield in M6 due to endogenous proteins in horse serum
Media Study 2	Compare protein expression across 7 different media cultures	7 media conditions, with different combinations of FBS and AA/L-Glu; grown in adherent cell culture	Low and variable protein expression. Highest protein yield in M1 (Ex-Cell CD CHO), but still inconsistent
Cell density 1	Evaluate protein expression at different seeding densities	20-120 x 10^6 Cells/100mL in T-175 cm^2 flasks; grown in adherent cell culture	No significant protein detected
Cell density 2	Repeat cell density study	20-140 x 10^6 Cells/100mL in T-175 cm^2 flasks; grown in adherent cell culture	No protein expression detected
Cell density 3	Evaluate protein expression in serum adapted cells	50-125 x 10^6 Cells/250mL in petri dishes; grown in adherent cell culture	No protein expression confirmed in CHO DP12 cell line

4.1.1 Anti-IL-8 mAb Cell Culture Overview

The mammalian cell line CHO DP12 was used for the production of anti-IL-8 monoclonal antibodies, with all experiments initiated from the WCB vials. The cells were cultured in a DMEM-complete medium. Cell culture was completed in adherent mode. The cells typically reached 100% confluency within 2 days and were sub-cultured accordingly up to the required volume or cell density required for production. In addition, during the production stage, glucose levels and viable cell count were generally measured every 2 days.

4.1.2 Independent Anti-IL-8 Monoclonal Antibodies Production

Batch 1

As part of cell culture familiarisation training, an initial batch was produced under supervision, with expansion to a final volume of 1000 mL with DMEM-complete media across 10 T-175 cm^2 flasks and a 10-day production step. The conditioned media were harvested and purified using affinity chromatography using protein G FPLC.

The 1.2 mL in each elution fraction was measured for protein concentration, as shown in **Figure 24**. There was a distinct protein peak at fraction 4. Fractions 3 to 7 were pooled together and dialysed into sucrose-histidine buffer. The final pooled antibody concentration was determined to be 1.144 mg/mL, corresponding to a total recovery of 6.9 mg protein from 6.0 mL pooled volume. Based on the 1 L production culture volume, the calculated protein titre for Batch 1 was 0.0069 mg/mL. This material was used for the stability study outlined in **section 4.2.**

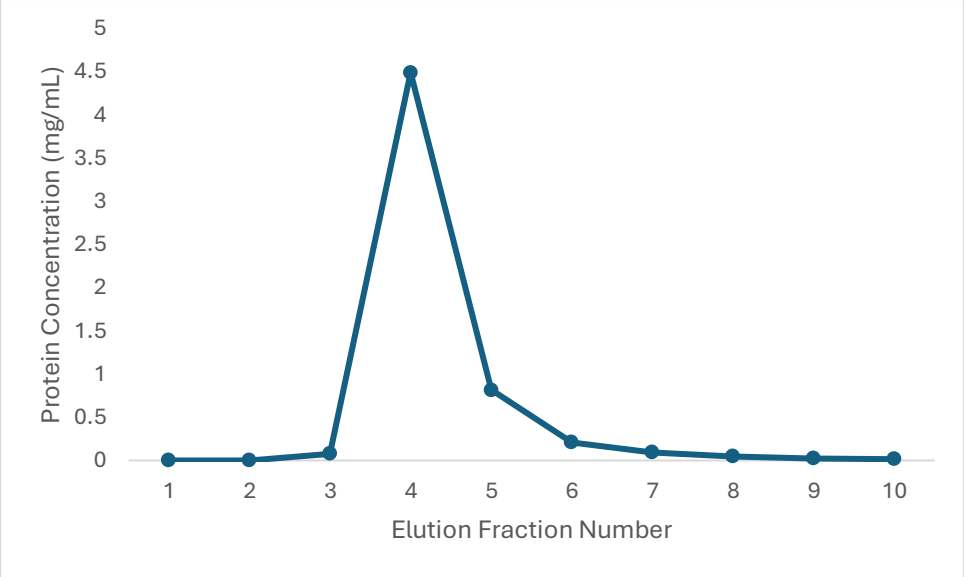


Figure 24: Protein concentrations of eluted fractions from Batch 1 of independent Anti-IL-8 mAbs production in CHO-DP12 cells, as measured by Nanodrop spectrophotometry at 280 nm.

Table 8: Calculated protein titre for independent anti-IL-8 mAb production: Batch 1.

Batch	Total Protein Mass Recovered (mg)	Culture Volume (mL)	Titre (mg/mL)
Independent anti-IL-8 mAb production Batch 1	6.9	1000	0.0069

Batch 2

In the second independent batch, CHO DP12 Anti-IL-8 cells were cultured in 1 litre of Ex-Cell CD CHO medium in a single shaking bottle for 10 days, incubated with agitation for 10 days under standard suspension culture conditions. Glucose levels and viable cell percentage were measured throughout.

As shown in **Figure 25**, the initial glucose level was 30 mmol, which declined sharply till Day 4, after which they were restored. Following that, the glucose levels remained stable till Day 10. Correspondingly, the viable cell percentage remained in the range of 50-60 % as displayed in **Figure 26**. These results indicate active glucose uptake during the initial phase of production and loss of cell viability towards later stages.

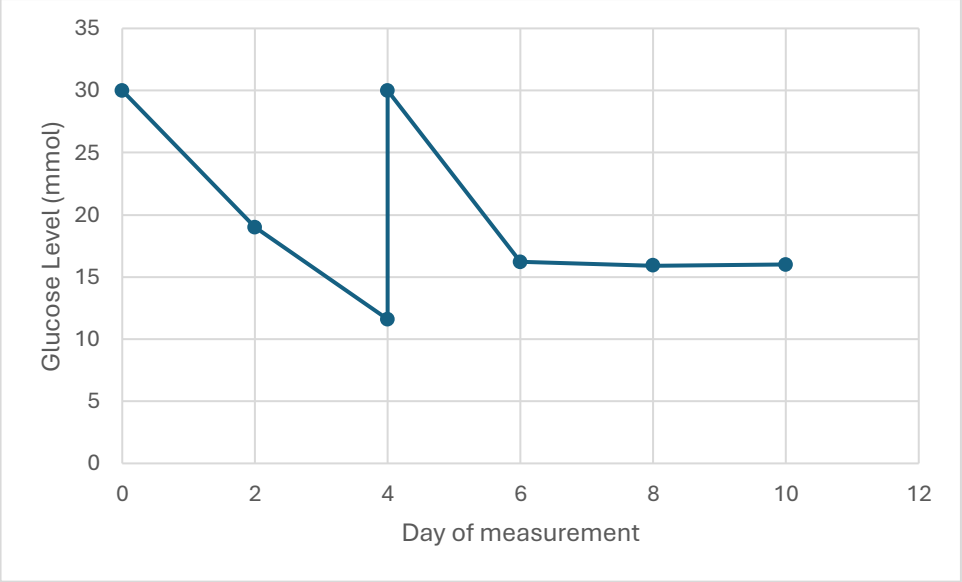


Figure 25: Glucose levels of Batch 2 of the independent CHO-DP12 Anti-IL-8 cell culture. Data are presented from one biological replicate (n=1). Glucose concentration was measured once per time point.

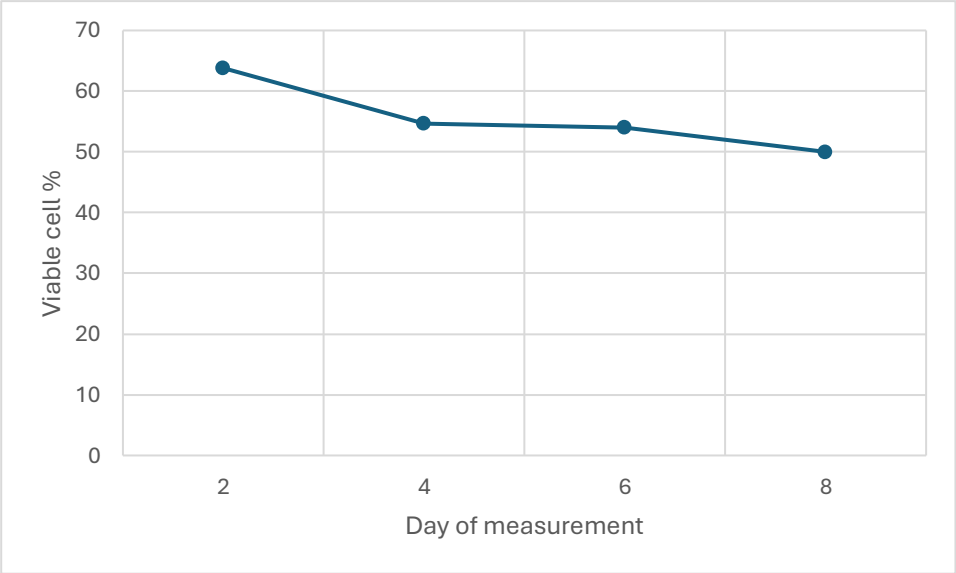


Figure 26: Cell viability percentages for Batch 2 of the independent CHO-DP12 Anti-IL-8 cell culture. Data are presented from one biological replicate (n=1). Cell viability at each time point was calculated as the average of two haemocytometer counting chambers.

The supernatant was collected on Day 10 and purified using FPLC. Protein quantification of the elution fractions (1.2 mL each) via Nanodrop revealed extremely low yields. There was no significant protein expression in this batch, as expected and assumed to be a result of culturing cells in suspension without an adaptation period.

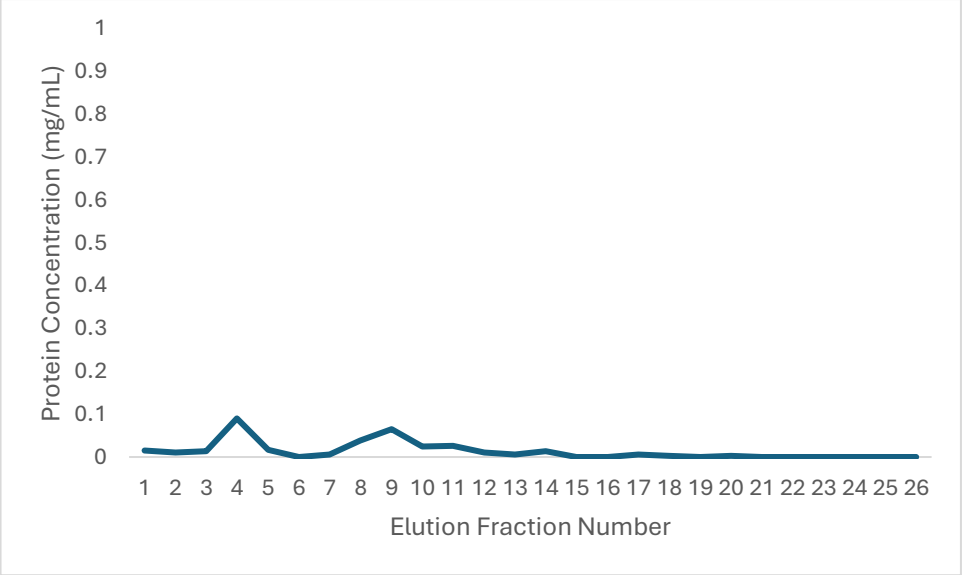


Figure 27: Protein concentrations of eluted fractions from Batch 2 independent Anti-IL-8 mAbs production in CHO-DP12 cells, as measured by Nanodrop spectrophotometry at 280 nm; n=1.

Table 9: Calculated protein titre for independent anti-IL-8 mAb production, Batch 2.

Batch	Total Protein Mass Recovered (mg)	Culture Volume (mL)	Titre (mg/mL)
Independent anti-IL-8 mAb production Batch 2	0.4152	1000	0.00042

4.1.3 Media Studies

Batch 1

Cell Culture

To evaluate the effect of different culture media on antibody production, CHO DP12 Anti-IL-8 cells were grown in various media compositions as adherent cells and monitored for protein expression levels as per **Table 10**.

After expansion to six T-175 cm^2 flasks, the cells at passage 14 were transferred to 8 different production conditions at $1x10^6$ cells/mL in 100 mL media per flask and maintained at standard incubation conditions for 10 days.

Each medium was supplemented with 1% HEPES, 1% penicillin-streptomycin, and 1% FBS or 1% horse serum (HS), depending upon the experimental condition. The experiment assessed both serum-containing and serum-free conditions, along with combinations of AA and L-glutamine to isolate the effects of base medium composition on protein expression. The different media conditions used were as follows:

Table 10: Batch 1 of different media conditions tested for CHO-DP12 Anti-IL-8 mAb production, showing variations in base medium and supplementation.

Media Condition	Base Medium	Supplements	Serum Type	Initial Glucose Concentration (mmol)
1	Ex-Cell CD CHO	-	None	30
2	RPMI	-	1% FBS	11
3	RPMI	AA, L-glutamine	None	11
4	DMEM	-	1% FBS	25
5	DMEM	AA, L-glutamine	None	25
6	DMEM	-	1% Horse Serum	25
7	McCoys	-	1% FBS	16
8	McCoys	AA, L-glutamine	None	16

Glucose Concentration

Glucose levels of all media conditions were monitored over a 10-day production period to evaluate cellular metabolic activity and nutrient uptake. **Figure 28** illustrates the levels of glucose measured for CHO DP12 Anti-IL-8 cells cultured in different media conditions, denoted M1-M8. As shown, glucose concentrations in all media conditions gradually declined over time. Media conditions M2 and M5 showed relatively lower and more stable glucose intake. M7 was refed with glucose on Day 6 to restore initial glucose levels following

a marked decline. These differences may be a factor in the variation of protein yield amongst different media conditions.

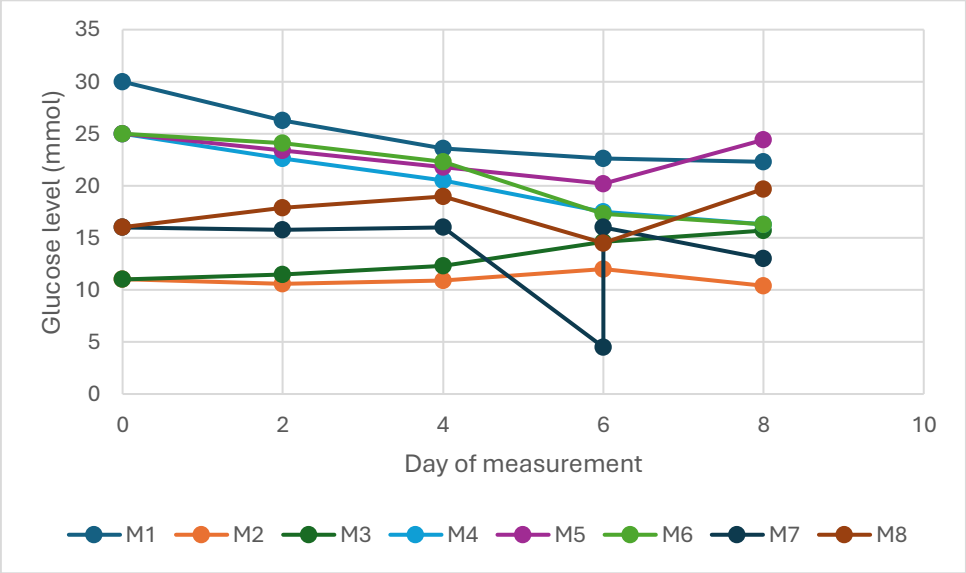


Figure 28: Glucose consumption profiles for Batch 1 of the different media study of CHO-DP12 Anti-IL-8 cell culture. Glucose levels were measured once per time point across eight media conditions (M1-M8); n=1 per condition.

Purification

The harvested supernatant was filtered through a 0.22 µm membrane to remove cellular debris and purified using FPLC, with a 1mL protein G affinity column. Approximately 60 mL of supernatant per media condition was loaded onto the column for purification. Due to accidental spillage of one of the samples, only 60 mL of cell culture supernatant could be used to maintain uniformity across different media samples, despite culturing 100 mL of media.

For each condition, six 1 mL elution fractions were collected for all samples except for M4, in which elution was unsuccessful due to technical errors during the FPLC run. M4 was subsequently removed from analysis.

All successful elution fractions per media condition were analysed for protein concentration using Nanodrop spectrophotometry at 280 nm. Values of each media condition were compared, and the results are presented in **Figure 29**.

As shown in the graph, media conditions M1, M2, M3, M4, M5, M7 and M8 exhibited comparable protein concentrations across elution fractions, with fractions 2 to 4 demonstrating the highest titres. However, media condition M6 (DMEM + 1% Horse Serum) had the highest concentration of 9.76 mg/mL compared to others, as shown separately in **Figure 30**. The markedly elevated protein yield in M6 can be attributed to the presence of endogenous proteins from HS. Therefore, the Nanodrop readings of M6 were not a reliable indicator of anti-IL-8 monoclonal antibodies.

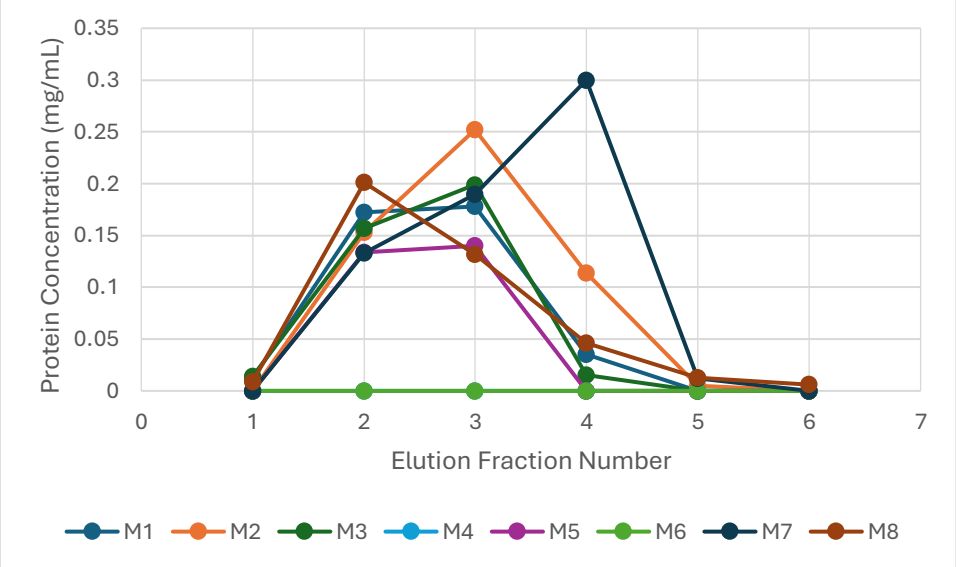


Figure 29: Protein concentrations of eluted fractions from Batch 1 media studies of CHO-DP12 Anti-IL-8 mAbs produced in media conditions M1, M2, M3, M5, M7 and M8, excluding M4 and M6, as measured by Nanodrop spectrophotometry at 280 nm; n=1 per condition.

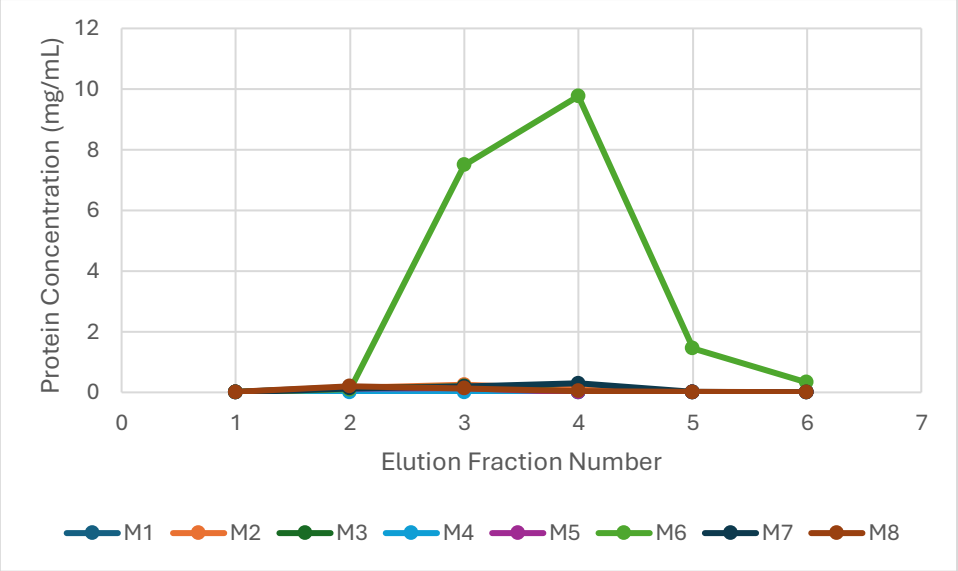


Figure 30: Protein concentrations of eluted fractions from Batch 1 media studies of CHO-DP12 Anti-IL-8 mAbs, including condition M6, shown separately due to significantly higher yields, as measured by Nanodrop spectrophotometry at 280 nm; n=1 per condition.

Table 11: Calculated titre values from Batch 1 media study of CHO DP12 Anti-IL-8 mAbs.

Media Condition (Batch 1)	Total Protein Recovered (mg)	Titre (mg/mL)
M1	0.476	0.0048
M2	0.6288	0.0063
M3	0.462	0.0046
M4	N/A	N/A
M5	0.3288	0.0033
M6	22.9776	0.2298
M7	0.762	0.0076
M8	0.4884	0.0049

Batch 2

Cell Culture

Building upon findings from Batch 1, a second batch of media studies was conducted to further evaluate the effect of culture media on Anti-IL-8 mAb production. This batch focused on a refined set of media conditions, specifically excluding HS.

A fresh vial of CHO DP12 cells was thawed and expanded. Due to the limited availability of T-175 cm^2 flasks, the cells were expanded into ten T-75 cm^2 flasks as an adherent culture. At

passage 12, cells were collected and divided among 7 T-175 cm^2 flasks with 5x10^6 cells/mL in 100 mL media per flask.

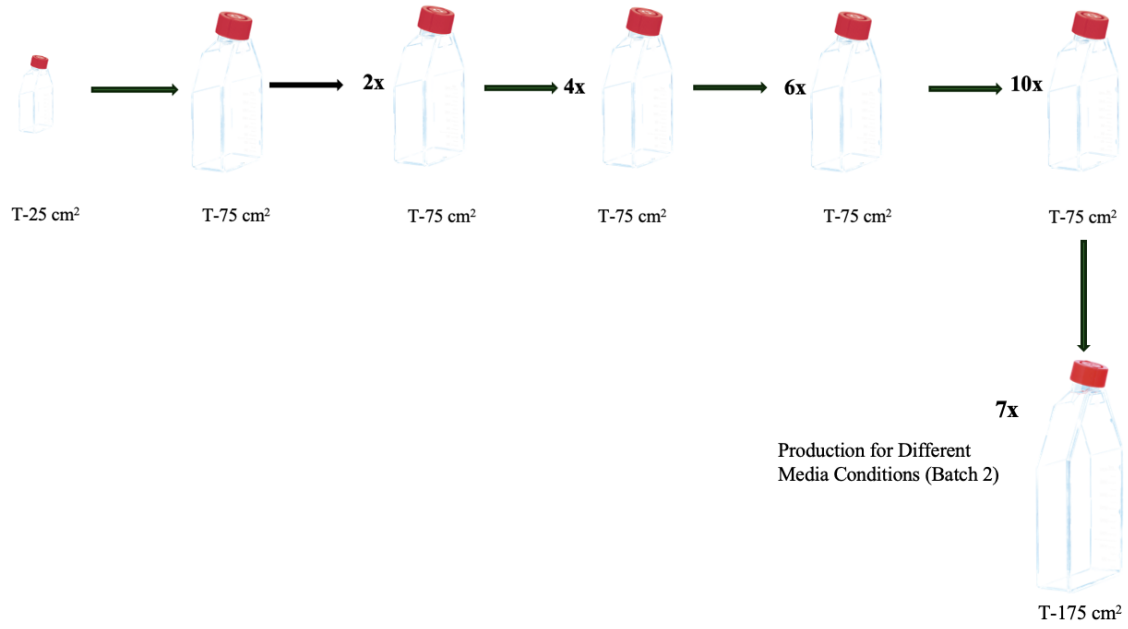


Figure 31: Expansion of CHO-DP12 Anti-IL-8 cell culture from T-25 cm^2 to ten T-175 cm^2 adherent flasks for Batch 2 of media studies.

All media formulations were supplemented with 1% HEPES, 1% penicillin-streptomycin and 1% FBS, depending upon the experimental condition. The flasks were kept in production for 10 days at standard incubation conditions, 37 °C, 5% CO_2.

Table 12: Batch 2 of different media conditions tested for CHO-DP12 Anti-IL-8 mAb production, showing variations in base medium and supplementation.

Media Condition	Base Medium	Supplements	Serum Type	Initial Glucose Concentration (mmol)
1	Ex-Cell CD CHO	-	None	30
2	RPMI		FBS	11
3	RPMI	AA, L-glutamine	None	11
4	DMEM	-	FBS	25
5	DMEM	AA, L-glutamine	None	25

6	McCoys	-	FBS	16
7	McCoys	AA, L-glutamine	None	16

Glucose Consumption

Glucose levels were measured over a 10-day production period and compared with different media conditions for glucose intake. **Figure 32** shows the glucose concentrations in mmol for the 7 media conditions (M1-M7) used in Batch 2.

To prevent nutrient limitation, cultures were restored to their initial glucose levels on Days 2, 6 and 8. Glucose levels declined steadily till Day 10, indicating continuous nutrient uptake.

Media conditions M1 (Ex-cell CD CHO) and M4 (DMEM + 1% FBS), which are considered to be ideal media samples for CHO DP12 cells, demonstrated the highest glucose consumption.

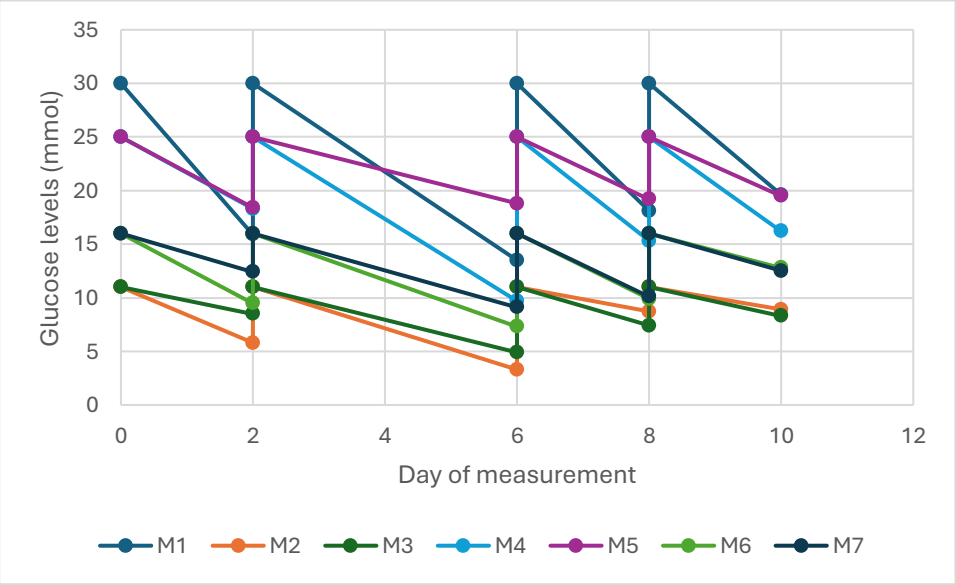


Figure 32: Glucose consumption profiles for Batch 2 of the different media study of CHO-DP12 Anti-IL-8 cell culture. Glucose levels were measured across seven media conditions (M1-M7); n=1 per condition.

Purification

The conditioned media samples were purified similarly to those in Batch 1 using FPLC and a 1 mL Protein G column. 60 mL of each filtered supernatant sample was loaded into the

system for purification. A total of 6 eluted fractions were collected for each media condition, and protein concentration was measured via Nanodrop Spectrophotometry at 280 nm, as shown in **Figure 33**.

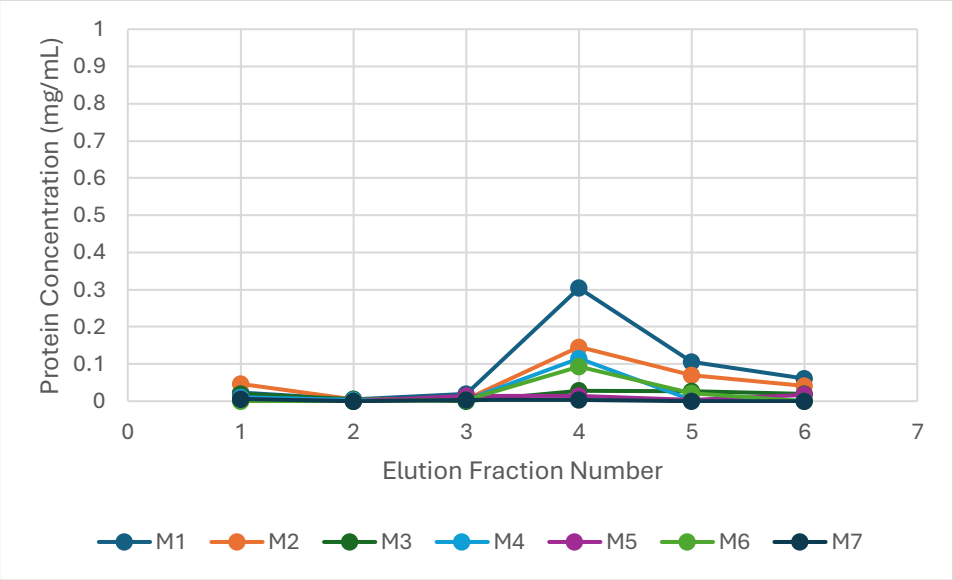


Figure 33: Protein concentrations of eluted fractions from Batch 2 media studies (M1-M7) of CHO-DP12 Anti-IL-8 mAbs as measured by Nanodrop spectrophotometry at 280 nm; n=1 per condition.

Table 13: Calculated titre values from Batch 2 of the media study of CHO DP12 Anti-IL-8 mAbs.

Media Condition (Batch 2)	Total Protein Recovered (mg)	Titre (mg/mL)
M1	0.6228	0.0062
M2	0.3768	0.0038
M3	0.12	0.0012
M4	0.16596	0.0017
M5	0.0648	0.00065
M6	0.1404	0.0014
M7	0.0168	0.00017

4.1.4 Cell Density Assessment

Batch 1

Cell Culture

CHO DP12 cells at passage 15 were put into the production phase in six different T-175 flasks, each containing 100 mL of Ex-Cell CD CHO serum-free medium, with the following seeding cell densities (CD1-CD6).

1. $2x10^5$ cells/mL
2. $4x10^5$ cells/mL
3. $6x10^5$ cells/mL
4. $8x10^5$ cells/mL
5. $10x10^5$ cells/mL
6. $12x10^5$ cells/mL

Throughout the 10-day production period, cell viability and glucose consumption were monitored at regular intervals to compare the cell growth and metabolic activity between different seeding densities.

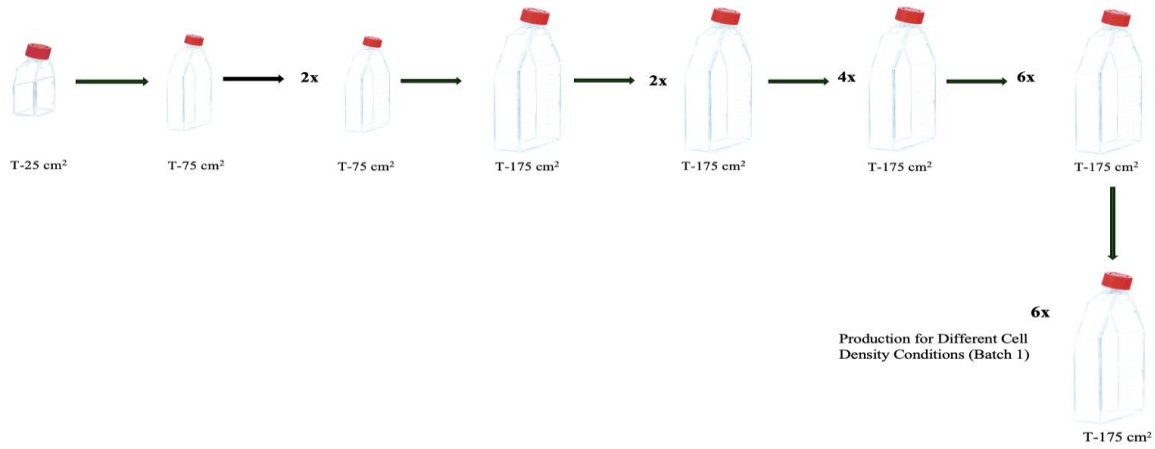


Figure 34: Expansion of CHO-DP12 Anti-IL-8 cell culture from T-25 cm^2 to T-175 cm^2 adherent flasks for Batch 1 of the different cell density study.

Glucose Consumption

All cultures were initiated in Ex-Cell CD CHO medium with an initial glucose concentration of 30 mmol. **Figure 35** shows the glucose concentrations over time for each cell density, indicating a gradual decrease over time across all seeding densities. Glucose was replenished on Days 4 and 8 to restore initial concentrations. By Day 12, glucose levels had stabilised across all conditions as cultures approached the stationary phase. The higher seeding densities exhibited a faster decline in glucose levels compared to lower densities, highlighting the relationship between initial cell density and nutrient consumption rate.

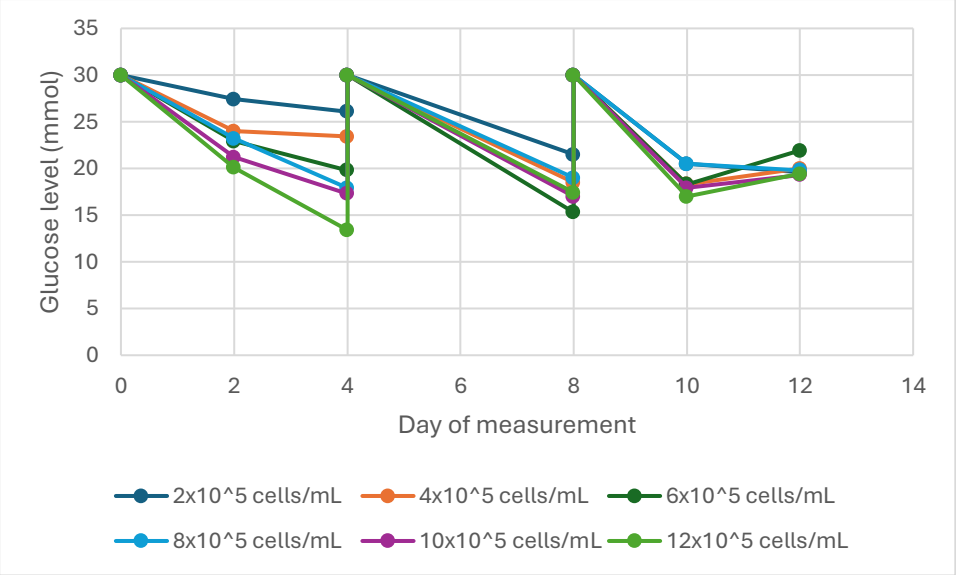


Figure 35: Glucose consumption profiles for Batch 1 of the different cell density study of CHO-DP12 Anti-IL-8 cell culture. Glucose levels were measured across six cell density conditions; n=1 per condition.

Cell Viability

Figure 36 represents the cell viability percentage across all cell densities. CD3 and CD6 consistently maintained high viability throughout the production period. In contrast, CD1 and CD2 showed a notable dip in cell viability around Day 4 and Day 8, respectively. Higher densities demonstrated better glucose utilisation and consistency in cell viability, compared to lower densities. The trends observed will be further correlated with protein yield in the next sections.

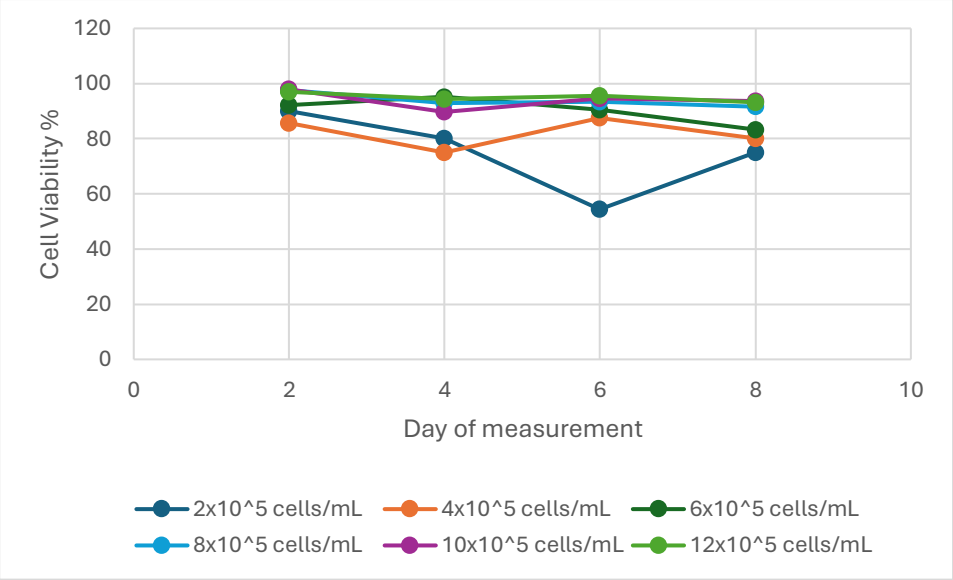


Figure 36: Cell viability percentages for Batch 1 of the different cell density study of CHO-DP12 Anti-IL-8 cell culture. Cell viability was calculated as the average of two haemocytometer counting chambers; n=1 per condition.

Purification

The conditioned media samples for Batch 1 of different cell densities experiments were purified using FPLC and a 1 mL Protein G column. For each condition, 80 mL of filtered supernatant was loaded into the system for purification. A total of 6 eluted fractions were collected for each density condition, and protein concentration was measured via Nanodrop Spectrophotometry at 280 nm, as shown in **Figure 37.**

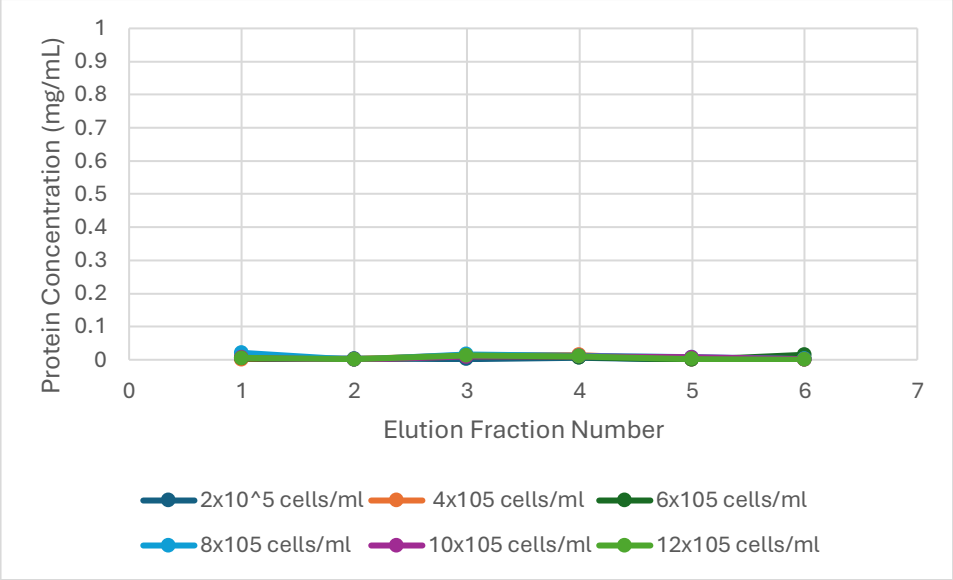


Figure 37: Protein concentrations of eluted fractions from Batch 1 cell density study of CHO-DP12 Anti-IL-8 mAbs as measured by Nanodrop spectrophotometry at 280 nm; n=1 per condition. The y-axis scale reflects the very low concentration range, as all readings were zero or close to zero.

Table 14: Calculated titre values from Batch 1 for the cell density study of CHO DP12 Anti-IL-8 mAbs.

Cell Density Condition (Batch 1)	Total Protein Mass Recovered (mg)	Culture Volume (mL)	Titre (mg/mL)
CD1 ($2x10^5$ cells/mL)	0.018	100	0.00018
CD2 ($4x10^5$ cells/mL)	0.0336	100	0.00034
CD3 ($6x10^5$ cells/mL)	0.0432	100	0.00043
CD4 ($8x10^5$ cells/mL)	0.0684	100	0.00068
CD5 ($10x10^5$ cells/mL)	0.0396	100	0.00040
CD6 ($12x10^5$ cells/mL)	0.0372	100	0.00037

All experimental cell densities consistently showed minimal protein concentration, with no variation among different seeding conditions. The maximum protein yield observed was 0.03 mg/mL, indicating low or no antibody expression at all in this batch. These findings suggest that varying initial seeding density did not impact antibody yield, and no detectable anti-IL-8 monoclonal antibodies were produced in this batch.

Batch 2

Cell Culture

CHO DP12 cells at passage 15 were put into the production phase in seven different T-175 flasks, each containing 100 mL of Ex-Cell CD CHO serum-free medium, with the following seeding cell densities (CD1-CD7).

1. $2x10^5$ cells/mL
2. $4x10^5$ cells/mL
3. $6x10^5$ cells/mL
4. $8x10^5$ cells/mL
5. $10x10^5$ cells/mL
6. $12x10^5$ cells/mL
7. $14x10^5$ cells/mL

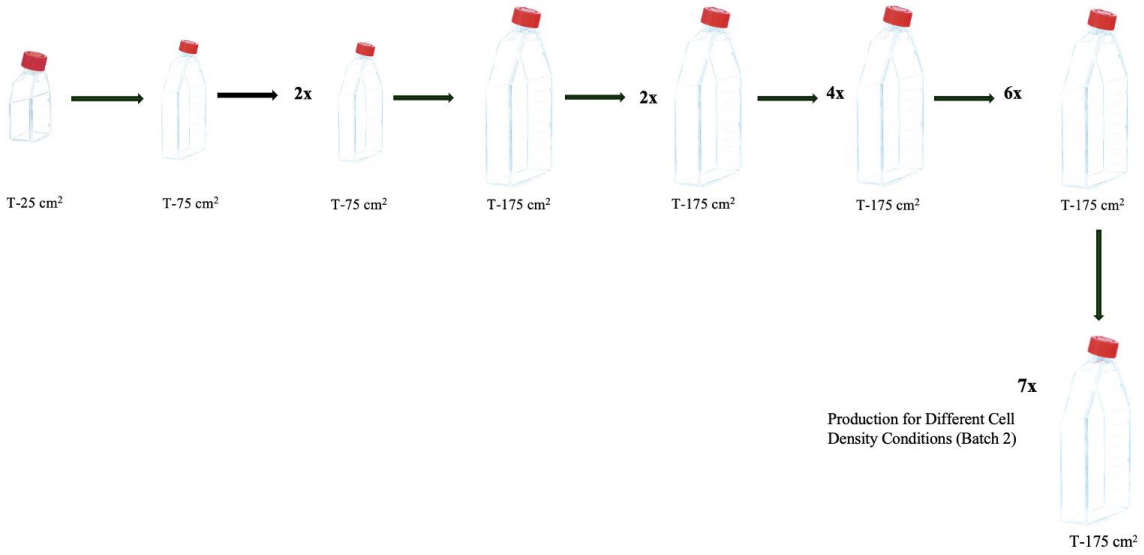


Figure 38: Expansion of CHO-DP12 Anti-IL-8 cell culture T-25 cm^2 to T-175 cm^2 adherent flasks for Batch 2 of the different cell density study.

Glucose Consumption

Figure 39 illustrates the glucose consumption of CHO DP12 cells seeded at seven different cell densities (CD1-CD7) from Day 0 to Day 7 during the production period. All conditions were in Ex-Cell CD CHO medium with an initial glucose level of 30 mmol. Glucose levels declined steadily from Day 0 to Day 3, and cultures were refed with glucose on Day 3 to restore glucose concentrations. Following this, glucose levels decreased progressively and

began to stabilise by Day 7. Similar to Batch 1, the higher seeding densities exhibited higher glucose consumption as compared to lower seeding densities.

No cell viability data were collected for this batch; therefore, comparative interpretation is limited to glucose consumption alone during the production phase.

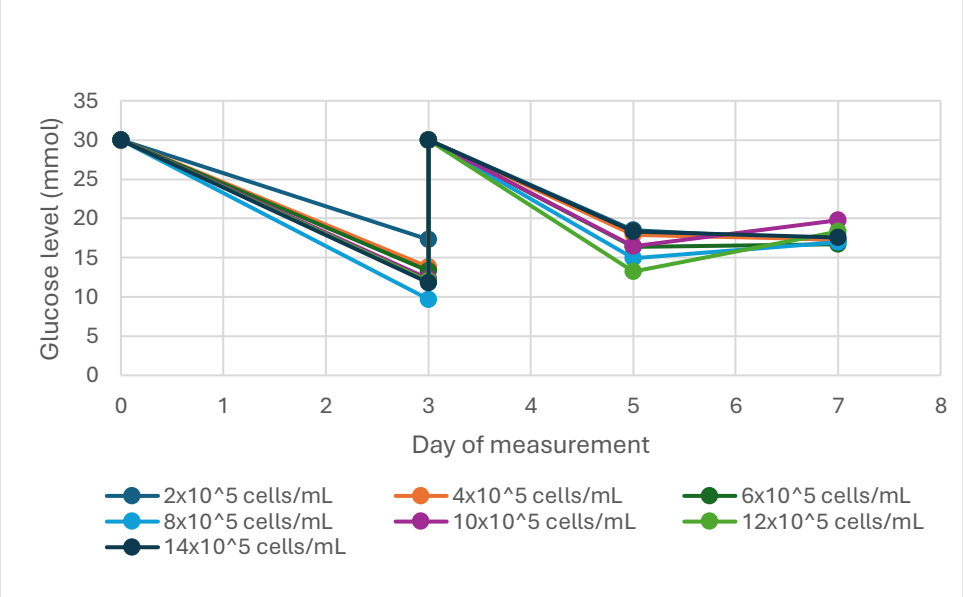


Figure 39: Glucose consumption profiles for Batch 2 of the different cell density study of CHO-DP12 Anti-IL-8 cell culture. Glucose levels were measured across seven cell density conditions; n=1 per condition.

Purification

The filtered supernatants were purified in the FPLC, using a 1 mL Protein G column. For each condition, 80 mL was loaded into the column for purification. The six eluted fractions were then analysed for protein concentration across all samples, using Nanodrop spectrophotometry at 280 nm, as shown in **Figure 40**.

All conditions showed very low protein concentrations, indicating minimal antibody production. These results indicated that despite being grown in ideal medium at different cell densities and measurable glucose uptake, there was no significant protein expressed in Batch 2, similar to the findings of Batch 1.

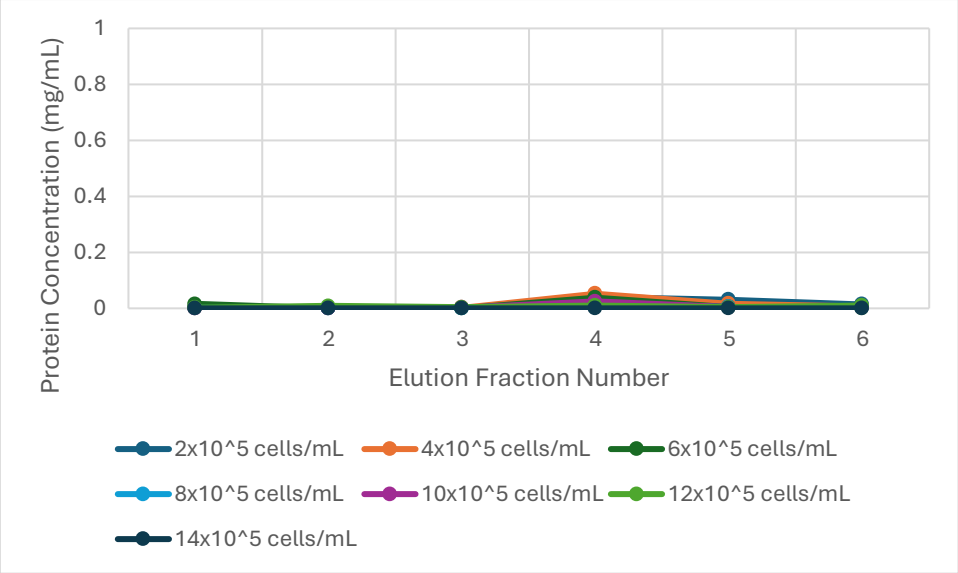


Figure 40: Protein concentrations of eluted fractions from Batch 2 cell density study of CHO-DP12 Anti-IL-8 mAbs as measured by Nanodrop spectrophotometry at 280 nm; n=1 per condition. The y-axis scale reflects the very low concentration range, as all readings were zero or close to zero.

Table 15: Calculated titre values for Batch 2 cell density study of CHO DP12 Anti-IL-8 mAbs.

Cell Density Condition (Batch 2)	Total Protein Mass Recovered (mg)	Culture Volume (mL)	Titre (mg/mL)
CD1 ($2x10^5$ cells/mL)	0.1044	100	0.0010
CD2 ($4x10^5$ cells/mL)	0.0972	100	0.00097
CD3 ($6x10^5$ cells/mL)	0.0708	100	0.00071
CD4 ($8x10^5$ cells/mL)	0.0372	100	0.00037
CD5 ($10x10^5$ cells/mL)	0.042	100	0.00042
CD6 ($12x10^5$ cells/mL)	0.0456	100	0.00046
CD7 ($14x10^5$ cells/mL)	0	100	0

Batch 3

Cell Culture

A third round of cell density study was conducted using a fresh vial of CHO DP12 cells to further explore the impact of cell seeding densities on antibody production in Gibco CD CHO medium, supplemented with 100 x Hypoxanthine-Thymidine (HT) solution. The cells were adapted to low serum conditions before production to reduce cellular stress and improve transition into serum-free conditions. Specifically, cells were gradually adapted from 10% FBS DMEM medium to 2.5% FBS DMEM. They were expanded to five T-175 flasks for 4

days. For this batch, each condition was set up using five petri dishes containing 50 mL medium each, resulting in 250 mL total volume per density condition. The four tested seeding cell densities were as follows (CD1-CD4):

1. $2x10^5$ cells/mL
2. $3x10^5$ cells/mL
3. $4x10^5$ cells/mL
4. $5x10^5$ cells/mL

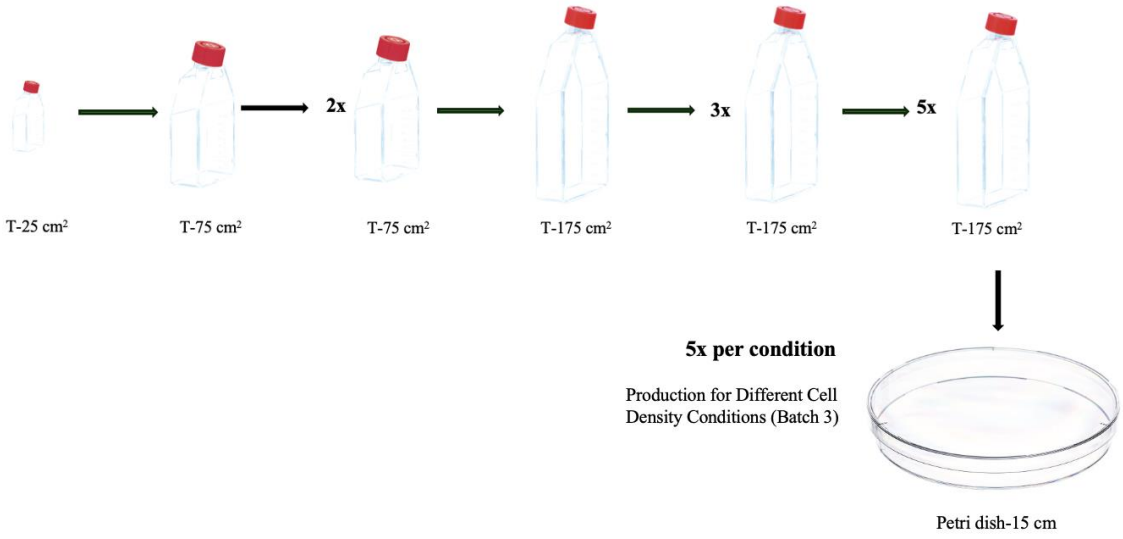


Figure 41: Expansion of CHO-DP12 Anti-IL-8 cell culture from T-25cm² to T-175cm² adherent flasks and 15 cm petri dishes for Batch 3 of the different cell density study.

Glucose consumption and cell viability percentage were monitored throughout the 10-day production phase to evaluate metabolic activity and cell health conditions. One of the petri dishes of CD4 had microbial contamination, which resulted in the loss of 50 mL of conditioned media.

Glucose Consumption

Figure 42 shows the glucose concentrations across the four different cell density conditions (CD1-CD4) during the production phase in Gibco CD CHO medium with initial value of 30 mmol. All conditions exhibited a sharp decline in glucose levels on Day 4, with the higher

cell density conditions (CD 3 and CD 4) being refed. Post that, glucose levels were stabilised by Day 8.

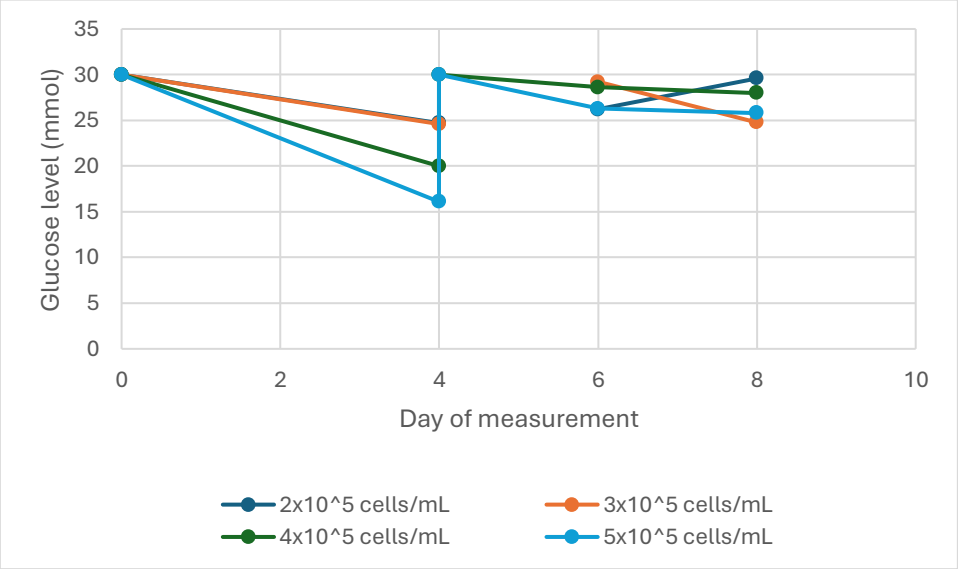


Figure 42: Glucose consumption profiles for Batch 3 of the different cell density study of CHO-DP12 Anti-IL-8 cell culture. Glucose levels were measured across four cell density conditions; n=1 per condition.

Cell Viability

The cell viability percentage was assessed across all four different seeding conditions on Days 4, 6 and 8 of the production phase, as presented in **Figure 43**. All conditions maintained relatively high cellular viability throughout the experiment, remaining above 70%. CD1 and CD2 displayed a steady increase in viability up to Day 6, followed by a slight decline around Day 8. In contrast, CD3 and CD4 started with higher initial viability on Day 4, experienced a drop on Day 6 and subsequently stabilised.

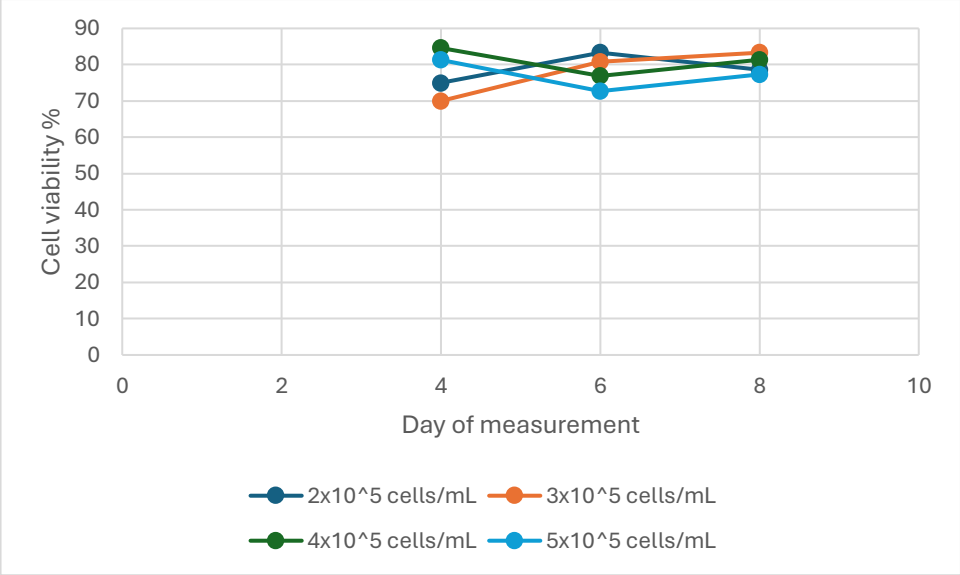


Figure 43: Cell viability percentages for Batch 3 of the different cell density study of CHO-DP12 Anti-IL-8 cell culture. Cell viability was calculated as the average of two haemocytometer counting chambers; n=1 per condition.

Purification

All four conditioned media were filtered and purified using FPLC and a 1 mL G protein column. For each condition, 180 mL was loaded into the column for purification. The six eluted fractions were then analysed for protein concentration across all samples, using Nanodrop spectrophotometry at 280 nm. As shown in **Figure 44**, negligible protein levels were detected across all four seeding densities (CD1- CD4).

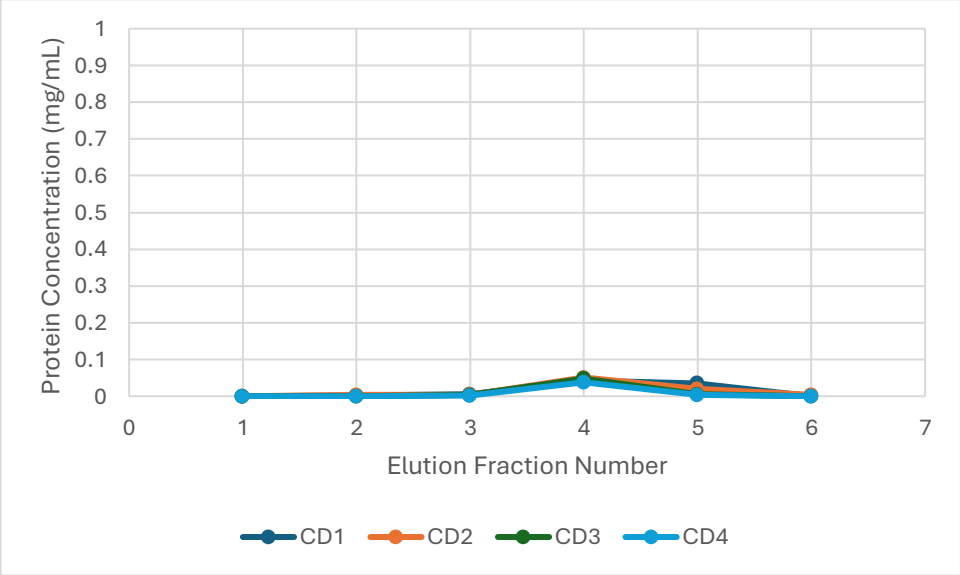


Figure 44: Protein concentrations of eluted fractions from Batch 3 cell density study of CHO-DP12 Anti-IL-8 mAbs as measured by Nanodrop spectrophotometry at 280 nm; n=1 per condition.

Table 16: Calculated titre values for Batch 3 cell density study of CHO DP12 Anti-IL-8 mAbs.

Cell Density Condition (Batch 2)	Total Protein Mass Recovered (mg)	Culture Volume (mL)	Titre (mg/mL)
CD1 ($2x10^5$ cells/mL)	0.1032	250	0.00041
CD2 ($3x10^5$ cells/mL)	0.0972	250	0.00039
CD3 ($4x10^5$ cells/mL)	0.0672	250	0.00027
CD4 ($5x10^5$ cells/mL)	0.0516	250	0.00021

Despite metabolic activity and high cell viability across all different seeding conditions during the production phase, no significant antibody expression was detected in any of the three cell density study batches. This consistent absence of detectable protein across multiple experiments strongly indicated a lack of protein expression by the CHO DP12 Anti-IL-8 cells.

4.2 Anti-IL-8 mAb Stability Study

A stability study was performed to assess the effects of varying temperature conditions for defined time periods on anti-IL-8 monoclonal antibodies produced in Independent Batch 1. All antibody samples were dialysed into a sucrose-histidine buffer at pH 6.0. The defined temperature conditions included -20°C, 4°C, 25°C and 40°C, over different time points from four days to two months. The samples taken at each time point were analysed using SDS-PAGE under reducing conditions to check for degradation over time, as detailed below.

4.2.1 Stability of Anti-IL-8 mAbs at -20°C

The first temperature condition assessed was -20°C which corresponds to a potential storage temperature used when formulations exhibit a high frozen glass transition temperature (Tg') e.g. greater than -20°C. This allows for use of -20°C freezers and shipping which can be cheaper and more favourable than -80°C storage and shipping. While technically frozen, amorphous components in the formulation (sucrose, mAb) may be in mobile rubber phase and prone to degradation, hence this temperature was assessed.

The SDS PAGE gel shows consistent bands at expected molecular weights, 50kDa for heavy chains and ~20kDa for lighter chains. Unexpectedly, strong bands were visible at 130 kDa, suggesting incomplete reduction of sample or an inherent level of aggregates. Over time, several faint, lower molecular weight bands were observed at 120 kDa, 100 kDa, suggesting aggregation or potential degradation of band at 130 kDa, which reduced in intensity. In particular, there was a time-dependent increase in the 100 kDa band, which could correspond to dimerization of the heavy chain band. Faint bands that may represent fragments were observed at 25 kDa and 35 kDa, which were again time dependent, indicative of degradation. At two months, a relatively weak fragment was observed at ~10kDa,

indicating fragmentation. In contrast, the -80°C control maintained a clearer and more stable band profile.

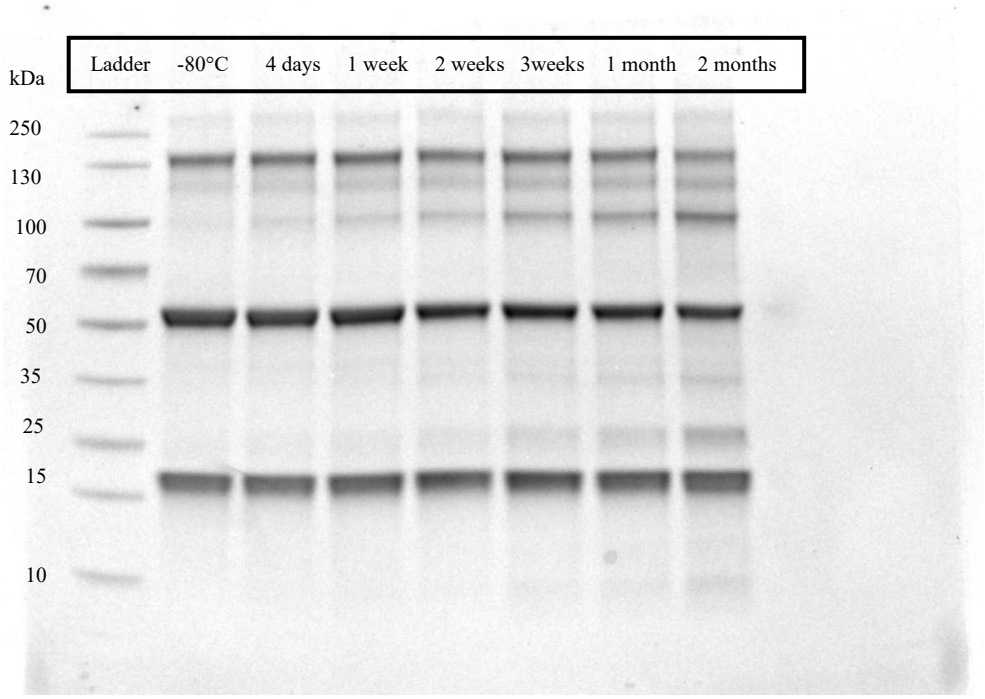


Figure 45: SDS-PAGE of anti-IL-8 mAb stored at -20°C for stability study.

4.2.2 Stability of Anti-IL-8 mAbs at 4°C

In this arm, samples were kept at 4°C, which is typical of storage conditions for mAbs formulated as commercial therapeutics in solution. The samples were analysed using SDS-PAGE and their bands were compared to a control stored at -80°C. Distinct bands were seen around 50 kDa and ~20 kDa as expected of intact, monomeric mAbs. Light smearing and subtle changes in band sharpness began to appear around 2 weeks at 100 and 120 kDa, suggestive of aggregation or degradation of 130 kDa band similar to samples at -20°C. However, degradation with time is reduced as compared to -20°C samples and relative to -80°C control.

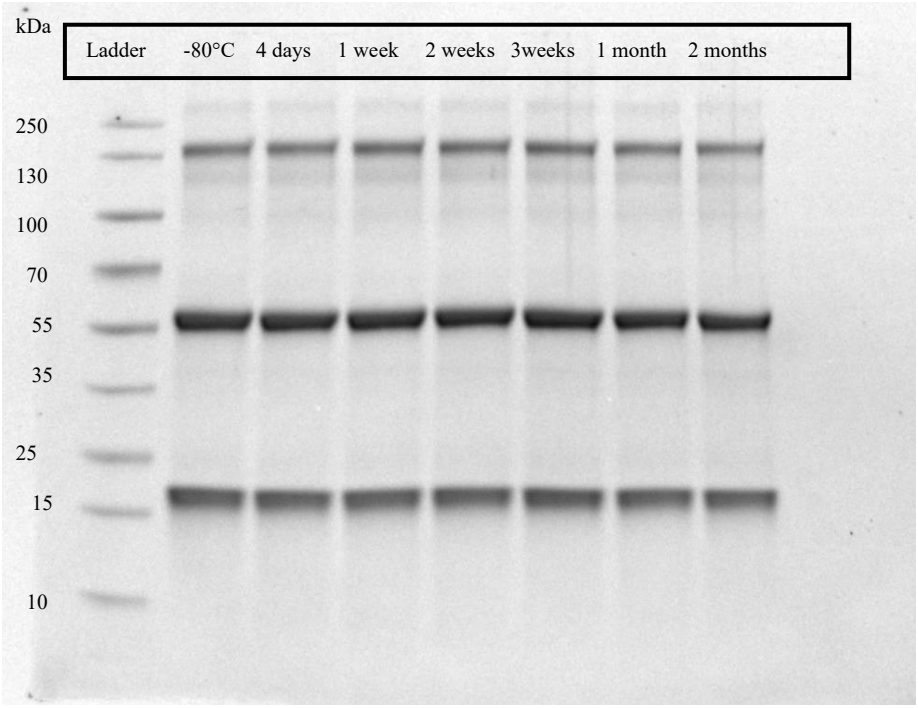


Figure 46: SDS-PAGE of anti-IL-8 mAb stored at 4°C for stability study.

4.2.3 Stability of Anti-IL-8 mAbs at 25°C

The accelerated stability of anti-IL-8 monoclonal antibodies produced in Batch 1 was assessed by storing at 25°C for up to two months and analysed using SDS-PAGE, as seen in **Figure 47**. The gel showed consistent heavy (50 kDa) and light (25 kDa) bands across all time points as expected as well as the unexpected band at 130 kDa observed at all timepoints and all stability conditions. Minor bands were observed towards the end of 2 months again at 100 and 130 kDa, representative of aggregation.

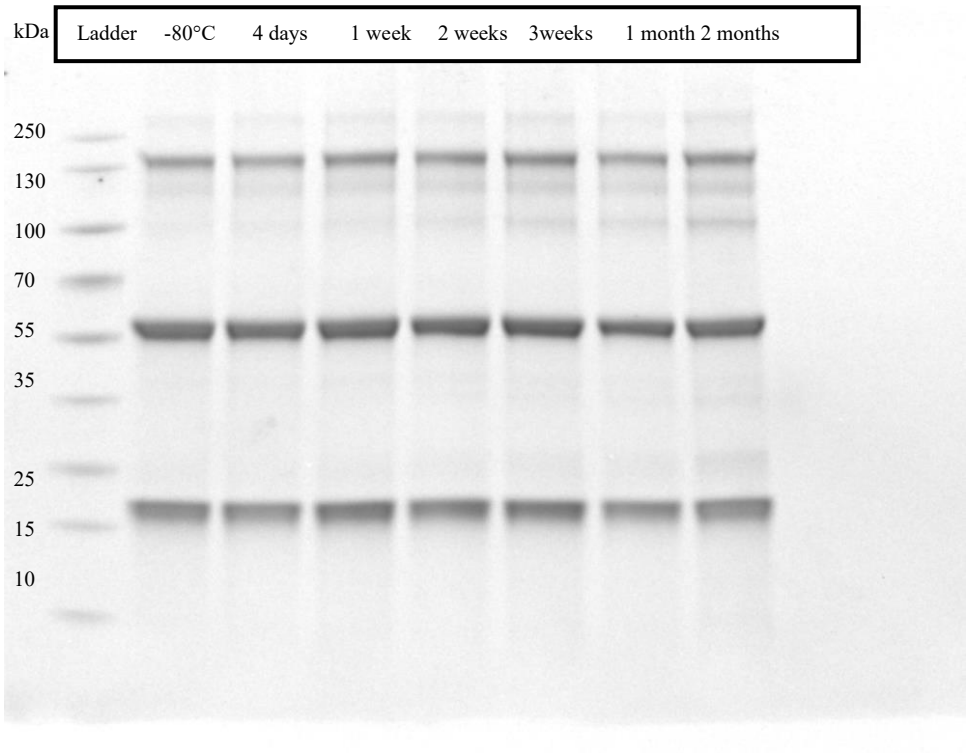


Figure 47: SDS-PAGE of anti-IL-8 mAb stored at 25°C for stability study.

4.2.4 Stability of Anti-IL-8 mAbs at 40°C

The stress stability of anti-IL-8 monoclonal antibodies produced in Batch 1 was assessed by storing them at 40°C for up to two months and analysed using SDS-PAGE, as seen in **Figure 48**. At 40°C, the heavy (50kDa) and light (25kDa) bands were consistently detected across all time points. The bands appeared slightly less intense at later time points, suggesting minor protein degradation.

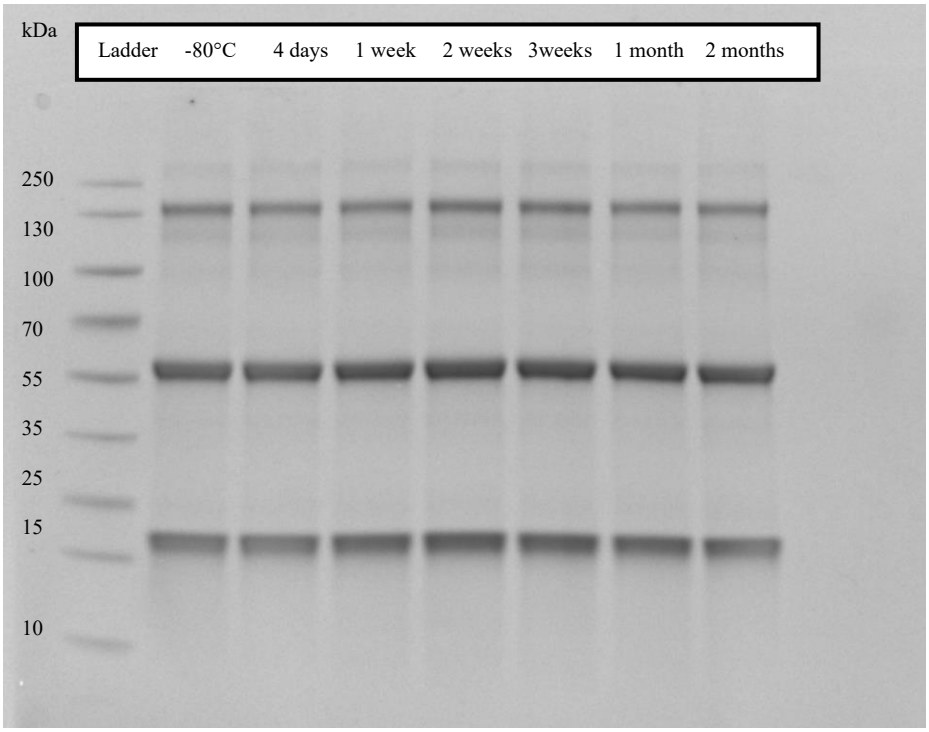


Figure 48: SDS-PAGE of anti-IL-8 mAb stored at 40°C for stability study.

5. Results - cNIST mAb Cell Culture

5.1 Batch 1

Cell Culture

To evaluate the impact of seeding density on cNIST mAb production, CHO NIST cells were cultured under four different initial cell density conditions. The cells were put into production at passage 15 in T-175 flasks containing 100 mL of Gibco CD CHO medium per flask and maintained under standard incubation conditions (37 °C, 5% CO_2) throughout the 10-day production period. The four seeding densities tested were as follows (CD1-CD4):

1. 2×10^5 cells/mL
2. 4×10^5 cells/mL
3. 6×10^5 cells/mL
4. 8×10^5 cells/mL

Cell growth, viability and glucose consumption were monitored regularly, and the harvested supernatant was processed for purification using FPLC and protein quantification via Nanodrop spectrophotometry.

Glucose Consumption

Glucose levels were monitored throughout the production phase to assess the metabolic activity of CHO NIST cells under different seeding densities. The initial glucose level of Gibco CD CHO medium was 30 mmol. As shown in **Figure 49**, glucose levels decreased steadily from Day 0 to Day 3 across all four conditions. Hence, all samples were fed with glucose to reach the initial glucose concentration. CD4, containing the highest cell number, showed the maximum amount of glucose consumed. Nutrient intake after Day 5 plateaued till

Day 10. Overall, the higher density conditions CD3 and CD4 utilised more glucose levels according to the demand of cell numbers.

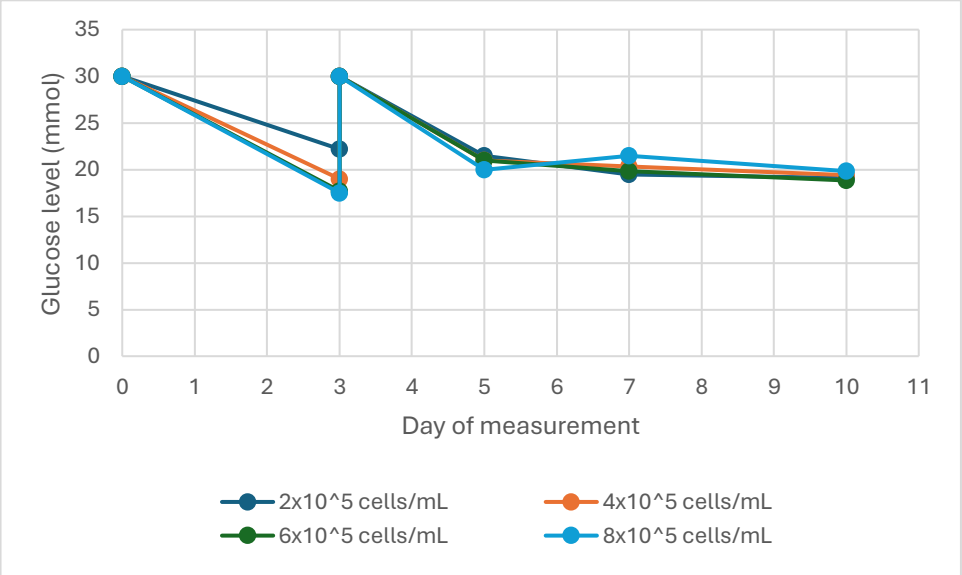


Figure 49: Glucose consumption profiles for Batch 1 of the different cell density study (CD1-CD4) in CHO-NIST cell culture; n=1 per condition.

Cell Viability

Cell viability percentage analysis was carried out for all four different cell density conditions on Days 3, 5 and 7 as shown in **Figure 50**. Viability of CD1 peaked at Day 5 with 43.5% and CD2 with 45% on Day 3, which was followed by a dip on Day 7. In contrast, the higher density conditions CD3 and CD4 demonstrated lower viability, with CD4 dropping below 20% by Day 7. Overall, the lower density conditions (CD1 and CD2) maintained higher viability compared to the higher density conditions (CD3 and CD4) over the week.

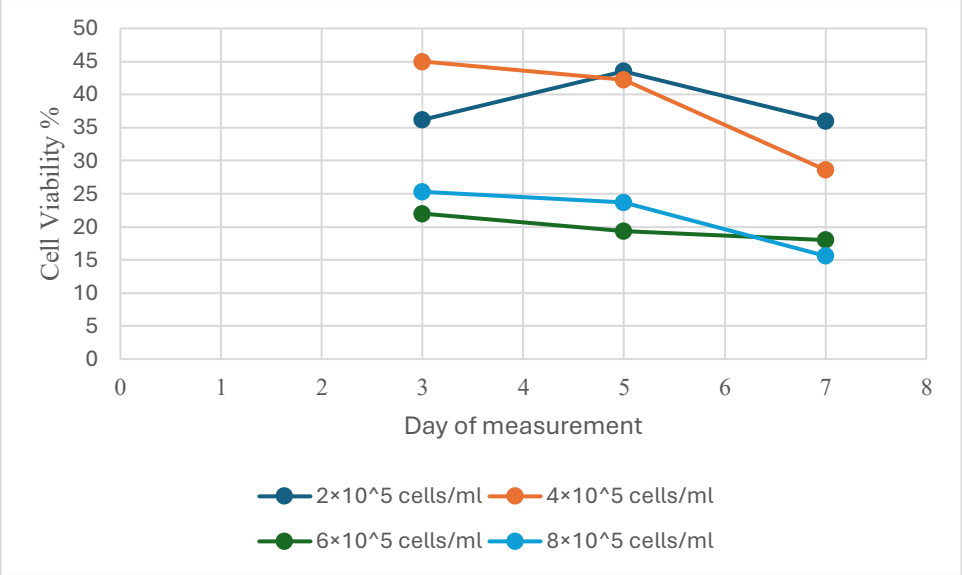


Figure 50: Cell viability percentages for Batch 1 of the different cell density study (CD1-CD4) of CHO-NIST cell culture; n=1 per condition.

Purification

The conditioned media from all four cultures were filtered and purified using FPLC and a 1 mL G protein column. For each experimental condition, 80 mL was loaded into the column for purification. The resulting six elution fractions were then analysed for protein concentration across all samples. As shown in **Figure 51**, the majority of protein was detected in fraction 4 across all conditions, with residual levels in fraction 5. The highest antibody concentration was obtained in the lowest cell density condition (CD 1) with 2×10^5 cells/mL, reaching ~0.027 mg/mL. With increasing seeding density (CD2-CD4), the protein yield progressively declined. This trend demonstrated that higher initial cell densities were associated with reduced mAb production under tested conditions.

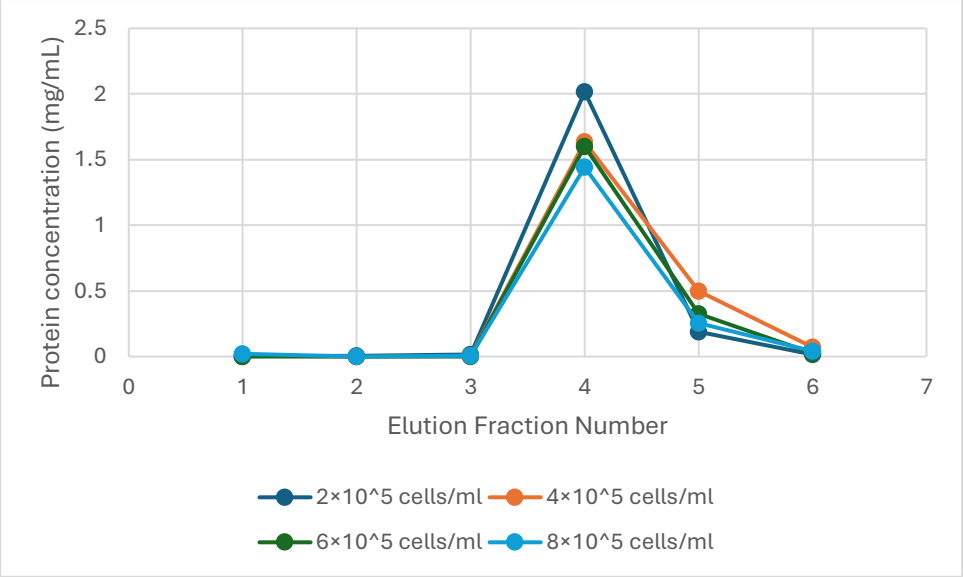


Figure 51: Protein concentrations of eluted fractions from Batch 1 cell density study for cNIST mAbs as measured by Nanodrop spectrophotometry at 280 nm; n=1 per condition.

Table 17: Calculated titre values for Batch 1 cell density study of cNIST mAbs.

Cell Density Condition (Batch 1)	Total Protein Mass Recovered (mg)	Culture Volume (mL)	Titre (mg/mL)
CD1 ($2x10^5$ cells/mL)	2.6952	100	0.027
CD2 ($4x10^5$ cells/mL)	2.6544	100	0.027
CD3 ($6x10^5$ cells/mL)	2.3484	100	0.023
CD4 ($8x10^5$ cells/mL)	2.1168	100	0.021

5.2 Batch 2

Cell Culture

To evaluate the impact of seeding density on cNIST mAb production, CHO NIST cells were cultured under four different initial cell density conditions. The cells were put into production at passage 18 in T-175 flasks containing 100 mL of Gibco CD CHO medium per flask and maintained under standard incubation conditions (37 °C, 5% CO_2) throughout the 10-day production period. The four seeding densities tested were as follows (CD1-CD4):

1. 2×10^5 cells/mL
2. 4×10^5 cells/mL
3. 6×10^5 cells/mL
4. 8×10^5 cells/mL

Cell growth, viability and glucose consumption were monitored regularly, and the harvested supernatant was processed for purification using FPLC, and protein quantification via Nanodrop spectrophotometry.

Glucose consumption

Glucose levels of all four seeding density samples were measured across the 10-day production period, as shown in **Figure 52**. The lowest cell density, CD1 (2×10^5 cells/mL), exhibited a major decline in glucose concentration on Day 3. All conditions were refed glucose on Day 3 and restored the glucose concentration to 30 mmol. Other conditions also indicated active metabolism and nutrient intake of cNIST cells. By Day 10, the levels had plateaued, and the media was collected for filtration.

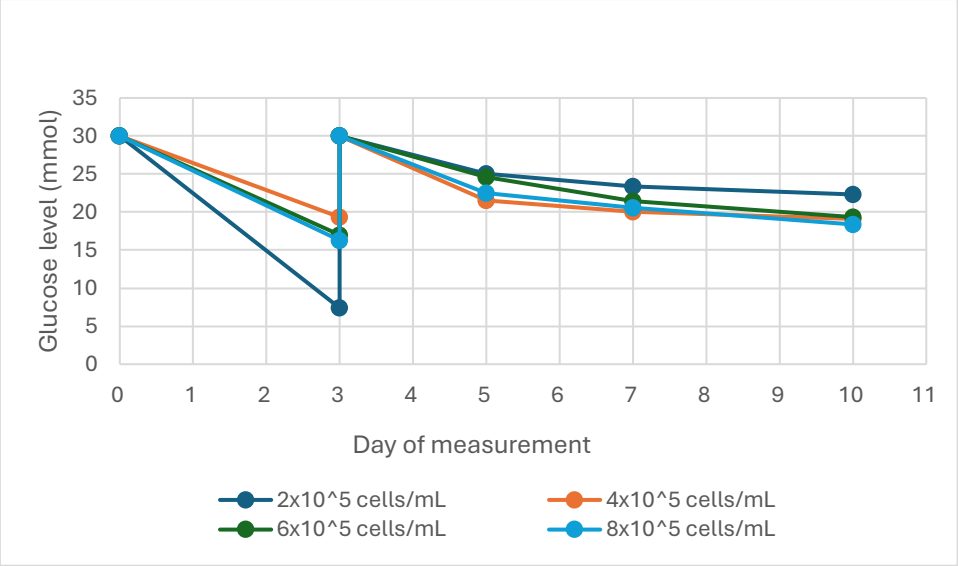


Figure 52: Glucose consumption profiles for Batch 2 of the different cell density study (CD1-CD4) of CHO-NIST cell culture; n=1 per condition.

Cell Viability

The cell viability profile was monitored regularly during the production phase, as displayed in **Figure 53**. The lower cell density conditions CD1 and CD2, with 2×10^5 cells/mL and 4×10^5 cells/mL, respectively, showed the highest viability percentage on Day 3 in the range of 70%. In contrast, the higher cell densities of CD3 and CD4, seeded at 6×10^5 cells/mL and 8×10^5 cells/mL, resulted in fewer viable cells. By Day 5, viability had declined across all conditions and reached the lowest values on Day 7.

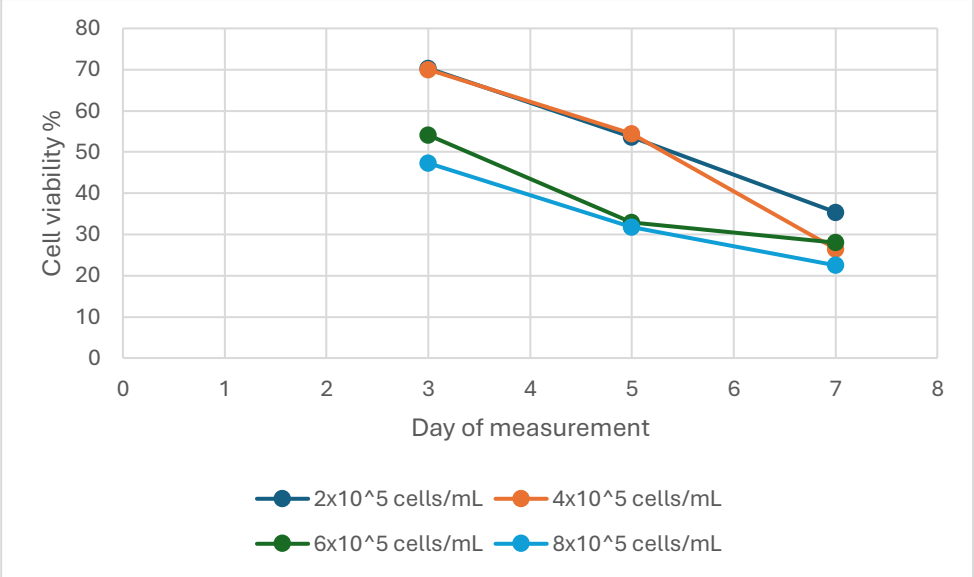


Figure 53: Cell viability percentages for Batch 2 of the different cell density study (CD1-CD4) of CHO-NIST cell culture; n=1 per condition.

Purification

The conditioned media from all samples were filtered through a 0.22 µm membrane and purified using the FPLC. As observed in **Figure 54** the antibody yield was the maximum in the lowest cell density condition (2×10^5 cells/mL) with 1.1 mg/mL. The trend was progressively decreasing with increasing cell densities, similar to Batch 1.

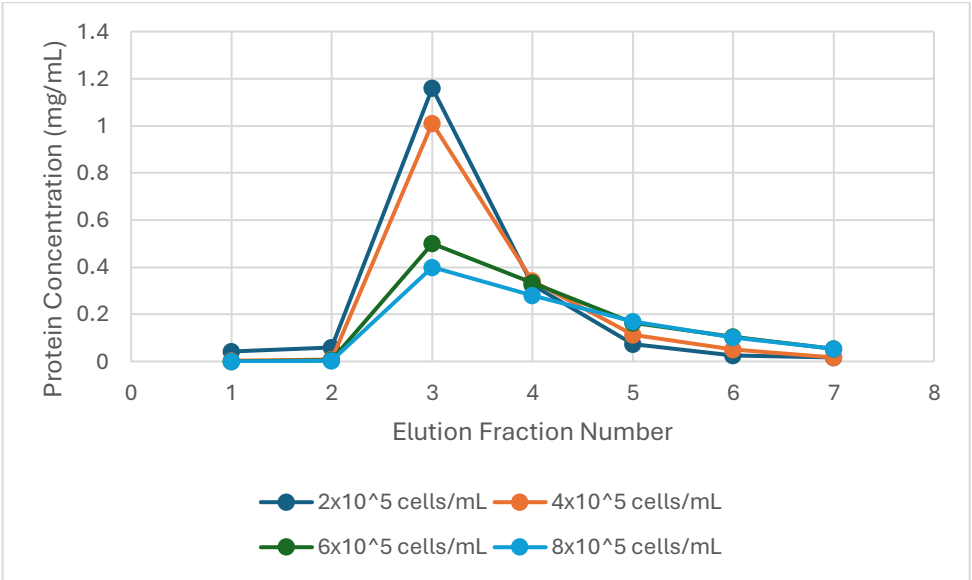


Figure 54: Protein concentrations of eluted fractions from Batch 2 cell density study for cNIST mAbs as measured by Nanodrop spectrophotometry at 280 nm; n=1 per condition.

Table 18: Calculated titre values for Batch 2 cell density study of cNIST mAbs.

Cell Density Condition (Batch 2)	Total Protein Mass Recovered (mg)	Culture Volume (mL)	Titre (mg/mL)
CD1 ($2x10^5$ cells/mL)	2.044	100	0.020
CD2 ($4x10^5$ cells/mL)	1.850	100	0.019
CD3 ($6x10^5$ cells/mL)	1.393	100	0.014
CD4 ($8x10^5$ cells/mL)	1.201	100	0.012

5.3 cNIST mAb Forced Degradation Study

A forced degradation study was performed to assess the effects of varying conditions for defined time periods on cNIST mAb monoclonal antibodies produced in Batch 1 of the cell density study. All antibody samples were dialysed into a sucrose-histidine buffer at pH 6.0 prior to study commencement. The defined stress conditions included extremes of temperature, pH, light, freeze-thaw and agitation. The samples taken at each time point were analysed using SDS-PAGE under reducing conditions to check for degradation over time as well as SEC-HPLC as an orthogonal means of antibody size analysis. The overall study negative control used was a sample that was stored at -80°C immediately post formulation, while within each arm, study-specific controls were used.

The cNIST mAb sample stored at -80°C served as the control condition for the forced degradation study. As shown in **Figure 55**, the size-exclusion chromatogram displayed a single and sharp peak at approximately 4.5 minutes retention time when analysed by software. This peak initially appeared to account for 100% of the area, corresponding to the monomeric form of the antibody. However, upon closer inspection, two additional peaks were present in the right-hand shoulder, indicating minor fragments at 4.7 and 5.0 minutes. These fragments represent 12% and 3.7% of the total area, respectively. Such fragments were not clearly visible in SDS-PAGE but may have been lost in the thick heavy chain band at ~50 kDa. Overall, the -80°C control sample demonstrated high stability, low aggregation and minimal fragmentation. This profile was used as the baseline reference for comparison with samples subjected to stress conditions.

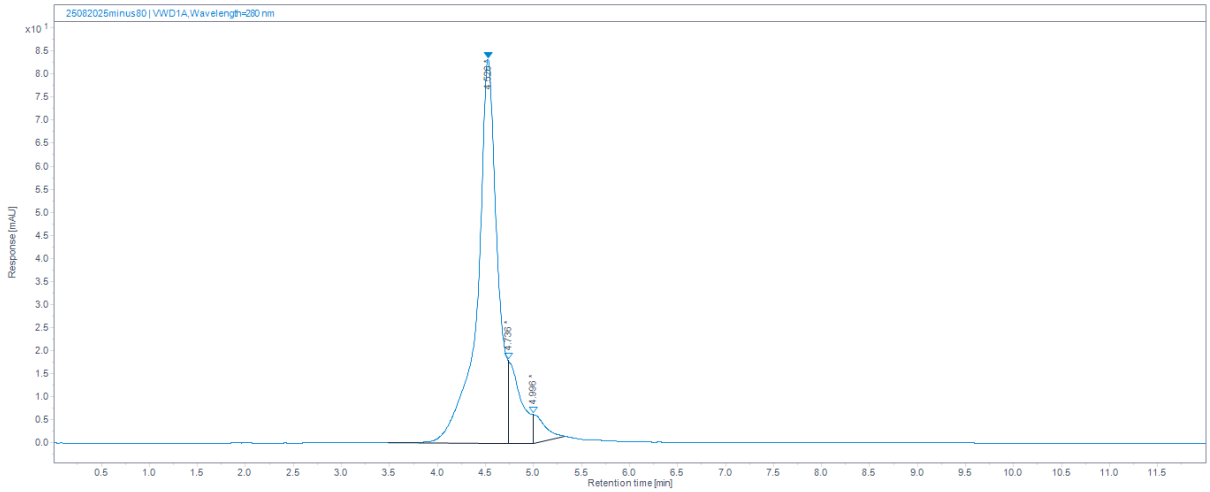


Figure 55: SEC-HPLC chromatogram of study control (-80°C) sample of cNIST mAb for forced degradation study, showing the main monomer at 4.5 minutes.

5.3.1 Temperature

For the temperature arm, the control sample was stored at 4°C for 2 weeks, while the test samples were incubated at 40°C for 1 week and 2 weeks. The 4°C sample displayed intact heavy and light chain bands comparable to the -80°C control, indicating stability under refrigerated conditions when assessed by SDS-PAGE. Faint bands were observed at ~35 and ~45 kDa, demonstrating fragmentation. In contrast, the 40°C samples showed visibly thinner bands compared to the 4°C control, with the 2-week sample appearing fainter than the 1-week sample. The progressive thinning of bands indicates degradation of the antibody over time at higher temperatures. In addition, light bands were observed at ~100 kDa after 1- and 2-weeks, indicating aggregation and at ~45 and ~35 kDa, demonstrating fragmentation.

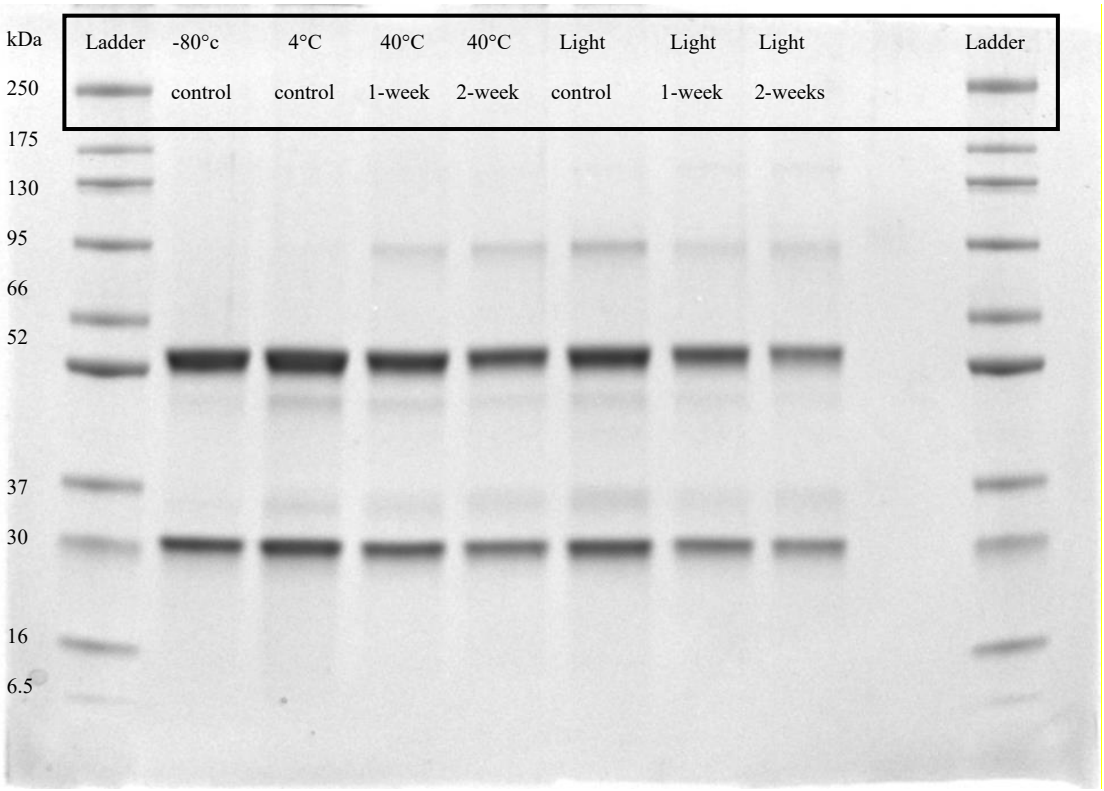


Figure 56: SDS-PAGE of cNIST mAbs subjected to forced degradation under temperature and light conditions. Temperature stability was assessed at 4°C (control) and 40°C for 1 and 2 weeks. Light exposure was measured up to 2 weeks, with a tin foil-wrapped serving as the light control. A -80°C sample was included as an overall stability reference.

The stability of cNIST mAb under different temperature conditions was assessed by SEC-HPLC. At 4°C (control), the monomer main peak demonstrated a decrease in area with a parallel increase in the smallest fragment area. This fragment area increased from 3.7% in the -80°C control to 12.7%, with a negligible increase in the larger fragment. This indicates that the antibody was partially unstable in the given liquid formulation even at 4°C.

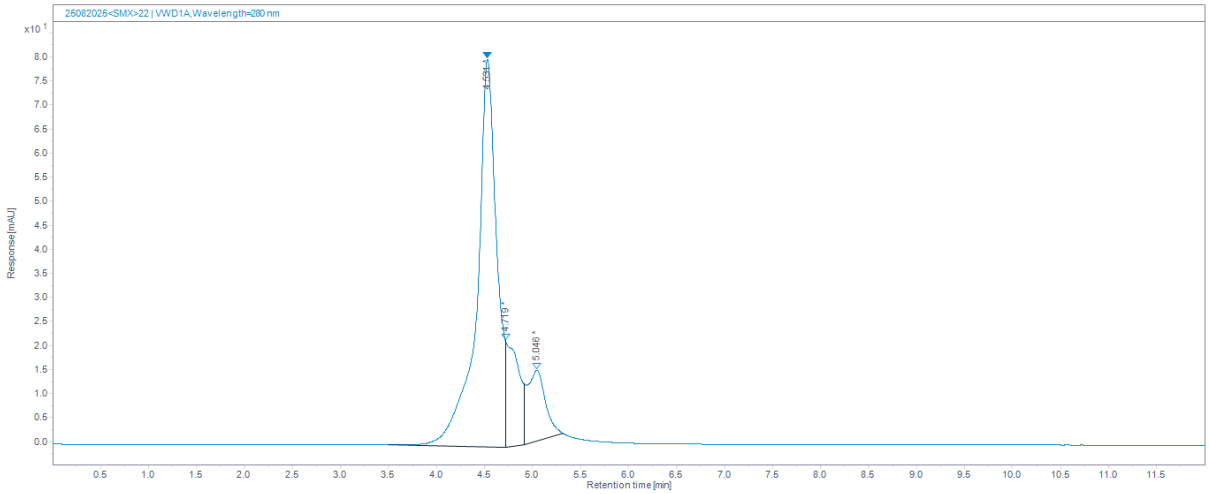


Figure 57: SEC-HPLC chromatogram of temperature control (4°C) sample of cNIST mAb for forced degradation study, showing the main monomer at 4.5 minutes.

At 40°C for 1 week, three peaks were detected: the monomer was reduced to 68.1% due to thermal stress-induced degradation. Two secondary species at 4.8 minutes (16.8%) and 5.0 minutes (15.1%), generating around 32% fragmentation, as seen in **Figure 58**.

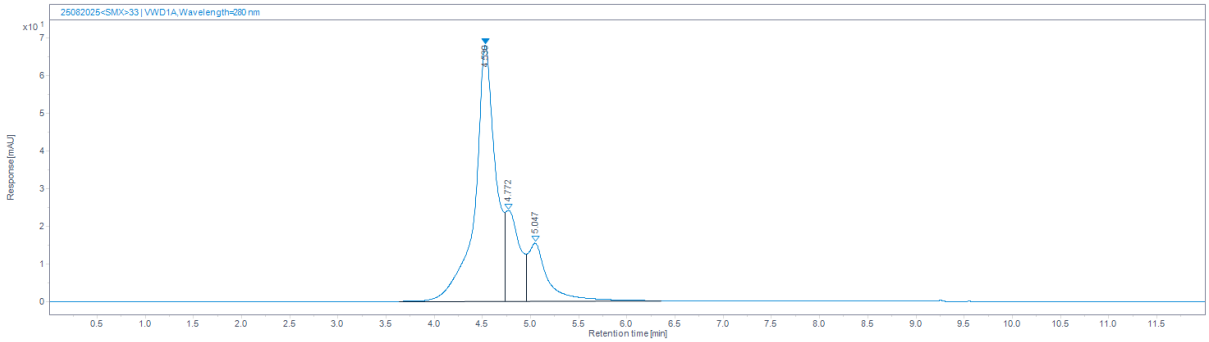


Figure 58: SEC-HPLC chromatogram of temperature (40°C, 1 week) sample of cNIST mAb for forced degradation study, showing the main monomer at 4.5 minutes.

At 40°C after 2 weeks, degradation became more evident. The monomer peak decreased to 48.0% of the total area while two secondary peaks at 4.7 minutes (42.2%) and 5.0 minutes (11.8%) were observed. These results indicate significant fragmentation and progressive destabilisation of the antibody during prolonged thermal stress.

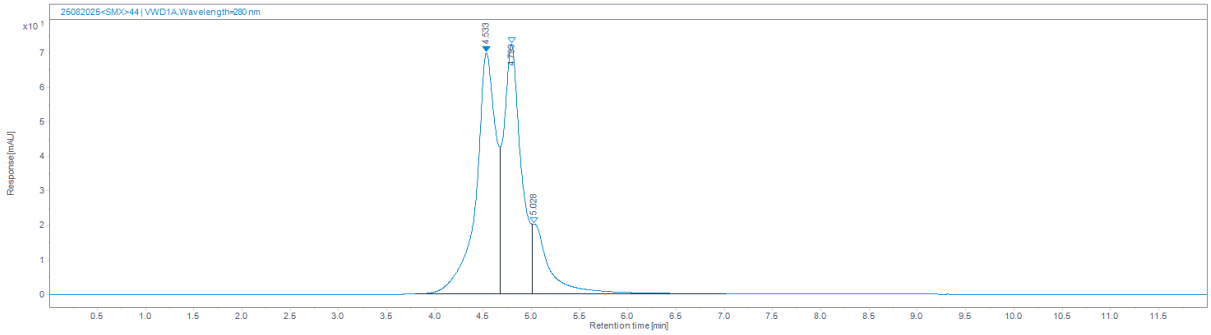


Figure 59: SEC-HPLC chromatogram of temperature (40°C, 2 weeks) sample of cNIST mAb for forced degradation study, showing the main monomer at 4.5 minutes.

5.3.2 Light Exposure

The effect of light exposure on cNIST mAb stability was assessed under controlled conditions for up to 2 weeks at 25°C, with samples analyzed by SDS-PAGE and SEC-HPLC. The light control sample was kept covered and protected from UV for 2 weeks in a photostability chamber, and it demonstrated three peaks on the chromatogram. SDS-PAGE analysis demonstrated main bands at ~55 and ~30 kDa, representative of heavy and light mAb chains. Similar to the temperature arm, additional bands were observed in light control and samples at ~100 kDa, ~45 kDa and ~35 kDa with loss in band density over time.

The light control sample demonstrated a monomer at 4.5 minutes, representative of 52.3% of total area, and two secondary peaks at 4.8 and 5.0 minutes that covered 21.9% and 25.8% of total area, respectively (**Figure 60**). This indicated partial instability of the antibody when stored for prolonged periods at ambient temperature, although the monomer remained the dominant species.

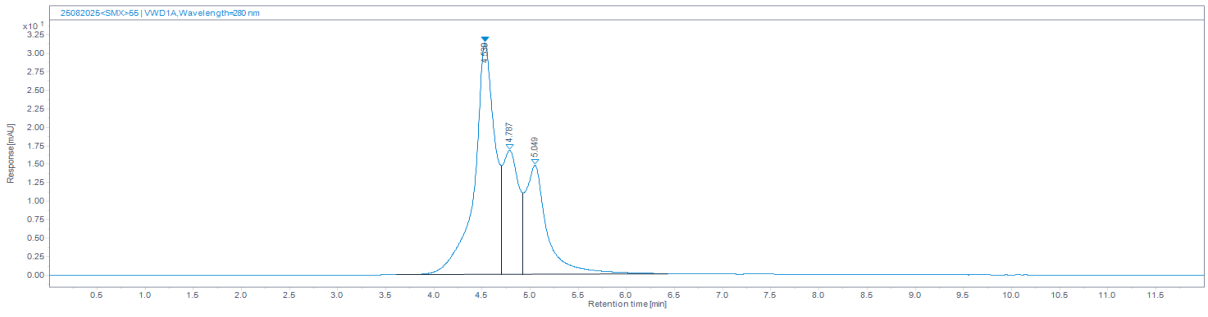


Figure 60: SEC-HPLC chromatogram of light control sample of cNIST mAb for forced degradation study, showing the main monomer at 4.5 minutes.

After 1 week of light exposure, the chromatogram showed a shift in distribution, with the monomer peak decreasing to 43.7% and a significant increase in the secondary species, accounting for 49.3% of the total area and the smaller fragment representing 7%. This suggests that light stress accelerated degradation, resulting in a major proportion of antibody fragments, as seen in **Figure 61**.

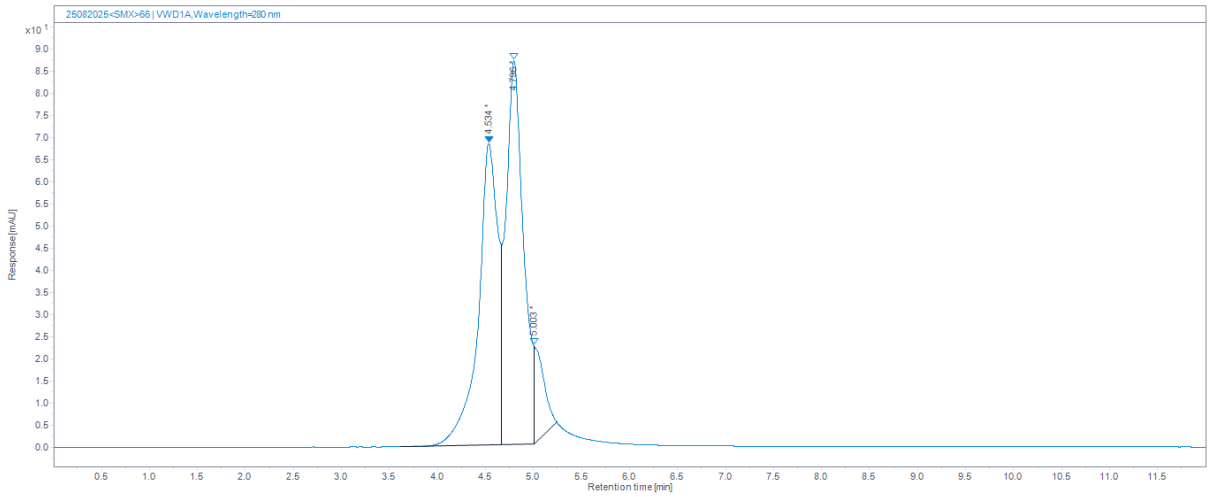


Figure 61: SEC-HPLC chromatogram of light (1 week) sample of cNIST mAb for forced degradation study, showing the main monomer at 4.5 minutes and fragments and 4.8 and 5.0 minutes.

2 weeks of light exposure exhibited a persistent degradation pattern, with the monomer content at 47.9% and two secondary low molecular weight peaks contributing to 36.1% and 16.0% respectively (**Figure 62**). Heterogeneous fragmentation was observed in this extended light-induced stress condition when compared to the 1-week light exposure sample.

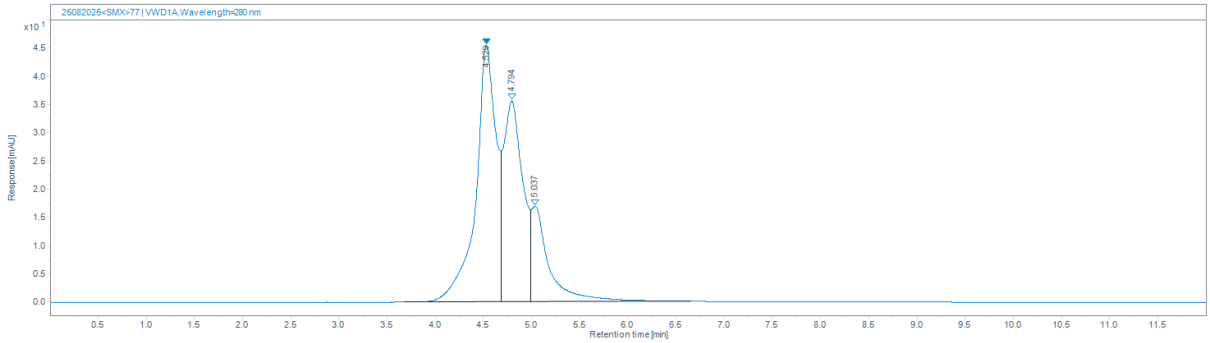


Figure 62: SEC-HPLC chromatogram of light (2 weeks) sample of cNIST mAb for forced degradation study, showing the main monomer at 4.5 minutes.

5.3.3 pH

cNIST mAb samples were dialyzed into buffers of pH 2.7 and pH 11 to evaluate their stability at pH 2.7 (acidic) and pH 11 (alkaline) using SEC-HPLC and SDS-PAGE. Characteristic heavy and light chain bands were observed for both acid and base-treated samples. The light chain in both samples, but in particular the basic sample, was of lower intensity compared to the control.

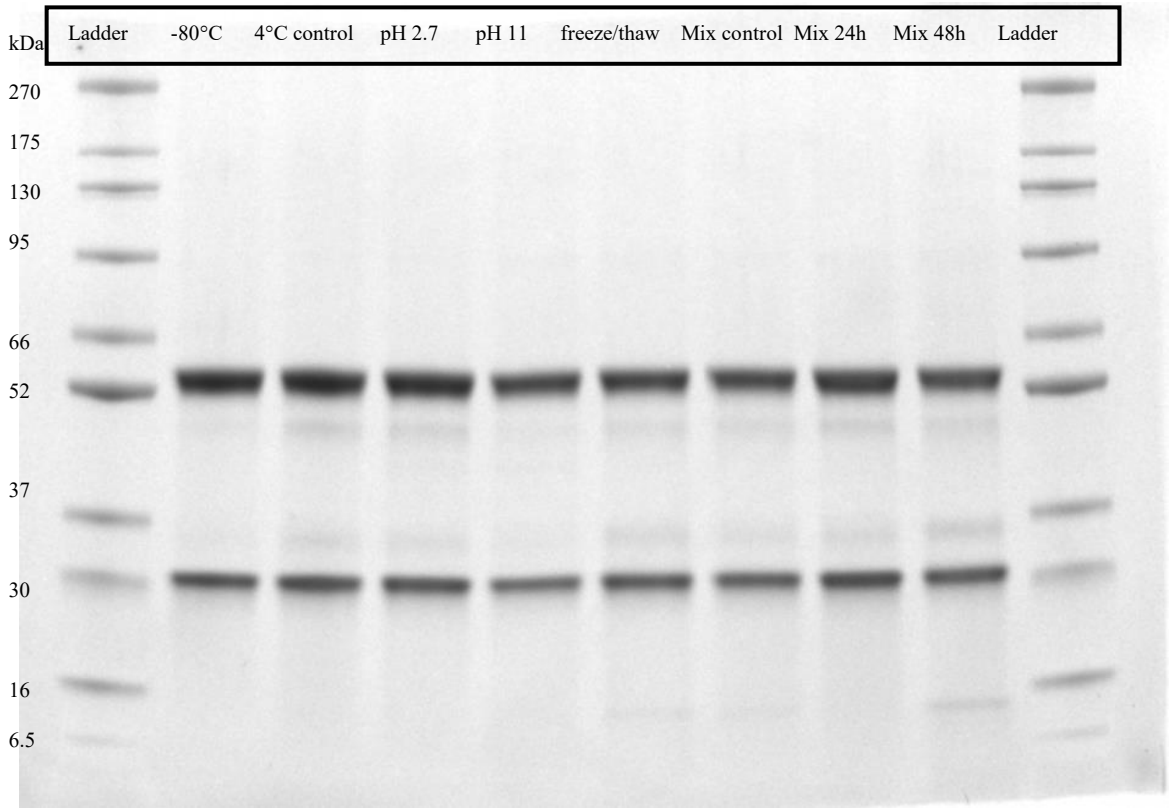


Figure 63: SDS-PAGE of cNIST mAbs subjected to forced degradation under pH, freeze-thaw and mixing conditions. Exteme pH values (2.7 and 11) were evaluated with 4°C serving as a control. Freeze-thaw stability was tested after three cycles, and mixing stress was assessed at 24 and 48 hours with a still sample as the control. A -80°C sample was included as an overall stability reference

Under acidic conditions at pH 2.7, a dominant monomeric peak elutes at 4.5 minutes, accounting for 82.0% of the total area and a secondary peak at 5.1 minutes contributes 18.0%. This shows the formation of a low molecular weight (LMW) fragment, consistent with limited acid-induced clipping.

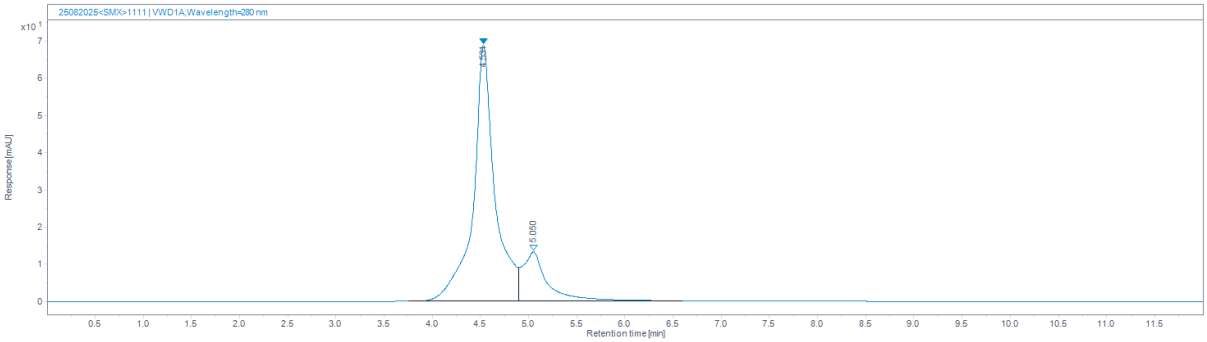


Figure 64: SEC-HPLC chromatogram of cNIST mAb at pH 2.7 for forced degradation study, showing the main monomer at 4.5 minutes.

At pH 11 in alkaline conditions, the monomeric peak was observed for only 44.1% of the total area. Fragmentation proportion increased to 49.4% for the larger fragment and 6.5% for the smaller fragment, indicating extensive degradation but with a different pathway compared to acidic degradation. Overall, alkaline conditions were more detrimental for cNIST mAb than acidic stress due to higher fragmentation.

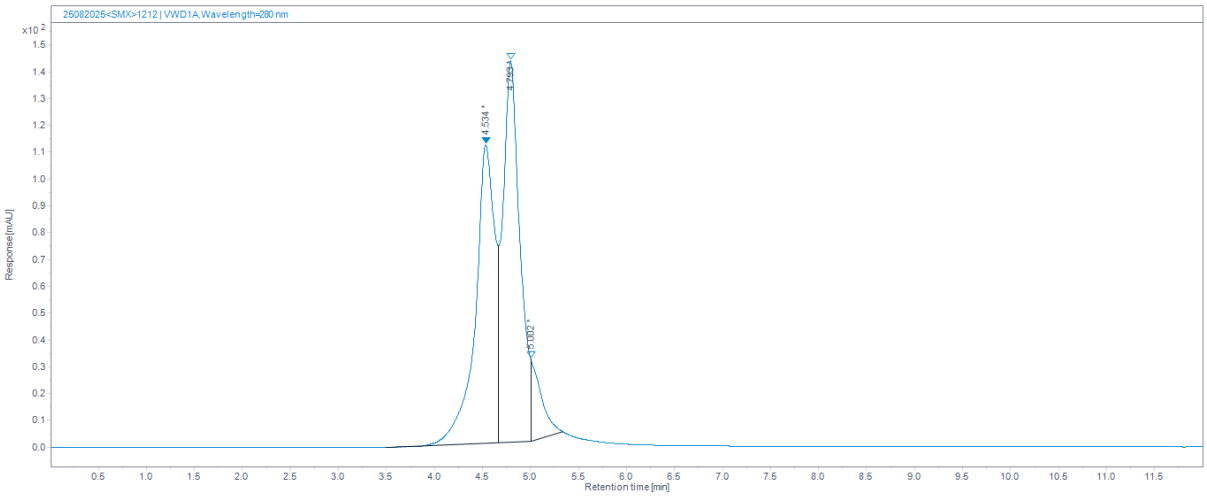


Figure 65: SEC-HPLC chromatogram of cNIST mAb sample at pH 11 for forced degradation study, showing the main monomer at 4.5 minutes.

5.3.4 Freeze-Thaw cycles

After three freeze-thaw cycles of 24 hours each, the SEC-HPLC data showed the monomer at 4.5 minutes, contributing to 55.4% of the total area with two later-eluting LMW peaks at 4.8 minutes (28.6%) and 5.0 minutes (16.1%). The results indicate fragmentation into multiple

species, which caused ~45% loss of monomer. The SDS-PAGE bands did not provide any additional insight apart from displaying lower band intensity compared to the -80° control.

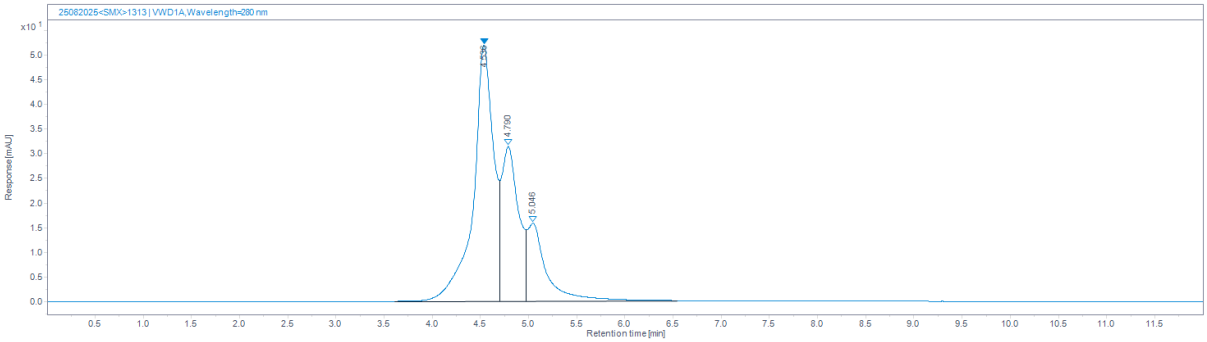


Figure 66: SEC-HPLC chromatogram of freeze-thaw sample of cNIST mAb for forced degradation study, showing the main monomer at 4.5 minutes.

5.3.5 Agitation

cNIST mAb samples were subjected to continuous mixing for 24 hours and 48 hours at room temperature, while a non-agitated sample held for 48 hours under otherwise identical conditions served as the control. SDS-PAGE analysis did not demonstrate any clear changes between arm control and mixed samples outside of some faint bands at ~35 and ~45 kDa.

The control sample showed three peaks with monomers at 4.5 minutes with 42.5% of the area, and a secondary peak at 4.8 minutes with a larger proportion of area of 48.6%. The third peak, representing second smallest fragment, was observed to have an area of 8.9%.

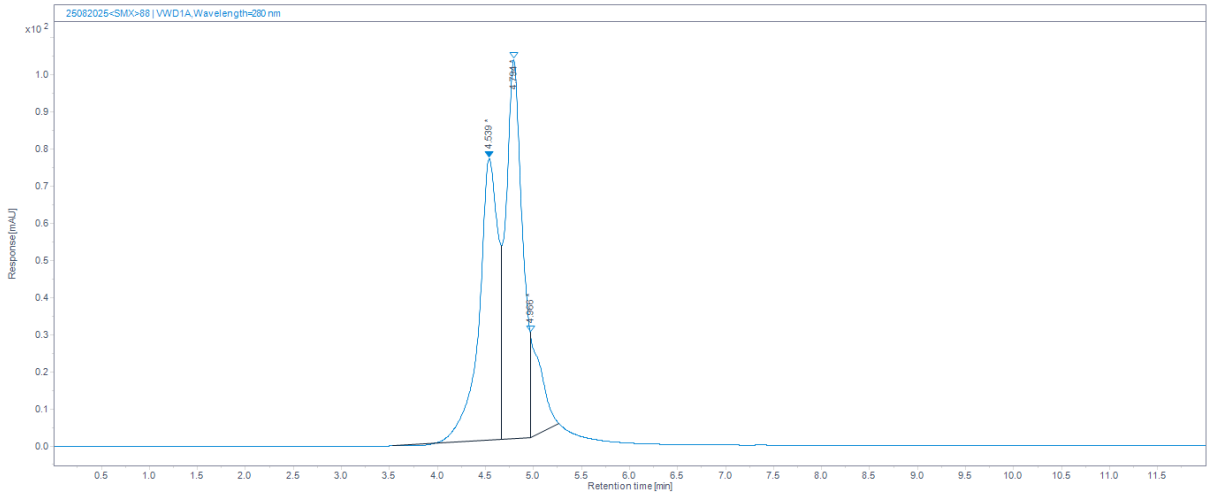


Figure 67: SEC-HPLC chromatogram of mixing control sample of cNIST mAb for forced degradation study, showing the main monomer at 4.5 minutes.

The 24-hour mixing sample demonstrated an increase in area as compared to the control at 52.5%, while fragmented species occupied 40.2 and 7.3% of the total area. The 48-hour mixing sample distribution was slightly different from 24 h sample, with the monomer covering 49% of the total area and fragments 41.3 and 9.6%. Overall, agitation did not drive further degradation, but 24-hour mixing modestly increased monomer as compared to the control and 48-hour mixing sample.

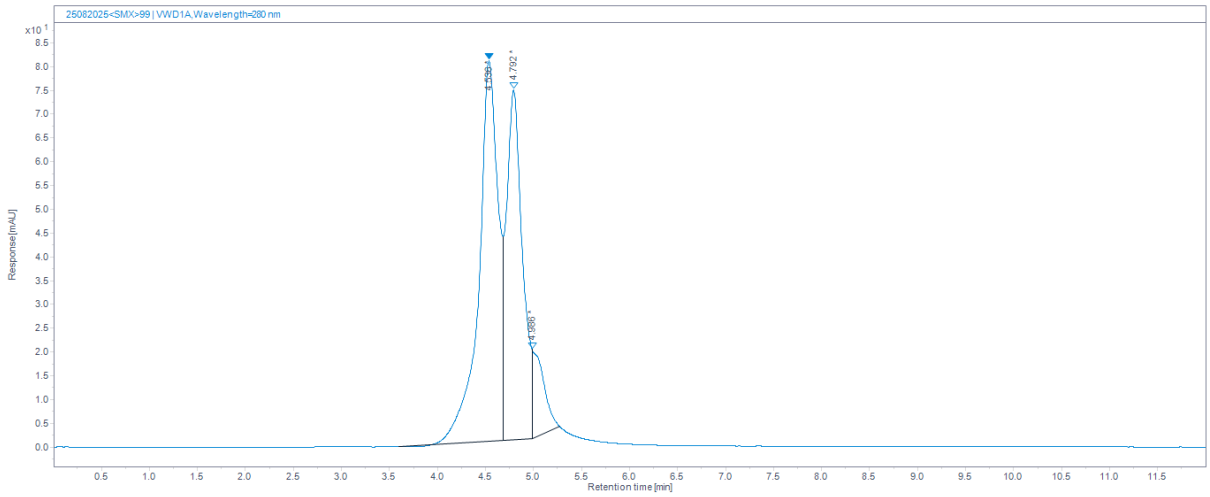


Figure 68: SEC-HPLC chromatogram of the 24-hour mixing sample of cNIST mAb for forced degradation study, showing the main monomer at 4.5 minutes.

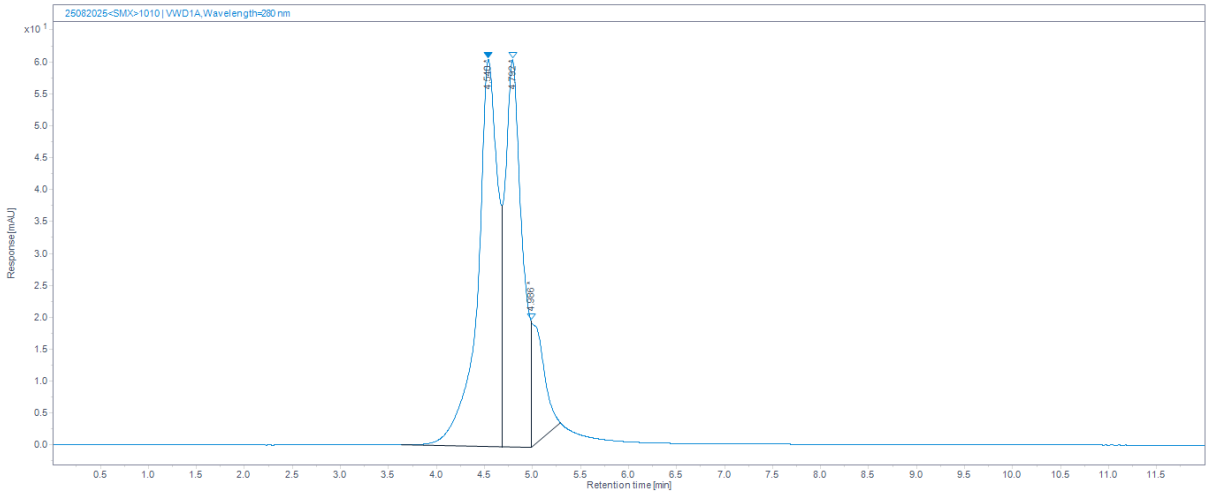


Figure 69: SEC-HPLC chromatogram of the 48-hour mixing sample of cNIST mAb for forced degradation study, showing the main monomer at 4.5 minutes.

5.3.6 Summary Analysis of SDS-PAGE AND SEC-HPLC

In order to correlate SDS-PAGE data and SEC-HPLC, **Table 19** was generated which captures bands, peak retention times, areas and proportions for all samples and controls.

Table 19: Summary of forced degradation study across SDS-PAGE and SEC-HPLC.

Condition	SDS-PAGE	SEC-HPLC Peak	RT (min)	Peak Area (mAU-s)	Area %
Control -80°C	Intact heavy/light chains, no degradation	Peak 1	4.5	1196.9	84.3
		Peak 2	4.7	170.3	12.0
		Peak 3	5.0	52.1	3.7
Temp 4°C control (2 week)	Comparable to -80°C control, minimal degradation	Peak 1	4.5	1157.2	73.8
		Peak 2	4.7	210.3	13.4
		Peak 3	5.0	199.5	12.7
Temp 40°C (1 week)	Thinner bands than temp control, early degradation	Peak 1	4.5	1005.9	68.1
		Peak 2	4.8	248.0	16.8
		Peak 3	5.0	222.8	15.1
Temp 40°C (2 weeks)	Thinner bands than 40°C 1 week, more degradation	Peak 1	4.5	1000.8	48.0
		Peak 2	4.7	918.5	42.2
		Peak 3	5.0	255.7	11.8

Condition	SDS-PAGE	SEC-HPLC Peak	RT (min)	Peak Area (mAU-s)	Area %
Light control (2 weeks)	Intact bands with slight degradation	Peak 1	4.5	465.2	52.3
		Peak 2	4.8	194.7	21.9
		Peak 3	5.0	229. 5	25.8
Light (1 week)	Thinner bands	Peak 1	4.5	971.0	43.7
		Peak 2	4.8	1096.0	49.3
		Peak 3	5.0	155.9	7.0
Light (2 weeks)	Further band thinning	Peak 1	4.5	664.8	47.9
		Peak 2	4.8	499.9	36.1
		Peak 3	5.3	221.9	16.0
pH 2.7	Intact bands as compared to pH 11	Peak 1	4.5	1077.7	82.0
		Peak 2	5.1	236.9	18.0
pH 11	Thinner bands compared to pH 2.7	Peak 1	4.5	1569.6	44.1
		Peak 2	4.8	1758.7	49.4
		Peak 3	5.0	231.0	6.5
Freeze-thaw	Less intense bands compared to control	Peak 1	4.5	756.4	55.4
		Peak 2	4.8	389.9	28.6
		Peak 3	5.0	219.3	16.1
Mixing control (48 hrs)	Slight reduction in band thickness	Peak 1	4.5	1054.3	42.5
		Peak 2	4.8	1205.3	48.6
		Peak 3	5.0	220.0	8.9
Mixing 24 hours	Bands more intact than 48 hours	Peak 1	4.5	1117.6	52.5
		Peak 2	4.8	857.0	40.2
		Peak 3	5.0	155.2	7.3
Mixing 48 hours	Thinner bands than 24 hours, more degradation	Peak 1	4.5	889.2	49.0
		Peak 2	4.8	749.2	41.3
		Peak 3	5.0	174.6	9.6

6. Cell-Based Potency Assay Method Development

To evaluate the biological activity of IL-8 antigen and assess the functional activity of the anti-IL-8 mAb, cell-based potency assay development was performed. Two models were assessed, using HL-60 and HCT-116 cell lines. The HL-60 cell line assay was based on replicating IL-8 i*n vivo* cell signalling cascade in neutrophil cells, with assessment of cell signalling by western blotting. The HCT-116 assay was based on the ability of IL-8 to promote cell proliferation in tumour cells, with cell proliferation measured as a marker of IL-8 activity.

Initially, HL-60 cells were stimulated with IL-8, both in the presence and absence of retinoic acid (RA). Retinoic acid was used to differentiate HL-60 cells into neutrophil-like cells, which are more responsive to stimulation.

Further, the assay focused on using HCT-116 colorectal carcinoma cells as the primary model, due to stable cell growth, which enabled consistent experimental handling and downstream analysis. The HCT-116 cells were stimulated with recombinant human IL-8 across varying concentrations to investigate dose-dependent cellular response and to establish neutralising effects of the anti-IL-8 mAb.

The cellular responses were measured using multiple analytical methods. Western blotting was used to detect signalling responses with IL-8. In parallel, cell count assays were used to monitor changes in cell proliferation and ATP analysis for metabolic activity with IL-8 and anti-IL-8 mAb.

No bioassay characterisation was performed for the cNIST mAb, as the antigen of cNIST mAb is not public information as part of its licensing agreement.

6.1 HL-60 Cell Assay

HL-60 cells, with and without retinoic acid, were treated with human IL-8 (50 ng/mL) at various time points: 0, 0.25, 0.5, 1, 2 and 4 hours to generate a signalling cascade. Cells were then lysed to quantify cell signalling through the detection of specific proteins (pERK and pRPS6). The lysed samples were normalised after protein quantification using the BCA assay.

Multiple experimental batches of HL-60 cells were treated with retinoic acid and subsequently stimulated with IL-8 to investigate expression of pERK and pRPS6 by western blotting. These biomarkers are expressed when IL-8 binds to CXCR1/CXCR2 receptors, activating MAPK pathway for pERK and indirectly activating mTOR via P13-Akt signalling for pRPS6. The general method development approach is detailed below **(Figure 70)**.

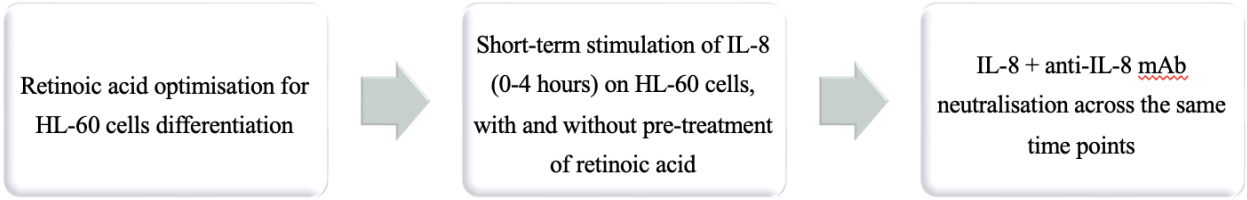


Figure 70: Schematic diagram of the HL-60 cell assay workflow with RA and human IL-8.

Cell Culture

HL-60 cells were initially grown in RPMI 1640 supplemented with 20% FBS. It took 1 week to expand to sufficient numbers to allow transition into 10% FBS RPMI. The cells grew in suspension culture and were progressively expanded up to four T-175 flasks to get the maximum cell population for treatment with retinoic acid. It was noted that RA-treated HL-60 cells exhibited reduced proliferation compared to untreated cells.

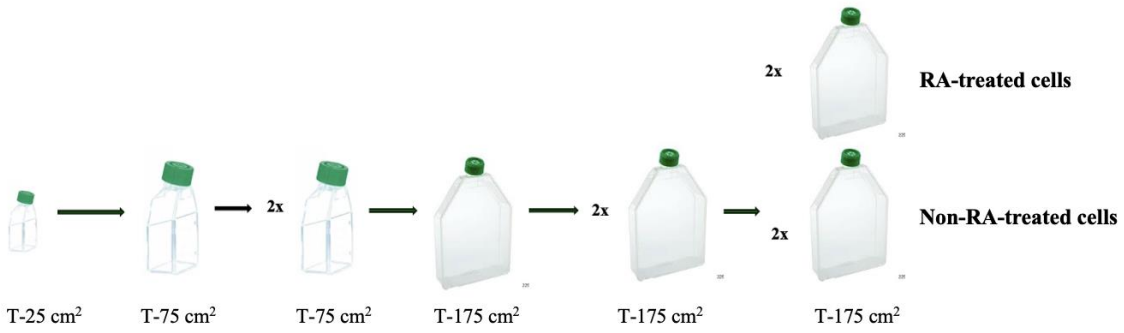


Figure 71: Expansion of HL-60 cells from T-25 cm² to T-175 cm² suspension flasks into differentiated and undifferentiated cells.

Western Blotting

Batch 1: Optimisation of Retinoic Acid Concentration for HL-60 Cells Differentiation

HL-60 cells were treated with increasing concentrations of retinoic acid (0, 0.25, 0.5 and 1 µM) for 7 days and stimulated with 10 ng/mL human IL-8 for 4 hours. Protein lysates were analysed by Western Blotting for phosphorylation of ERK (pERK) and ribosomal protein S6 (pRPS6). In both cases, the effect of increasing concentrations of retinoic acid was seen. However, no significant increase in phosphorylation was seen with IL-8 stimulation as compared to corresponding RA-only lanes.

Based on the observed differentiation response and guidance from the technical supervisor, 0.5 µM RA was selected as the working concentration for subsequent HL-60 potency assay experiments.

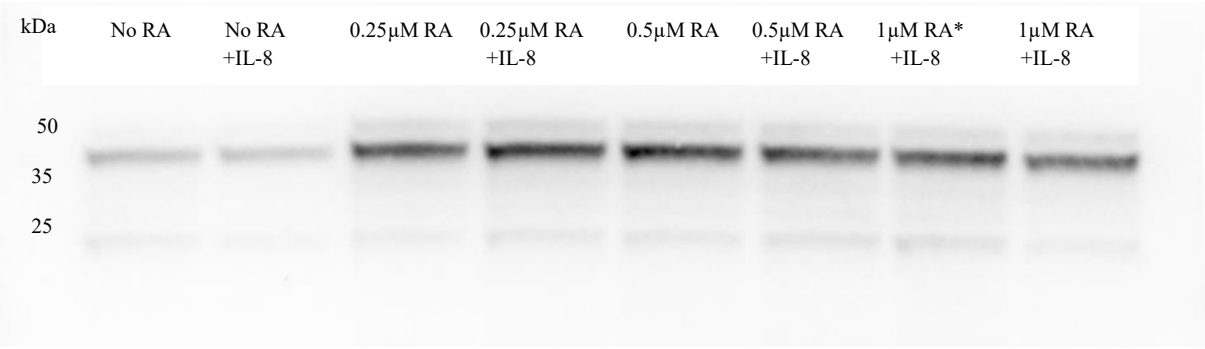


Figure 72: Western blot of pERK in HL-60 cells after RA treatment (0-1 µM, 7 days) with or without IL-8 (10 ng/mL, 4 hours).

Note: The lane labelled as "1 µM RA* + IL-8" represents a technical error where both 1 µM RA samples were inadvertently treated with IL-8.

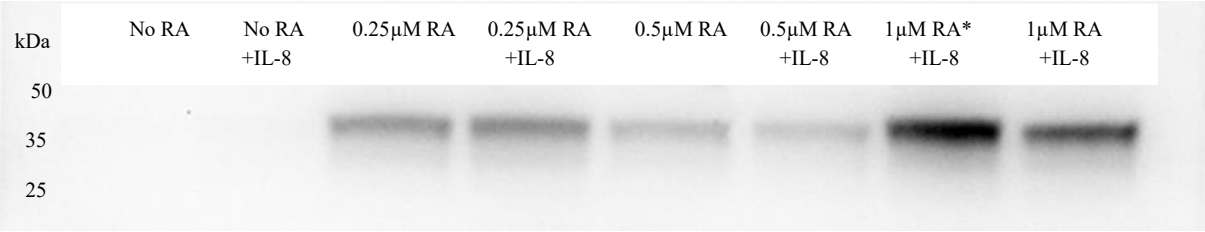


Figure 73: Western blot of pRPS6 in HL-60 cells after RA treatment (0-1 µM, 7 days) with or without IL-8 (10 ng/mL, 4 hours).

Note: The lane labelled as "1 µM RA* + IL-8" represents a technical error where both 1 µM RA samples were inadvertently treated with IL-8.

Batch 2-4

After identifying 0.5 µM RA as the working differentiation concentration, three further batches were conducted to examine IL-8-induced signalling in HL-60 cells. RA-treated and non-treated cells were stimulated with 50 ng/mL IL-8 for 0, 0.25, 0.5, 1, 2 and 4 hours. Although sufficient protein concentrations were confirmed in the BCA assay, no visible protein bands were seen on western blots. Band intensity remained faint or absent for all batches, preventing any reliable interpretation of IL-8 signalling. For Batches 3 and 4, β-tubulin was used as a housekeeping protein, confirming consistent protein loading and transfer across all samples within each batch. Due to technical limitations encountered with HL-60 cells and time constraints, these experiments were paused and activity focused on HCT-116 model development.

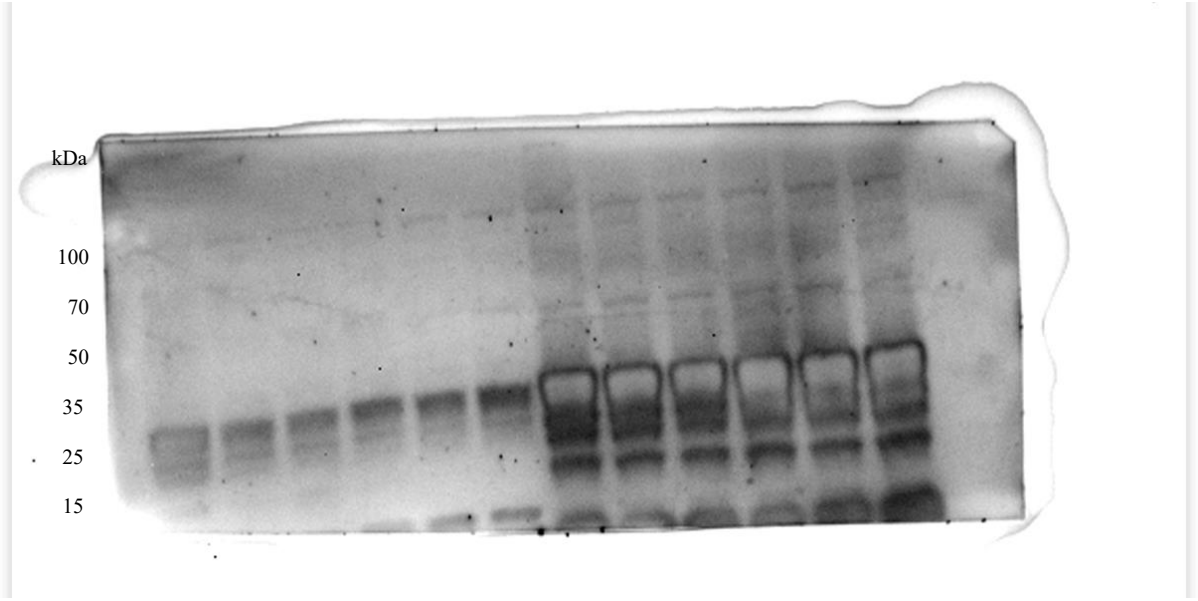


Figure 74: β-tubulin loading control for HL-60 samples western blot samples of Batch 3.

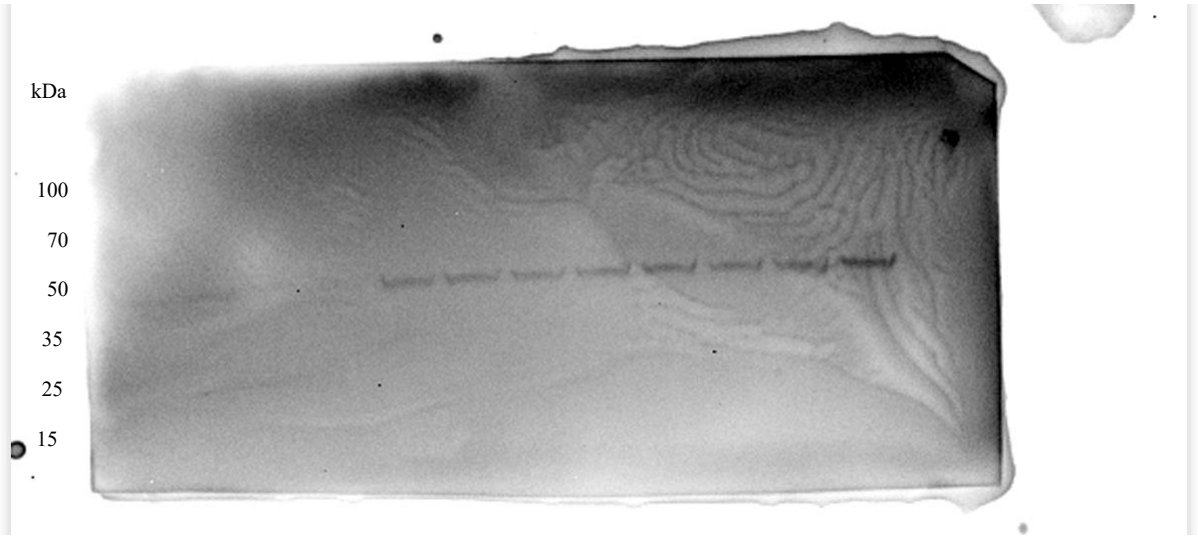


Figure 75: β-tubulin loading control for HL-60 samples western blot samples of Batch 4.

6.2 HCT-116 Cell Assay

Effect of IL-8 on HCT-116 Cells

HCT-116 cells were cultured in McCoy's 5A medium supplemented with 10% FBS, 1% HEPES and penicillin-streptomycin under standard conditions (37 °C, 5% CO_2). Cells were shifted into 2.5% FBS McCoy's 5A medium and seeded in 6-well or 96-well plates and stimulated with varying concentrations of human IL-8 and anti-IL-8, depending on the assay.

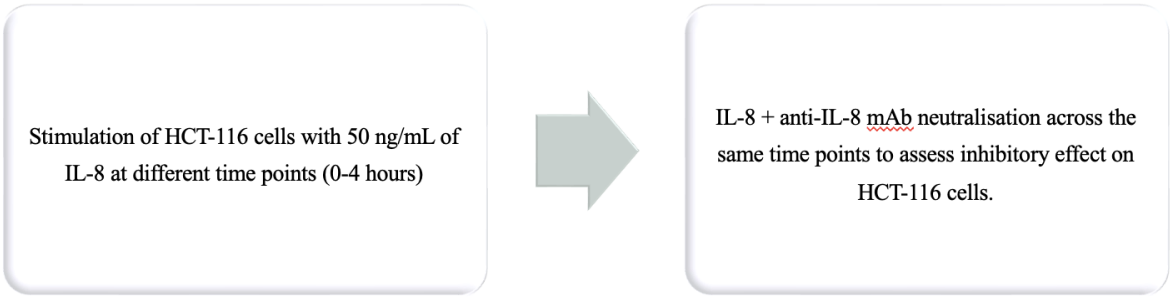


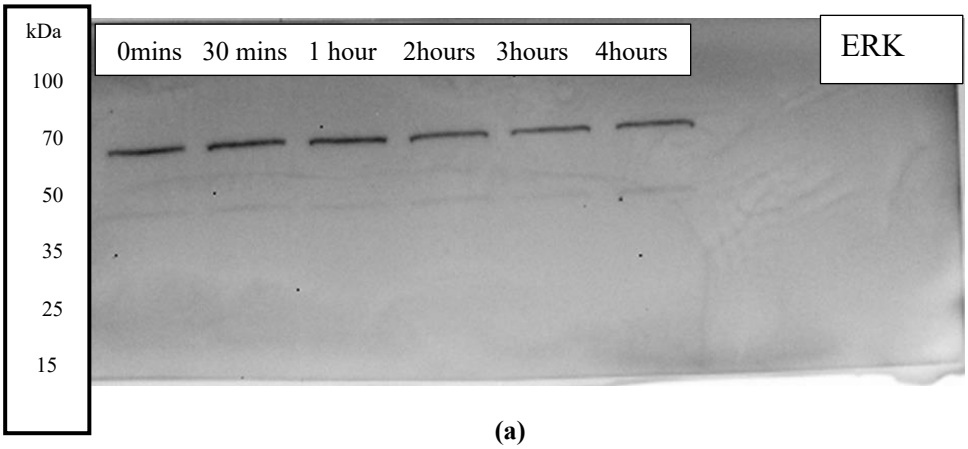
Figure 76: Schematic representation of the HCT-116 cell-based potency assay.

Western Blotting

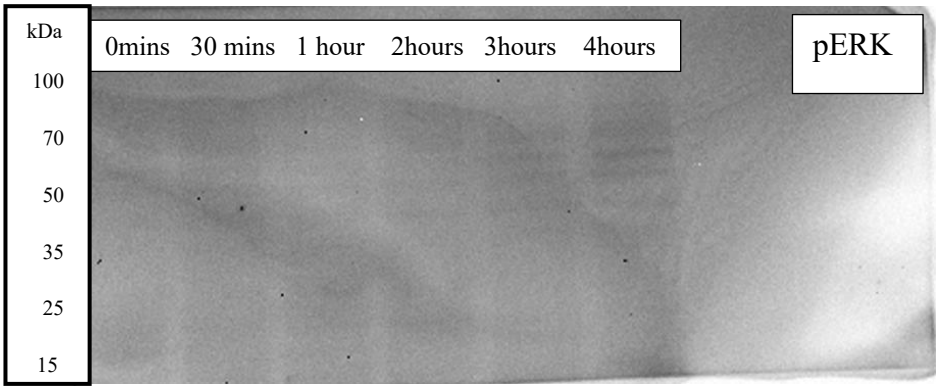
To investigate the effect of IL-8 stimulation on intracellular signalling pathways, HCT-116 cells were treated with 50ng/mL human IL-8 antigen at different time points ranging from 0 minutes to 4 hours. Protein lysates were analysed by SDS-PAGE followed by western blotting for ERK, phosphorylated ERK (pERK), ribosomal protein S6 (RPS6) and phosphorylated RPS6 (pRPS6).

Batch 1

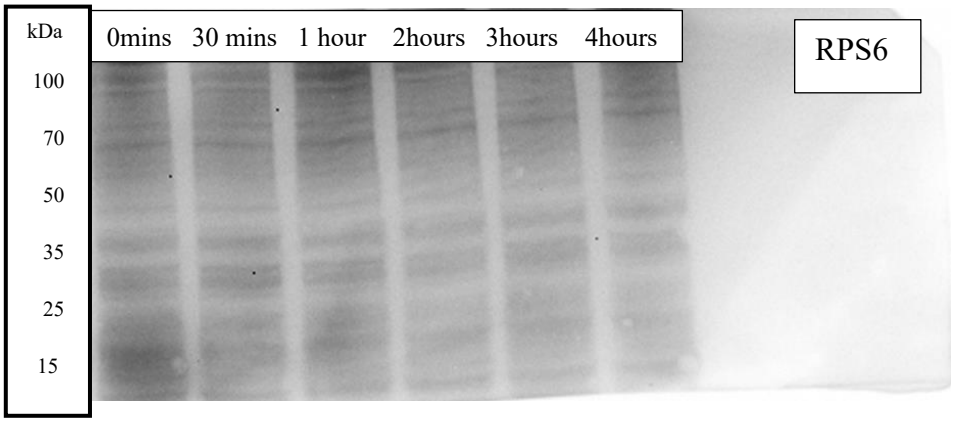
In the first batch, total ERK was detected across all time points with similar intensity, as shown in **Figure 77**. On the other hand, all other biomarkers i.e pERK, RPS6 and pRPS6 showed weak or absent signals with no certain time-dependent increase. This indicated that IL-8 stimulation did not induce detectable phosphorylation under the tested conditions.


kDa
100
70
50
35
25
15
0mins 30 mins 1 hour 2hours 3hours 4hours
ERK

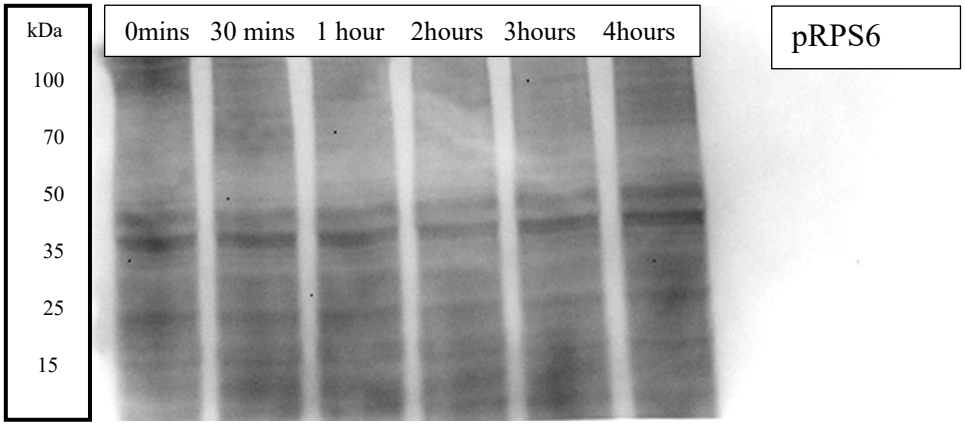
(a)


kDa
100
70
50
35
25
15
0mins 30 mins 1 hour 2hours 3hours 4hours
pERK

(b)


kDa
100
70
50
35
25
15
0mins 30 mins 1 hour 2hours 3hours 4hours
RPS6

(c)



(d)

Figure 77: Western blot analysis of IL-8 induced signalling in HCT-116 cells, Batch 1; (a) Total ERK, (b) pERK (c) RPS6, (d) pRPS6.

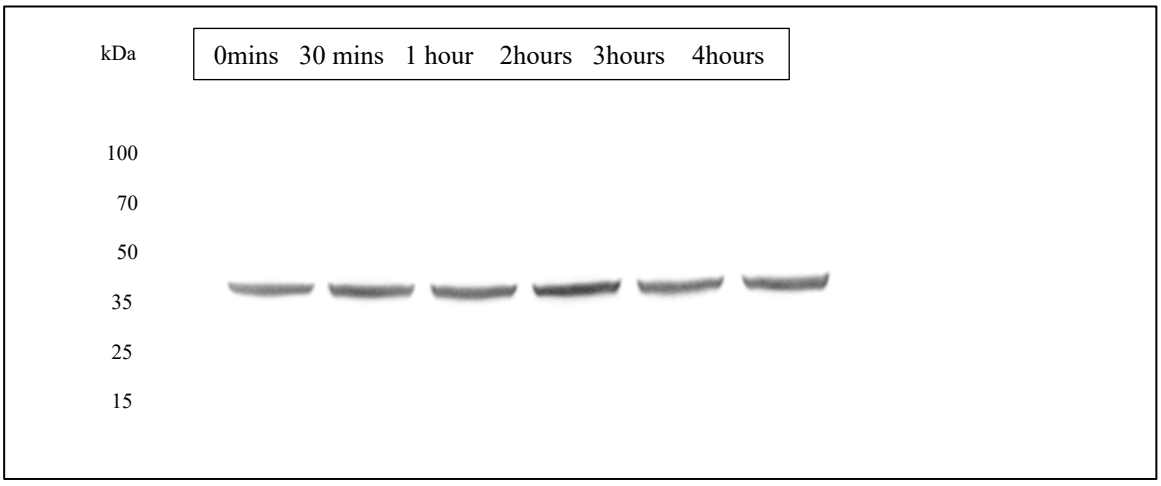
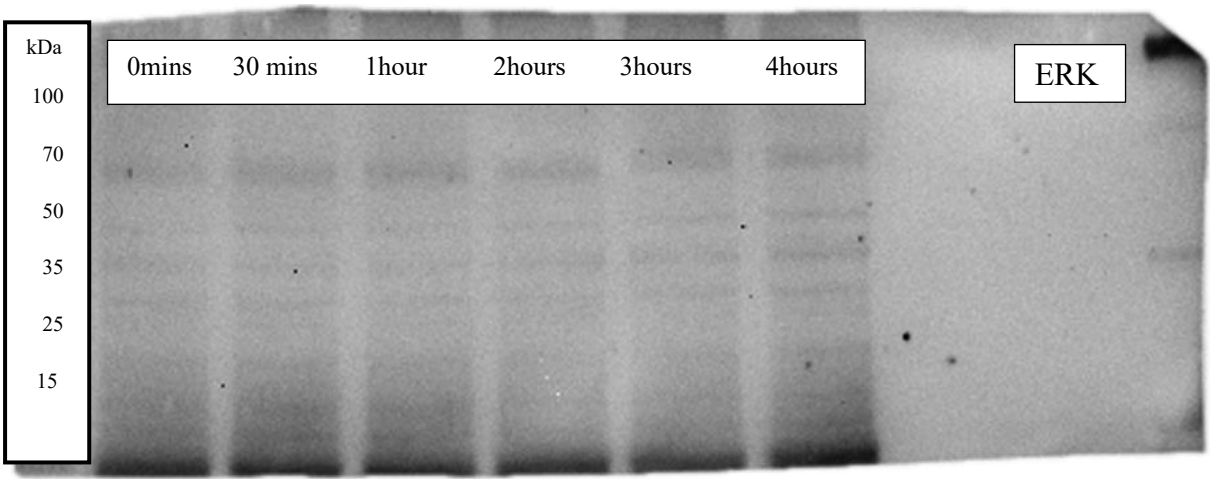


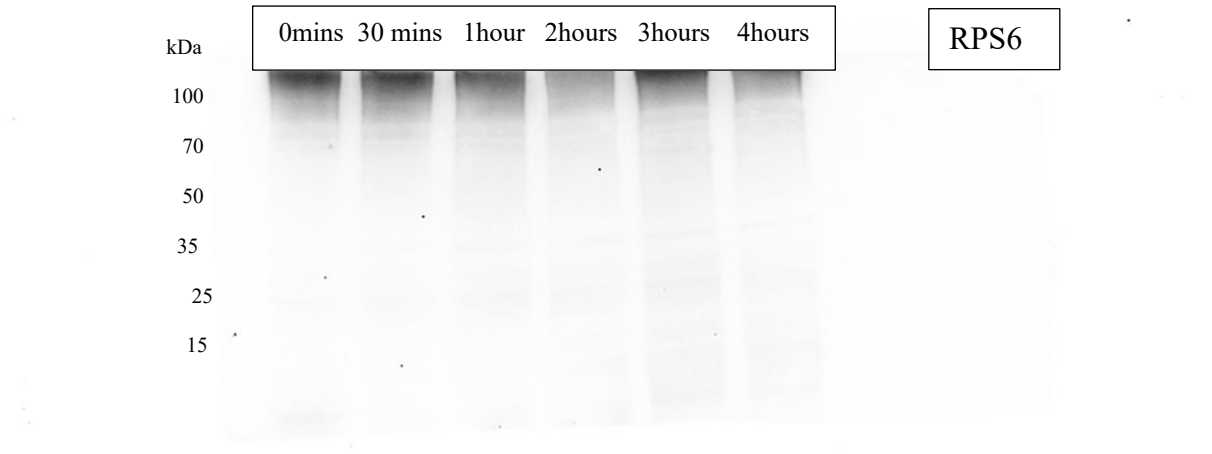
Figure 78: β-actin (~ 42 kDa) loading control for HCT-116 western blot samples of Batch 1. Comparable β-actin band intensity across lanes indicates similar protein loading in this batch.

Batch 2

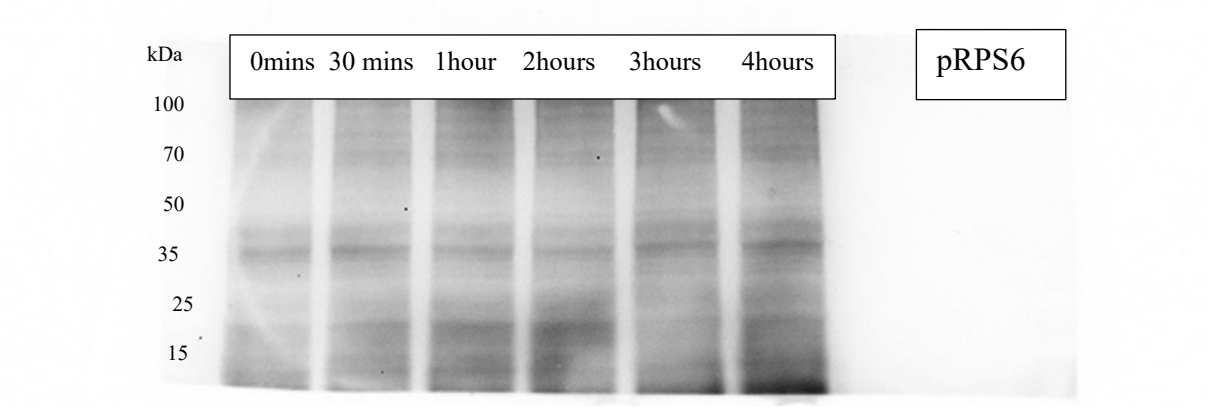
In the second batch, faint bands corresponding to phosphorylated ERK (pERK) were observed. However, the signals were weak making them difficult to interpret as a clear phosphorylation response. RPS6 and pRPS6 bands were not visible, with high background noise. Overall, the majority of blots remained undetectable.



(a)



(b)



(c)

Figure 79: Western blot analysis of IL-8-induced signalling in HCT-116 cells, Batch 2. (a) pERK (b) RPS6, (c) pRPS6

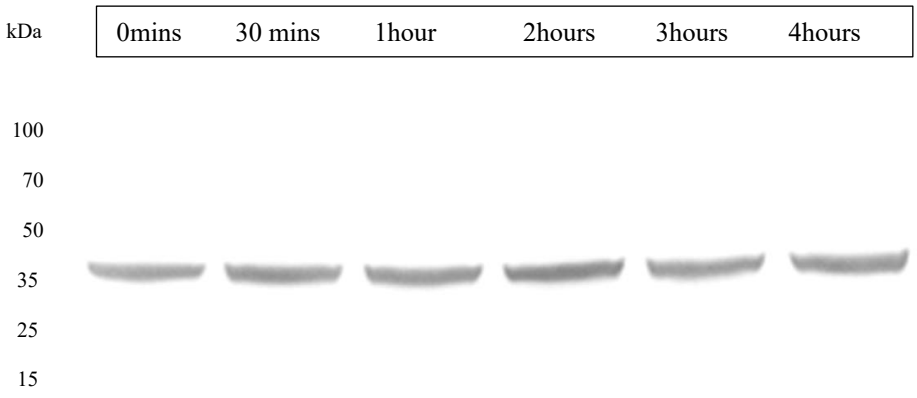
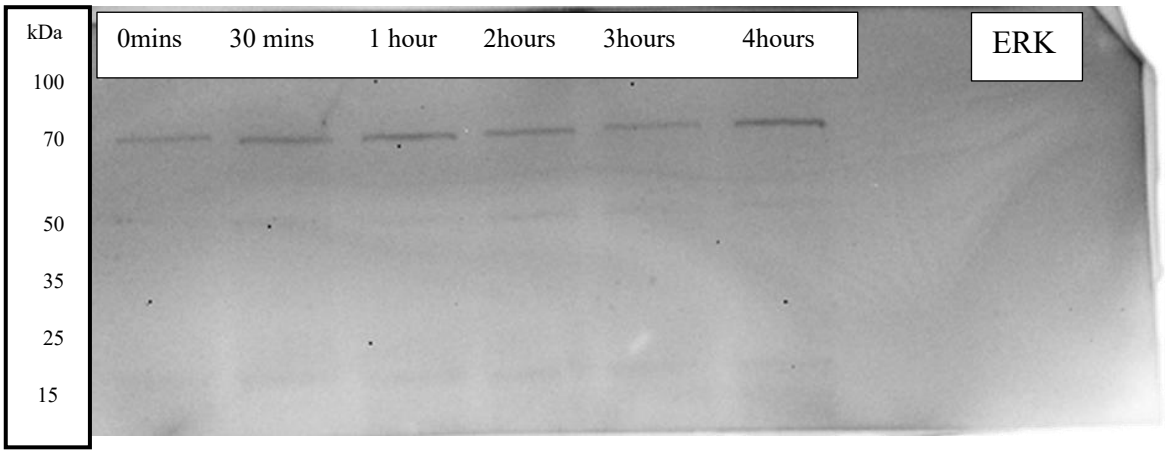


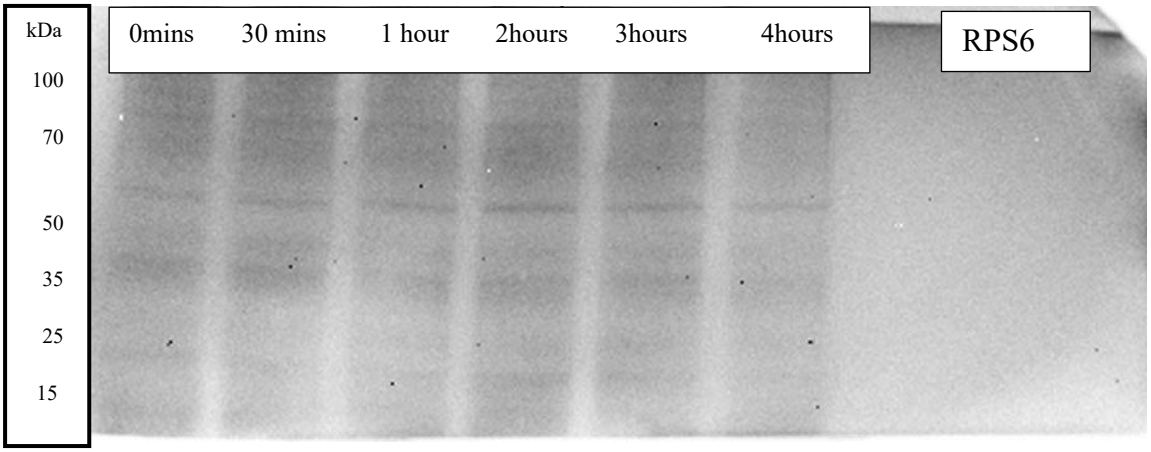
Figure 80: β-actin (~ 42 kDa) loading control for HCT-116 western blot samples of Batch 2. Comparable β-actin band intensity across lanes indicates similar protein loading in this batch.

Batch 3

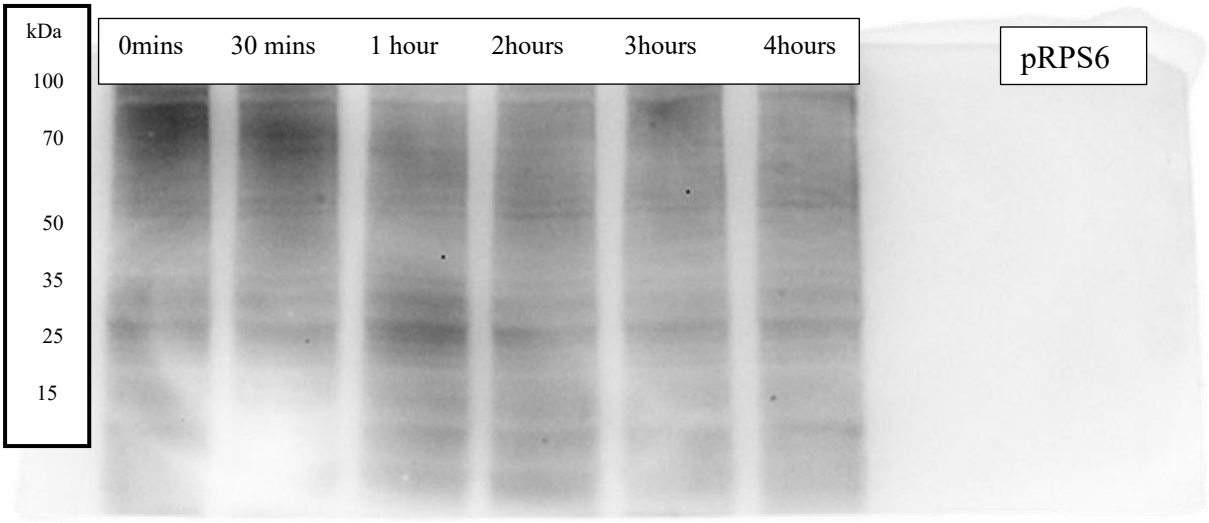
In the third batch, ERK was weakly but consistently detected across all time points with slight increase in intensity towards the 4-hour's time point, indicating adequate sample loading and transfer. RPS6 bands were present faintly, but the pRPS6 bands were accompanied with high background noise. Hence no clear activation trend was observed for IL-8-induced phosphorylation.



(a)



(b)



(c)

Figure 81: Western blot analysis of IL-8 induced signalling in HCT-116 cells, Batch 2 (a) Total ERK (b) RPS6, (c) pRPS6.

Cell Proliferation – Cell Count

To evaluate the proliferative effect of IL-8 on HCT-116 cells, cells were stimulated with increasing concentrations of recombinant IL-8 (0, 5, 10, 25, 50 and 100 ng/mL) and cultured for 72 hours. Mean cell counts were recorded across four batches of stimulation using a hemacytometer. As shown in **Figure 82,** a dose-dependent trend in cell count was observed with different concentrations of IL-8.

A rise in cell count was seen from an average cell count of 1.38 x 10^6 cells per well at baseline and a highest cell count of approximately 2 x 10^6 cells per well at 100 ng/mL. A moderate increase was seen at 5 ng/mL and 50 ng/mL as well, suggesting a proliferative response to IL-8. While there wasn't much rise in cell count numbers at 10 and 25 ng/mL.

The error bars in the graph reflect the substantial variability across batches. These results do not show a positive, robust proliferative effect of IL-8 on HCT-116 cells under the tested conditions.

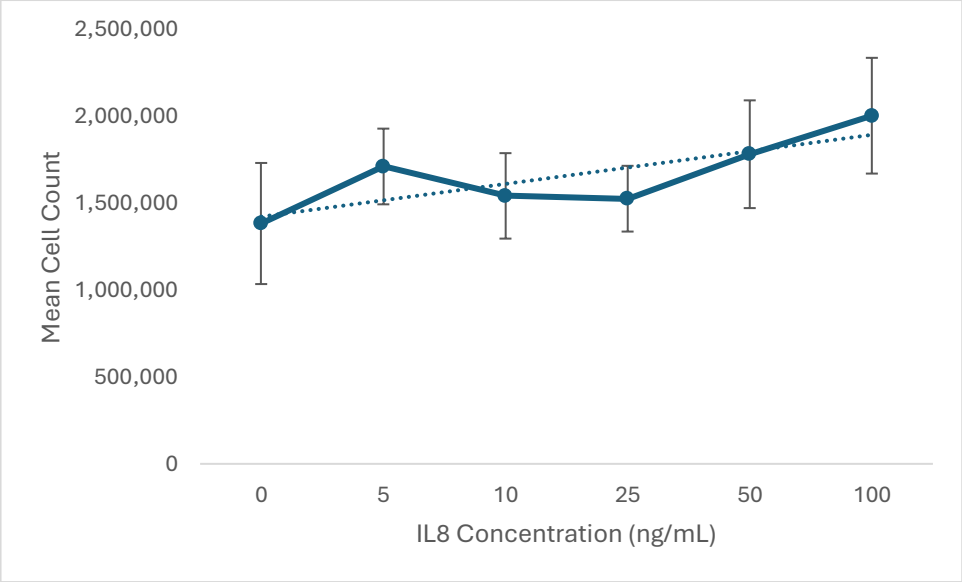


Figure 82: Mean cell counts of HCT-116 cells stimulated with increasing concentrations of IL-8 (0-100 ng/mL) across Batches 1-4 (n=4), each performed in duplicate. Error bars represent ± SD.

ATP Analysis

Batch 1

ATP analysis was measured in HCT-116 cells following stimulation with increasing concentrations of human IL-8 (0, 5, 10, 25, 50 and 100 ng/mL), using the CellTiter-Glo assay. As shown in **Figure 83**, an increase in luminescence can be seen till 10 ng/mL IL-8, after which the values saturate. This suggests maximum ATP activity occurred at 10 ng/mL and plateaued at higher concentrations, resulting in no significant increase in ATP levels.

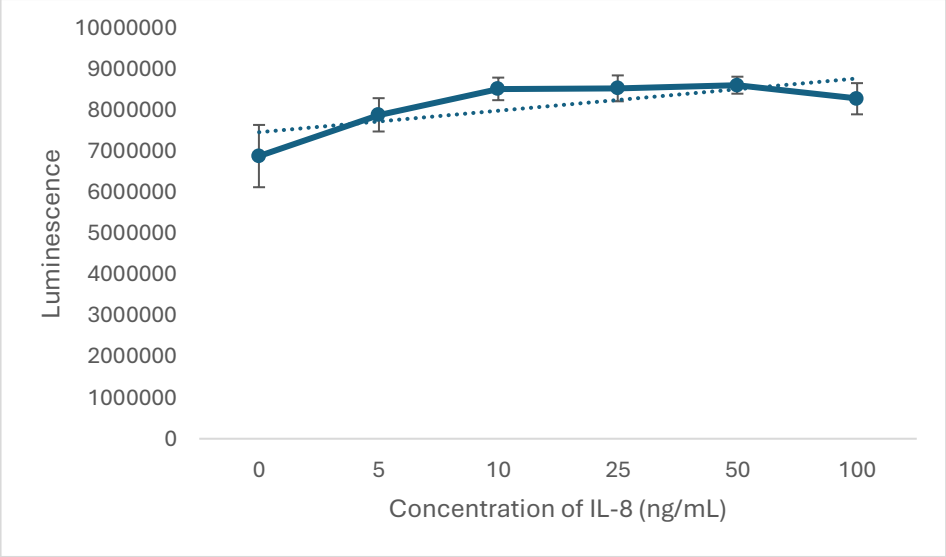


Figure 83: ATP analysis of HCT-116 cells stimulated with different concentrations of human IL-8 (0-100 ng/mL) in Batch 1. Luminescence values represent mean ± SD, with three replicates (n=3) per concentration.

Batch 2

For Batch 2, there were two sets of stimulation layouts, one in custom order (0 to 100 ng/mL) and one in randomised order to eliminate positional bias. While the luminescence values remain in a relevant range, the data did not exhibit a clear dose-dependent response trend. Both custom and randomised layouts showed a lack of consistency of results and minimal variation between IL-8 concentrations to determine a particular trend. Batch 2 data of both layouts are displayed in **Figure 84**.

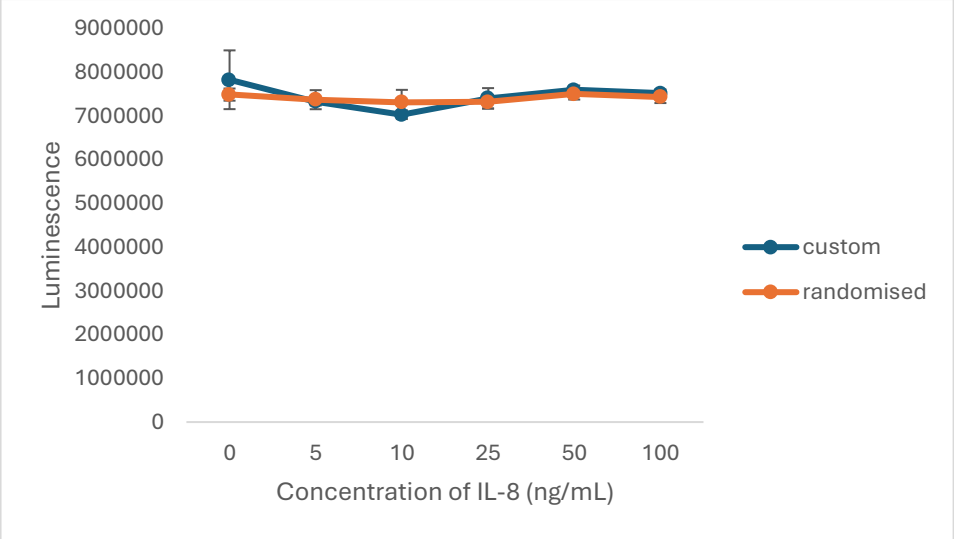


Figure 84: ATP analysis of HCT-116 cells stimulated with different concentrations of human IL-8 (0-100 ng/mL) in custom and randomised order for Batch 2. Luminescence values represent mean ± SD, with n=4 per concentration.

Batch 3

Batch 3 of ATP analysis was conducted in a similar manner as Batch 2, with one custom order layout and one randomised order layout of IL-8 stimulation at different concentrations. As shown in Figure 85, luminescence was not consistent in both layouts, which cannot be inferred as a dose-dependent response trend.

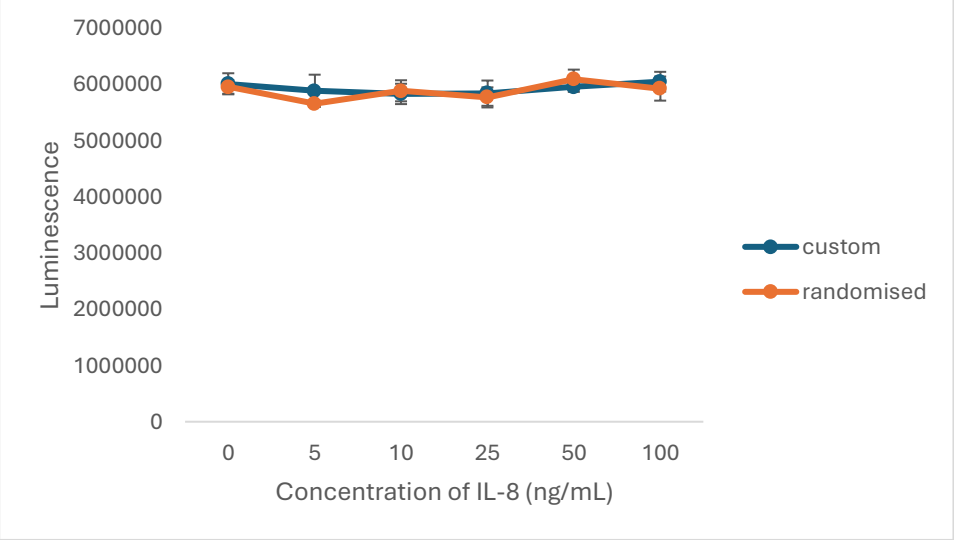


Figure 85: : ATP analysis of HCT-116 cells stimulated with different concentrations of human IL-8 (0-100 ng/mL) in custom and randomised order for Batch 2. Luminescence values represent mean ± SD, with n=4 per concentration.

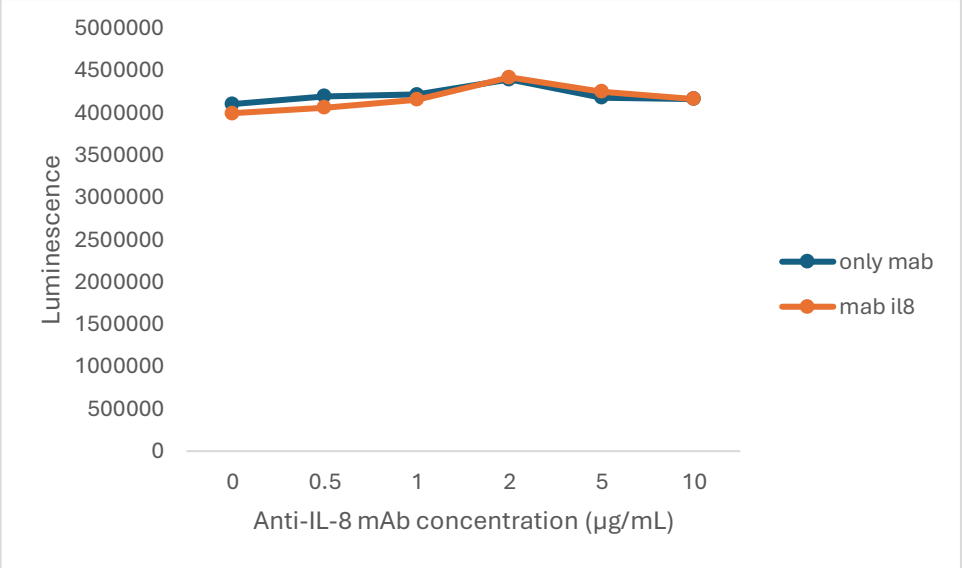
The ATP assay was conducted for three independent batches with both custom and randomised plate layouts to evaluate the metabolic activity of HCT-116 cells following IL-8 stimulation. Inconsistencies across all batches were observed and indicated a lack of reproducibility and reliability in the ATP assay under the tested conditions. Variability may have been due to metabolic fluctuations, plate handling or layout order effects. Consequently, a definitive conclusion regarding the effect of IL-8 on ATP levels of HCT-116 cells could not be established based on the data collected.

Effect of Anti-IL-8 Monoclonal Antibody on IL-8-stimulated HCT-116 Cells

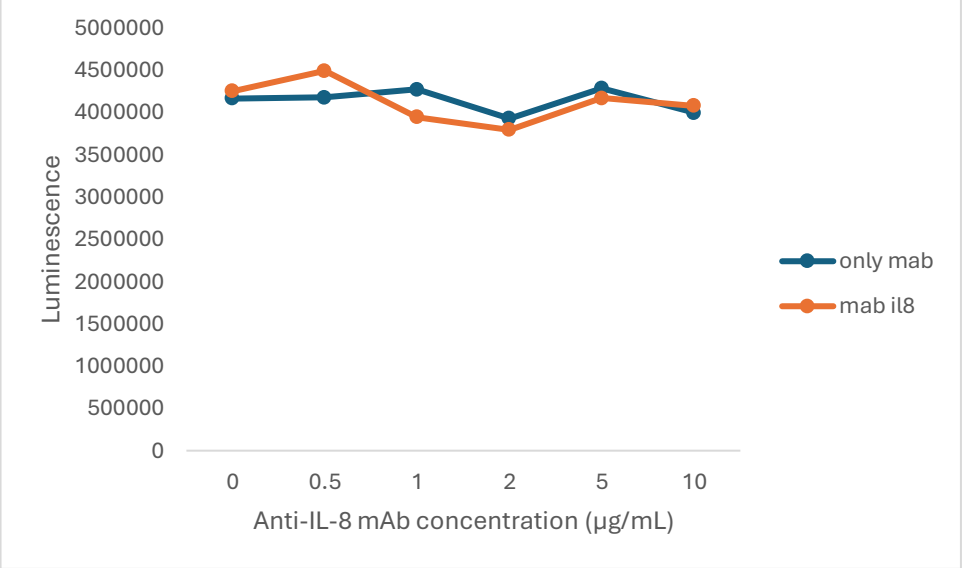
To further investigate the functional activity of the anti-IL-8 mAb, HCT-116 cells were stimulated with increasing concentrations of the mAb (0-10 μg/mL), both alone and in combination with IL-8 (10 ng/mL). ATP luminescence was measured to assess the change in metabolic activity with the mAb.

Batch 1

Batch 1 showed no clear and consistent trend in luminescence values across increasing antibody concentrations in either condition, as shown in **Figure 86**. In the custom order layout, both "mAb only" and "mAb+IL-8" groups show slight increases upto 2 μg/mL, but plateaus after that. In the randomised layout, the luminescence values fluctuated throughout and did not show any definitive suppressive effect of the antibody.



(a)

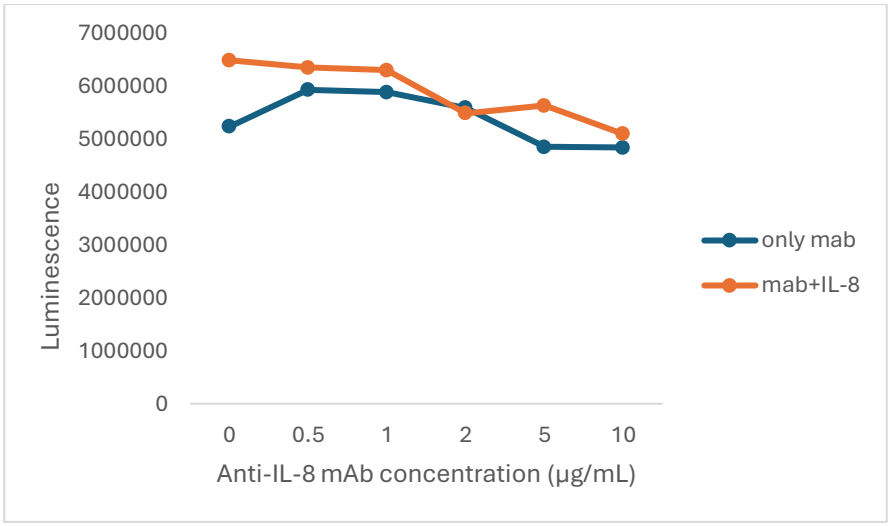


(b)

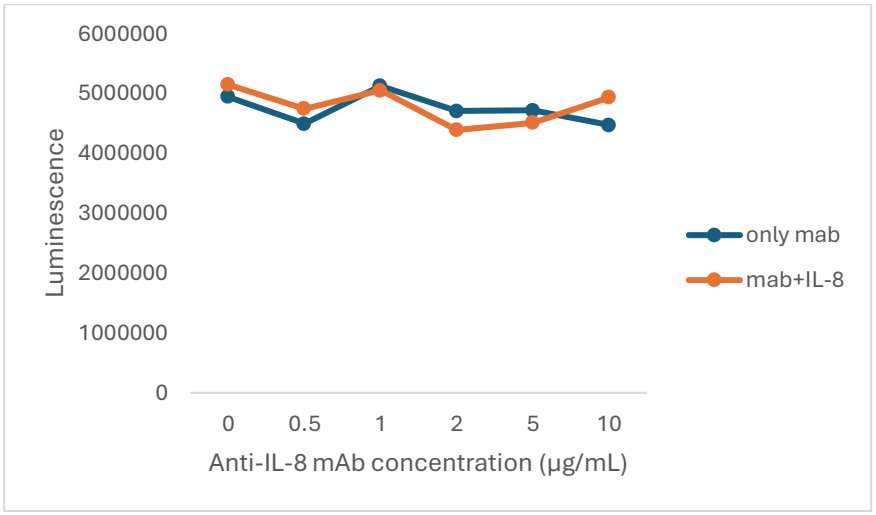
Figure 86: ATP assay of HCT-116 Batch 1 treated with anti-IL-8 mAb (0-10 µg/mL) alone and in combination with 10 ng/mL IL-8. (a) Custom order (b) Randomised order; n=1 per condition.

Batch 2

Similar variability was observed in Batch 2, as shown in **Figure 87**. In the custom order, ATP levels showed a slight decrease with increasing mAb concentrations, but the differences were not significant. In the randomised order, results were highly variable and lacked any particular trend indicating poor reproducibility.



(a)



(b)

Figure 87: ATP assay of HCT-116 Batch 2 treated with anti-IL-8 mAb (0-10 µg/mL) alone and in combination with 10 ng/mL IL-8. (a) Custom order (b) Randomised order; n=2 per condition.

Overall, across both batches and experimental layouts, the anti-IL-8 mAb did not produce a consistent or significant inhibitory effect on HCT-116 cells, in the presence and absence of IL-8. These findings suggest potential limitations in the bioactivity of the antibody, with further need for optimisation of assay conditions to reliably detect functional effects.

7. Discussion

Over the course of this 9-month research project, several experiments were conducted to investigate cell culture strategies to produce an anti-IL-8 mAb and characterise the potency of this mAb. The chosen cell line was donated to the ATCC by Genentech and is purported to have a titre of 250 mg/L under adherent cell culture conditions. In modern, commercial mAb production, this titre is relatively low compared to the 10 g/L CHO cell lines currently being licensed for therapeutic mAb production in intensified suspension cell culture processes. However, in an academic environment, such yields are substantial when compared to traditional hybridoma mAb procuring cell lines with titres often observed to be below <1 mg/L range (Li et al., 2010).

Initial cell culture studies focused on the production of an antibody with a previously used medium composition that was successful in the production of cNIST mAb from CHO cells within the research group. This medium was similar but not identical to the vendor's media, which was also composed of DMEM and 10% FBS. The process development strategy focused on media and seeding cell density optimisation, with replicate studies being performed. This strategy contrasted with prior work within the group, which prioritised experimental breadth over reproducibility in the course of a similar 9-month research programme (Pradeep, 2024).

A donated anti-IL-8 CHO cell vial of unknown passage number was initially used to develop a WCB, suggesting that the cells were likely to be of relatively high passage. A vial of known passage was not purchased from ATCC at the project initiation due to supply challenges with the vendor. High passage numbers are associated with genetic and phenotypic drift in CHO cells, including loss of transgene expression and reduced productivity (Dahodwala and Lee, 2019) . The first independent batch of anti-IL-8

monoclonal antibodies was produced in DMEM-complete medium. DMEM has been studied as an ideal medium for the growth of CHO cells; however, the presence of serum posed a critical drawback due to inherent IgG impurities in serum. This was reflected in Batch 1, which yielded a protein concentration of 1.144 mg/mL post-purification and a titre of 0.0069 mg/mL (**Table 8**); however, this yield included FBS-derived protein impurities, which meant that the results could not be attributed solely to the anti-IL-8 mAb. Similar challenges have been noted in studies where serum-supplemented media introduced contamination in mAb production (Ritacco et al., 2018). Nonetheless, these samples were used for a product stability study to assess storage conditions under different temperatures for predefined time periods. A second independent batch was cultured in suspension mode and as expected, failed to generate any titre due to a lack of adaptation to transition cells from adherent to suspension culture modes.

To evaluate the impact of different media compositions on protein expression for CHO DP12 cells, 2 batches of media studies were conducted. A range of media formulations was evaluated to assess how base medium composition and supplementation influence CHO DP12 cell growth and antibody production. Ex-Cell CD CHO served as a chemically defined control representative of industrial serum-free production conditions. DMEM, a commonly used glucose-rich medium for CHO cell growth, was selected with variants containing FBS, AA and HS. RPMI and McCoy's, though not typically used for CHO cells, were included to assess cell adaptability and productivity under non-ideal culture conditions. Each batch involved multiple media formulations, in the presence of FBS or the combination of AA and L-Glutamine in T-175 flasks. In Batch 1, 8 different media conditions (M1-M8) were tested, with regular monitoring of glucose levels and final protein yield being measured. Media condition 6 (M6) exhibited the highest apparent protein yield, which was later deemed unreliable due to contamination from HS endogenous antibodies (**Figure 30**). Other media

conditions had comparatively lower protein concentrations. Media Condition 1 (M1) with Ex-Cell CD CHO medium was hypothesised as most favourable due to its serum-free, chemically defined composition and CHO cell specificity. Yet unexpectedly, its protein yield was slightly lower than Media Condition 8 (M8), which contradicted initial expectations and suggested potential variability in CHO DP12 cell responses to complex media formulations (**Table 11**). In Batch 2, the HS condition was eliminated to reduce variability and refine the media conditions. This batch confirmed M1 with Ex-Cell CD CHO medium as the top-performing medium, aligning with established literature and industry standards for CHO-based protein expression. The remaining media conditions mirrored Batch 1 trends, though most protein yields remained low (**Table 13**). In addition, the variation across batches limits the results and requires further study. Further optimisation studies with replicates are required to conclusively determine the most effective media formulation for anti-IL-8 mAb production by CHO DP12 cells.

In parallel, a study was conducted to investigate the impact of seeding cell density on antibody expression. Three separate batches of cell density were executed using CHO DP12 anti-IL-8 cells produced in serum-free chemically defined media. This media was chosen as it is specifically designed for CHO cell culture, as well as being serum-free, reducing the impurity profile and had demonstrated the highest titres in media studies. Batch 1 had six different seeding densities per 100 mL of Ex-Cell CD CHO medium in T-175 flasks. Throughout the production, the cells remained metabolically active, and the cell viability percentage was in the range of 60-100% (**Figure 35 and Figure 36).** However, no protein was expressed across all conditions (**Table 14**). A similar trend was noted in batch 2, wherein seven different seeding conditions were tested with the same Ex-Cell CD CHO medium, but no antibodies were detected post-purification (**Table 15**). Antibody production in CHO DP12 cultures was not consistently proportional to viable cell density, reflecting limitations in

culture longevity and metabolic balance. Batch 3 of the cell density study was improvised by a low-serum (2.5% FBS) adaptation phase of 1 week before production in fully serum-free media supplemented with HT. The gradual serum reduction aimed to reduce cellular shock due to serum deprivation, as recommended by previous studies (Le Floch et al., 2006). The low glucose consumption observed in batch 3 after feeding contrasts with the work of Pérez-Rodriguez et al., 2020, who reported that anti-IL-8 CHO cells consumed approximately 60% glucose in non-supplemented cultures, whereas supplementation with PowerFeed A resulted in prolonged viability above 90%, complete glucose depletion, reduced lactate accumulation and a 1.9-2.5-fold increase in antibody titres. It was noted that integrated viable cell density and efficient nutrient metabolism, rather than peak cell density alone, are critical determinants of antibody yield (Pérez-Rodriguez et al., 2020).

In summary, both media and cell density seeding optimisation strategies did not lead to meaningful antibody production. The root cause being that the CHO DP12 cell line had undergone a loss of expression, leading to the absence of antibody production The initial independent study that produced a minor yield of antibodies, but with high impurities from FBS, should have merited further examination and potentially a bioassay such as ELISA to confirm the presence of anti-IL-8 mAbs. Previous internal assessments had established that 1% FBS contributed ~22% of total protein. Thus, at 10% FBS, the majority of protein in the harvest was polyclonal antibodies originating from serum components rather than the intended mAb. The results demonstrate the danger of relying solely on purification yields post-affinity chromatography when using serum in basal media. The titres are far from the vendor specified yields as well as yields observed in the literature (American Type Culture Collection (ATCC), n.d.). This is an important signal that should inform future studies, with a potential metric of actual yields versus theoretical yield measured, to monitor cell line productivity and the limit of in vitro cell age. Furthermore, the vendor-recommended media

and culturing strategy should be initially followed to establish a baseline rather than reliance on a common laboratory media composition developed for a different CHO cell line (cNISTmAb). This would also require the addition of methotrexate to basal media to ensure that high-copy cells are preserved throughout cell culture. In hindsight, this was a notable gap in the cell culture media formulations proposed.

Accordingly, as the likelihood of anti-IL-8 mAbs being present in high purity in the stability study executed in section 4.2 is low, the stability study performed is required to be repeated when an anti-IL-8 mAb is confirmed to be produced from a cell culture process. The stability study performed will not be discussed any further in the context of the anti-IL-8 cell culture studies performed.

In response to this lack of anti-IL-8 mAb production, the experiments were shifted to CHO NIST cells cultured in serum-free Gibco CD CHO medium supplemented with 8mM L-Glutamine as advised by the manufacturer. This contrasts with the EX-CELL CD CHO media used previously to culture the same cell line within the research group.

cNIST cell line demonstrated measurable mAb production under all four seeding densities and a slightly higher rate of glucose depletion as compared to CHO DP12 cells. Notably, protein yield was inversely correlated with seeding density, as the lowest density condition (2×10^5 cells/mL) produced the highest concentration (0.027 mg/mL) and progressively lower levels were observed at higher inoculation densities. Previous studies show that extremely low inoculation densities in rich media can limit growth due to insufficient cellular communication and autocrine signalling (Kim et al., 2020). While the tested cell densities were above this threshold, it was observed that increasing initial density reduced antibody production, which is consistent with reports that higher densities can impose nutrient and metabolic constraints that suppress productivity (Bokelmann et al.,

2024). Thus, both observations are complementary, highlighting the importance of an optimal cell density for CHO cell culture. The cell viability data showed two distinct groupings which indicates that there may be an optimal cell density value before viability drops off.

In comparison to prior work with EX-CELL CD CHO media, cell culture expansion was slower with GIBCO media and titres were also reduced (0.05mg/mL versus 0.027mg/mL) demonstrating the importance of cell culture media optimisation.

A forced degradation study was performed material produced in Batch 1 of cNIST mAbs to evaluate the impact of induced stress conditions such as extremes of temperature, light, pH, agitation and freeze-thaw cycles, on the stability of mAbs. As a result of their protein structure, therapeutic mAbs are particularly vulnerable to fragmentation, aggregation and conformational changes when exposed to physical and chemical stresses (Basle et al., 2020). Both SDS-PAGE and SEC-HPLC provided complementary insights into the forced degradation study **(Table 19)**. SDS-PAGE exhibited degradation with the presence of additional bands of lower molecular weight (30-40 kDa) in extreme stress conditions over time (**Figure 56 and Figure 63**). In SEC-HPLC degradation was characterised by a reduction in monomer peak area and the appearance of minor peaks at later retention times, suggesting fragmented species or conformationally destabilised monomers. SEC-HPLC did not reveal any substantial high molecular weight species (dimers and trimers), implying that aggregation was not the dominant degradation pathway under the applied conditions. The overall results were consistent for all conditions on SDS-PAGE and SEC-HPLC, confirming fragmentation into low molecular weight species (LMWS) and minimal aggregation under induced stress. The ratio of fragmentation between the two LMWS did differ across stressors and within groups, and in some studies, such as agitation, the pattern was not linear, which requires further investigation. Of note, acidic degradation produced a unique degradation profile whereby peak 2, the larger fragment, was visibly absent, and peaks were separated with the

absence of shoulders in the chromatogram. Further work is required to characterise the exact nature and molecular weight of the LMWS species observed. In addition, the instability at refrigerated conditions and low starting percentage of monomer requires further study and potential reformulation or purification using ion-exchange in a polishing step. This forced degradation study combined with anti-IL-8 mAb study (albeit with high impurities) demonstrate the sensitive but varying nature of mAb stability and the requirement for mAb specific studies to characterise the specific degradation and instability pathways for a given mAb.

Potency assays are a regulatory requirement for biological product batch release and accordingly, cell-based potency assay development was conducted for the anti-IL-8 mAb to be produced in cell culture studies. Potency assays were designed to assess the effect of anti-IL-8 monoclonal antibodies on HL-60 and HCT-116 cells to evaluate downstream signalling markers pERK and pRPS6 by western blotting. This approach was taken in lieu of potentially more challenging but published chemotaxis-based assays.

The first part of the assay involved stimulation of both differentiated and undifferentiated HL-60 cells with IL-8 antigen alone, expecting to result in detectable phosphorylation of the signalling biomarkers. However, immunoblot analysis did not reveal any visible bands at the anticipated molecular weights for multiple batches, nor was any consistent trend of increasing signal intensity observed with longer exposure times. β-tubulin was successfully detected as a loading control in all samples, confirming that protein transfer was successful. To further rule out the possibility of operator error, the assay was repeated by an experienced senior technical officer, but without any success ruling out analyst inexperience as a root cause. Subsequently due to time restrictions and limitations with the HL-60 cell line, further experiments were discontinued and efforts focused on the HCT-116 cell line.

The potency assay for HCT-116 cells was also conducted in two parts, with the antigen, IL-8, alone and with anti-IL-8 mAb across western blot, proliferation assay and ATP analysis. There were several difficulties faced during Western blot analysis, as the blots consistently showed high background noise and lacked clear detection of IL-8 effect on HCT-116 cells over short-term stimulation. In an effort to address this, the western blot protocol was optimised by adjusting blocking conditions and using a new of set of primary and secondary antibodies. While β-actin was successfully detected as a loading control in HCT-116 batches as a housekeeping gel, detecting successful protein transfer. Despite these modifications, results remained suboptimal with poor signal resolution, and no definite bands were visible at the corresponding molecular targets. Such outcomes are not uncommon, as Western Blot sensitivity can be influenced by several factors such as antibody specificity, protein expression levels, protein degradation or improper transfer (Mahmood and Yang, 2012).

Given these limitations, functional assays were performed in parallel to further investigate the effect of different IL-8 concentrations on HCT-116 cells over 72 hours. The proliferation assay demonstrated that stimulation of HCT-116 cells with increasing concentrations of IL-8 (0-100ng/mL) resulted in a modest upward trend in cell numbers. However, the overlapping error bars across concentrations indicate that the effect was not statistically significant (**Figure 82**). The ATP assay was performed to evaluate the metabolic activity of HCT-116 cells in response to human IL-8 antigen stimulation. In Batch 1 (n=3 per concentration), luminescence values peaked at an IL-8 concentration of 10 ng/mL and further reached a plateau (**Figure 83**). But this result could not be justified alone, considering the positional bias with stimulation on a 96-well plate; hence the next two batches included a randomised order of different concentrations of IL-8 stimulation. The trend could not be reproduced in Batch 2 (n=4 per concentration), as the luminescence values remained largely

unchanged across the IL-8 concentration range (0-100 ng/mL), with only minor fluctuations (**Figure 84**). Batch 3 (n=4 per concentration), demonstrated a similar response as previous batches, with no consistent response to a particular concentration of IL-8 (**Figure 85**). Interestingly, in the randomised batches, the luminescence values between the control condition (0 ng/mL IL-8) and the higher concentrations showed no major differences, indicating that exogenous supplementation of IL-8 did not significantly alter ATP levels. An important factor to consider is that HCT-116 cells are known to endogenously produce IL-8, leading to an established baseline of IL-8 signalling through autocrine mechanisms (Wigmore et al., 2001). This may mask the effect of externally stimulated IL-8, explaining why only subtle differences were observed across all tested conditions. Furthermore, Interleukin-8 has been strongly linked with functions beyond proliferation, such as migration, invasion, angiogenesis and inflammatory signalling (Ning et al., 2011). The variability between batches could also reflect differences in passage number, culture conditions or manual handling. Nevertheless, it was concluded that a significant effect was not observed, and a reproducible effect of IL-8 antigen stimulation on HCT-116 cell proliferation and metabolic activity was not achieved.

The next stage of potency assay involved treatment of HCT-116 cells with anti-IL-8 mAb, separately and in the presence of IL-8 antigen and evaluation of the metabolic activity via ATP analysis. Different concentrations of mAb were used for treatment along with 10 ng/mL of IL-8 antigen, with custom and randomised order of concentrations to eliminate positional bias. It should be noted that the anti-IL-8 mAb used in these experiments was commercially sourced and not derived from internal studies. In Batch 1 (n=1 per condition), the luminescence values remained variable with no clear dose-dependent reduction in ATP levels (**Figure 86**). The overlap between “only mAb” and “mAb+IL-8” groups indicated that the antibody treatment did not substantially reduce metabolic activity under the tested

conditions. Similarly, in Batch 2 (n=2 per condition), no reproducible or definite trend was observed as the luminescence values were fluctuating across concentrations (**Figure 87**). Altogether, these findings were limited, and the anti-IL-8 mAb did not demonstrate any significant inhibitory effect on HCT-116 cells. Further studies need to be continued to investigate the therapeutic potential of these monoclonal antibodies targeting migration, invasion or drug resistance rather than solely relying on ATP-based assays for HCT-116 cell cultures.

Future work in this space, should focus on identifying root cause analysis of HL-60 cell line not working as this cell line is well established for the characterisation of IL-8 signalling. Potentially, chemotaxis could be used as a readout instead of western blots which require several steps and are biomarker specific. Alternatively, reporter cell lines could be investigated as a means of assessing IL-8 signalling and Anti-IL-8 mAb potency.

8. Conclusion

In summary, this research study investigated the cell culture processes involved in the development of monoclonal antibodies on a laboratory scale, with a primary focus on anti-IL-8 and cNIST monoclonal antibodies.

For anti-IL-8 mAb, a series of experiments was conducted to optimise media conditions and seeding density while assessing parameters affecting cell culture performance and antibody yield. While the use of serum-supplemented DMEM medium supported cell viability, it introduced impurities from FBS and HS, which resulted in the detection of non-specific polyclonal antibodies rather than the desired anti-IL-8 mAb. Despite lengthy experimentation and multiple approaches, consistent expression could not be achieved, suggesting that the cell line was genetically unstable and had lost expression ability as a result of prolonged passaging prior to donation. The experience highlighted the importance of genetic stability, ensuring robustness of master cell bank vial and the use of bioassays to ensure product quality. The studies performed, including stability study, are required to be repeated in future work.

Subsequently, commercially sourced CHO-NIST cells at a lower passage number were used for the cell density study using serum-free Gibco CD-CHO medium. The NIST cell line successfully produced detectable antibodies across all tested densities, with the trend of lowest seeding cell density yielding the highest titre. Forced degradation studies of the produced and formulated mAb indicated the presence of fragments that require further purification and or reformulation to ensure monomer purity of >95%. Additional analytical efforts can guide and inform this work.

Preliminary potency assays were developed using HL-60 and HCT-116 cell lines to assess anti-IL-8 mAb activity. Western blot analysis of phosphorylated signalling proteins

(pERK and pRPS6) was unsuccessful in consistently determining any significant effect. ATP-based metabolic assays showed variable results in HCT-116 cells treated with IL-8 and anti-IL-8 mAb. These results were likely impacted by the endogenous IL-8 secretion in HCT-116 cells and the limited sensitivity of metabolic assays for cytokine-mediated effects. Future bioassays should target more specific IL-8 functions, such as migration, invasion or angiogenesis, to accurately evaluate antibody potency.

In alignment with the findings and limitations of this project, several areas of additional work have been identified to strengthen the production and analytical evaluation of anti-IL-8 monoclonal antibodies. Future work should aim to repeat CHO-DP12 Anti-IL-8 cell cultures with MTX supplementation to determine if the lack of a selection marker resulted in the non-expression of mAb. The use of serum-free media should be incorporated to further enhance product specificity and characterisation. Analytical improvements must include adopting SEC-HPLC as the primary method for aggregation analysis and implementing ELISA as a quantitative QC tool to confirm specific antibody production.

Collectively, the proposed experiments will enable a more complete understanding of upstream and downstream factors affecting mAb production and stability. A full list of future work to be completed is listed below.

Further Work:

Section	Detail	Rationale
4	Repeat cell culture studies for anti-IL 8 lots with existing and new stocks in the presence of methotrexate. Perform ELISA and SEC-HPLC on production products.	Determine if lack of selection marker resulted in non-expression of mAb
	Repeat cell culture studies for anti-IL 8 lots with existing and new stocks in the presence of vendor complete medium. Perform ELISA and SEC-HPLC on production products.	Determine if use of non-vendor recommended media resulted in non-expression of mAb

	Move to using SEC-HPLC in lieu of SDS-PAGE as primary assay for aggregation	SEC-HPLC demonstrates improved sensitivity and assess native structure
	Implement ELISA as a QC method to quantify anti-IL-8 specific mAb production	Confirm post-purification yields are anti-IL-8 specific when using FBS
	Remove IgG in FBS before use	Remove IgG contaminants
5	Perform head-to-head studies comparing GIBCO media and EX-CELL CD CHO media	Allow for a direct comparison between media in lieu of comparing studies executed at different times and different analysts.
	Optimise SEC-HPLC method	Allow for fragment 2 to be separated from monomer peak. Currently it forms a shoulder with monomer.
	Define molecular weight of fragments	Determine their potential degradation pathway
	Purify with a polishing chromatography step	Remove any potential impurities that may be causing LMWS
	Reformulate cNISTmAb	Current stability is poor even when refrigerated
6	Assess HL-60 cell line as bioassay using migration/chemotaxis as readout	Current study left incomplete due to timing
	Assess the feasibility of IL-8 reporter cell line	To ensure a potency bioassay is available for any future anti-IL-8 mAb developed.

9. References

1. Abraham, J., 2010. International Conference On Harmonisation Of Technical Requirements For Registration Of Pharmaceuticals For Human Use, in: Tietje, C., Brouder, A. (Eds.), Handbook of Transnational Economic Governance Regimes. Brill | Nijhoff, pp. 1041–1053. https://doi.org/10.1163/ej.9789004163300.i-1081.897
2. Adams, G.P., Weiner, L.M., 2005. Monoclonal antibody therapy of cancer. Nat. Biotechnol. 23, 1147–1157. https://doi.org/10.1038/nbt1137
3. Agilent, B., n.d. Charge Variant Analysis Application Compendium.
4. Alejandra, W.-P., Miriam Irene, J.-P., Fabio Antonio, G.-S., Patricia, R.-G.R., Elizabeth, T.-A., Aleman-Aguilar, J.P., Rebeca, G.-V., 2023. Production of monoclonal antibodies for therapeutic purposes: A review. Int. Immunopharmacol. 120, 110376. https://doi.org/10.1016/j.intimp.2023.110376
5. Alhuthali, S., Kotidis, P., Kontoravdi, C., 2021. Osmolality Effects on CHO Cell Growth, Cell Volume, Antibody Productivity and Glycosylation. Int. J. Mol. Sci. 22, 3290. https://doi.org/10.3390/ijms22073290
6. Alt, N., Zhang, T.Y., Motchnik, P., Taticek, R., Quarmby, V., Schlothauer, T., Beck, H., Emrich, T., Harris, R.J., 2016. Determination of critical quality attributes for monoclonal antibodies using quality by design principles. Biologicals 44, 291–305. https://doi.org/10.1016/j.biologicals.2016.06.005
7. American Type Culture Collection (ATCC), n.d. American Type Culture Collection (ATCC). (n.d.). CHO DP-12 clone #1934 (ATCC CRL-12445) Product Sheet. - Google Search [WWW Document]. URL https://www.atcc.org/products/crl-3614 (accessed 9.17.25).
8. Atkinson, T.P., 2022. Immunoglobulins, Structure, and Function, in: Immunoglobulins, Structure, and Function.
9. Aydin, S., 2015. A short history, principles, and types of ELISA, and our laboratory experience with peptide/protein analyses using ELISA. Peptides 72, 4–15. https://doi.org/10.1016/j.peptides.2015.04.012
10. Basle, Y.L., Chennell, P., Tokhadze, N., Astier, A., Sautou, V., 2020. Physicochemical Stability of Monoclonal Antibodies: A Review. J. Pharm. Sci. 109, 169–190. https://doi.org/10.1016/j.xphs.2019.08.009
11. Bellani, C.F., Ajeian, J., Duffy, L., Miotto, M., Groenewegen, L., Connon, C.J., 2020. Scale-Up Technologies for the Manufacture of Adherent Cells. Front. Nutr. 7. https://doi.org/10.3389/fnut.2020.575146

12. Berger, M., Shankar, V., Vafai, A., 2002. Therapeutic Applications of Monoclonal Antibodies. Am. J. Med. Sci. 324, 14–30. https://doi.org/10.1097/00000441-200207000-00004

13. Bernhard, S., Hug, S., Stratmann, A.E.P., Erber, M., Vidoni, L., Knapp, C.L., Thomaß, B.D., Fauler, M., Nilsson, B., Nilsson Ekdahl, K., Föhr, K., Braun, C.K., Wohlgemuth, L., Huber-Lang, M., Messerer, D.A.C., 2021. Interleukin 8 Elicits Rapid Physiological Changes in Neutrophils That Are Altered by Inflammatory Conditions. J. Innate Immun. 13, 225–241. https://doi.org/10.1159/000514885

14. Bilusic, M., Heery, C.R., Collins, J.M., Donahue, R.N., Palena, C., Madan, R.A., Karzai, F., Marté, J.L., Strauss, J., Gatti-Mays, M.E., Schlom, J., Gulley, J.L., 2019. Phase I trial of HuMax-IL8 (BMS-986253), an anti-IL-8 monoclonal antibody, in patients with metastatic or unresectable solid tumors. J. Immunother. Cancer 7, 240. https://doi.org/10.1186/s40425-019-0706-x

15. Bokelmann, C., Ehsani, A., Schaub, J., Stiefel, F., 2024. Deciphering Metabolic Pathways in High-Seeding-Density Fed-Batch Processes for Monoclonal Antibody Production: A Computational Modeling Perspective. Bioengineering 11, 331. https://doi.org/10.3390/bioengineering11040331

16. Breedveld, F.C., n.d. Therapeutic monoclonal antibodies.

17. Chames, P., Van Regenmortel, M., Weiss, E., Baty, D., 2009. Therapeutic antibodies: successes, limitations and hopes for the future. Br. J. Pharmacol. 157, 220–233. https://doi.org/10.1111/j.1476-5381.2009.00190.x

18. Chung, H.-L., 2007. Clinical significance of serum IgE. Korean J. Pediatr. 416–421.

19. Combe, M., Sokolenko, S., 2021. Quantifying the impact of cell culture media on CHO cell growth and protein production. Biotechnol. Adv. 50, 107761. https://doi.org/10.1016/j.biotechadv.2021.107761

20. Crowther, J.R. (Ed.), 2001. The ELISA guidebook, Methods in molecular biology. Humana Press, Totowa, NJ.

21. Cytiva, n.d. CellbagTM bioreactor containers with BioclearTM 10 film.

22. Dabhadkar, M., Palekar, S., Pawar, K., 2022. A review on “monoclonal antibodies: effective treatment against COVID-19.” Int. J. Community Med. Public Health 10, 525. https://doi.org/10.18203/2394-6040.ijcmph20223584

23. Dahodwala, H., Lee, K.H., 2019. The fickle CHO: a review of the causes, implications, and potential alleviation of the CHO cell line instability problem. Curr. Opin. Biotechnol. 60, 128–137. https://doi.org/10.1016/j.copbio.2019.01.011

24. David, J.M., Dominguez, C., Hamilton, D.H., Palena, C., 2016. The IL-8/IL-8R Axis: A Double Agent in Tumor Immune Resistance. Vaccines 4, 22. https://doi.org/10.3390/vaccines4030022

25. de Sousa-Pereira, P., Woof, J.M., 2019. IgA: Structure, Function, and Developability. Antibodies 8, 57. https://doi.org/10.3390/antib8040057

26. Dhar, S.K., Das, M., 2018. Engineering Antibodies. J. Indian Inst. Sci. 98, 5–20. https://doi.org/10.1007/s41745-018-0061-9

27. Eibl, R., Kaiser, S., Lombriser, R., Eibl, D., 2010. Disposable bioreactors: the current state-of-the-art and recommended applications in biotechnology. Appl. Microbiol. Biotechnol. 86, 41–49. https://doi.org/10.1007/s00253-009-2422-9

28. Fan, G., Li, Y., Ye, Q., Niu, Q., Zhao, X., Chen, L., Gu, Q., Zhang, Y., Wei, X., Wu, S., Wu, Q., Wu, Y., 2024. Animal-derived free hydrolysate in animal cell culture: Current research and application advances. J. Tissue Eng. 15, 20417314241300388. https://doi.org/10.1177/20417314241300388

29. Fekete, S., Beck, A., Veuthey, J.-L., Guillarme, D., 2015. Ion-exchange chromatography for the characterization of biopharmaceuticals. J. Pharm. Biomed. Anal. 113, 43–55. https://doi.org/10.1016/j.jpba.2015.02.037

30. Freshney, R.I., 2010. Culture of animal cells: a manual of basic technique and specialized applications, 6th ed. ed. Wiley-Blackwell, Hoboken, N.J. https://doi.org/10.1002/9780470649367

31. Freund, N.W., Croughan, M.S., 2018. A Simple Method to Reduce both Lactic Acid and Ammonium Production in Industrial Animal Cell Culture. Int. J. Mol. Sci. 19, 385. https://doi.org/10.3390/ijms19020385

32. Gabellini, C., Trisciuoglio, D., Desideri, M., Candiloro, A., Ragazzoni, Y., Orlandi, A., Zupi, G., Del Bufalo, D., 2009. Functional activity of CXCL8 receptors, CXCR1 and CXCR2, on human malignant melanoma progression. Eur. J. Cancer 45, 2618–2627. https://doi.org/10.1016/j.ejca.2009.07.007

33. Gahoual, R., Beck, A., Leize-Wagner, E., François, Y.-N., 2016. Cutting-edge capillary electrophoresis characterization of monoclonal antibodies and related products. J. Chromatogr. B, Analytical characterization of biopharmaceuticals 1032, 61–78. https://doi.org/10.1016/j.jchromb.2016.05.028

34. Ghizzani, V., Ascione, A., Gonnella, F., Massolini, G., Luciani, F., 2025. Exploring imaged capillary isoelectric focusing parameters for enhanced charge variants quality control. Front. Chem. 13, 1536222. https://doi.org/10.3389/fchem.2025.1536222

35. Golay, J., Introna, M., 2012a. Mechanism of action of therapeutic monoclonal antibodies: Promises and pitfalls of in vitro and in vivo assays. Arch. Biochem. Biophys., Antibody Engineering 526, 146–153. https://doi.org/10.1016/j.abb.2012.02.011

36. Golay, J., Introna, M., 2012b. Mechanism of action of therapeutic monoclonal antibodies: Promises and pitfalls of in vitro and in vivo assays. Arch. Biochem. Biophys. 526, 146–153. https://doi.org/10.1016/j.abb.2012.02.011

37. Gronemeyer, P., Ditz, R., Strube, J., 2014. Trends in Upstream and Downstream Process Development for Antibody Manufacturing. Bioengineering 1, 188–212. https://doi.org/10.3390/bioengineering1040188

38. Harada, A., Sekido, N., Akahoshi, T., Wada, T., Mukaida, N., Matsushima, K., 1994. Essential involvement of interleukin-8 (IL-8) in acute inflammation. J. Leukoc. Biol. 56, 559–564. https://doi.org/10.1002/jlb.56.5.559

39. Harris, R.J., Shire, S.J., Winter, C., 2004. Commercial manufacturing scale formulation and analytical characterization of therapeutic recombinant antibodies. Drug Dev. Res. 61, 137–154. https://doi.org/10.1002/ddr.10344

40. Huang, S., Mills, L., Mian, B., Tellez, C., McCarty, M., Yang, X.-D., Gudas, J.M., Bar-Eli, M., 2002. Fully Humanized Neutralizing Antibodies to Interleukin-8 (ABX-IL8) Inhibit Angiogenesis, Tumor Growth, and Metastasis of Human Melanoma. Am. J. Pathol. 161, 125–134. https://doi.org/10.1016/S0002-9440(10)64164-8

41. Humphreys, D.T., Wilson, M.R., n.d. MODES OF L929 CELL DEATH INDUCED BY TNF-· AND OTHER CYTOTOXIC AGENTS.

42. InvivoGen, n.d. TNF-α Reporter HEK 293 Cells.

43. Janeway, C.A., Jr., Travers, P., Walport, M., Shlomchik, M.J., 2001. Immunobiology: The Immune System in Health and Disease. 5th edition.

44. Kim, J.Y., Kim, Y.-G., Lee, G.M., 2012. CHO cells in biotechnology for production of recombinant proteins: current state and further potential. Appl. Microbiol. Biotechnol. 93, 917–930. https://doi.org/10.1007/s00253-011-3758-5

45. Kim, Y.J., Han, S.K., Yoon, S., Kim, C.W., 2020. Rich production media as a platform for CHO cell line development. AMB Express 10, 93. https://doi.org/10.1186/s13568-020-01025-3

46. Klimovich, V.B., 2011. IgM and its receptors: Structural and functional aspects. Biochem. Mosc. 76, 534–549. https://doi.org/10.1134/S0006297911050038

47. Köhler, G., Milstein, C., 2005. Pillars Article: Continuous cultures of fused cells secreting antibody of predefined specificity. Nature, 1975, 256 (5517): 495–497. J. Immunol. 174, 2453–2455. https://doi.org/10.1093/jimmunol/174.5.2453

48. Kornecki, M., Strube, J., 2018. Process Analytical Technology for Advanced Process Control in Biologics Manufacturing with the Aid of Macroscopic Kinetic Modeling. Bioengineering 5, 25. https://doi.org/10.3390/bioengineering5010025

49. Kothari, M., Wanjari, A., Acharya, S., Karwa, V., Chavhan, R., Kumar, S., Kadu, A., Patil, R., n.d. A Comprehensive Review of Monoclonal Antibodies in Modern Medicine: Tracing the Evolution of a Revolutionary Therapeutic Approach. Cureus 16, e61983. https://doi.org/10.7759/cureus.61983

50. Kumar, A., Starly, B., 2015. Large scale industrialized cell expansion: producing the critical raw material for biofabrication processes. Biofabrication 7, 044103. https://doi.org/10.1088/1758-5090/7/4/044103

51. Li, F., Vijayasankaran, N., Shen, A. (Yijuan), Kiss, R., Amanullah, A., 2010a. Cell culture processes for monoclonal antibody production. mAbs 2, 466–477. https://doi.org/10.4161/mabs.2.5.12720

52. Li, F., Vijayasankaran, N., Shen, A. (Yijuan), Kiss, R., Amanullah, A., 2010b. Cell culture processes for monoclonal antibody production. mAbs 2, 466–477. https://doi.org/10.4161/mabs.2.5.12720

53. Li, H., Liu, S., Yin, Y., Ji, S., Dong, D., Zhang, J., Fu, L., Xu, J., Chen, W., 2011. High-level Expression of Mycobacterium tuberculosis Protein EspB in E. coli and Preparation of Novel Anti-EspB Monoclonal Antibodies. Hybridoma 30, 341–346. https://doi.org/10.1089/hyb.2011.0013

54. Li, J., Huang, L., Zhao, H., Yan, Y., Lu, J., 2020. The Role of Interleukins in Colorectal Cancer. Int. J. Biol. Sci. 16, 2323–2339. https://doi.org/10.7150/ijbs.46651

55. Li, W., Prabakaran, P., Chen, W., Zhu, Z., Feng, Y., Dimitrov, D., 2016. Antibody Aggregation: Insights from Sequence and Structure. Antibodies 5, 19. https://doi.org/10.3390/antib5030019

56. Lipman, N.S., Jackson, L.R., Trudel, L.J., Weis-Garcia, F., 2005. Monoclonal Versus Polyclonal Antibodies: Distinguishing Characteristics, Applications, and Information Resources. ILAR J. 46, 258–268. https://doi.org/10.1093/ilar.46.3.258

57. Liu, J.K.H., 2014. The history of monoclonal antibody development - Progress, remaining challenges and future innovations. Ann. Med. Surg. 3, 113–116. https://doi.org/10.1016/j.amsu.2014.09.001

58. Luca, M., Huang, S., Gershenwald, J.E., Singh, R.K., Reich, R., 1997. Expression of Interleukin-8 by Human Melanoma Cells Up-Regulates MMP-2 Activity and Increases Tumor Growth and Metastasis 151.

59. Mahmood, T., Yang, P.-C., 2012. Western Blot: Technique, Theory, and Trouble Shooting. North Am. J. Med. Sci. 4, 429–434. https://doi.org/10.4103/1947-2714.100998

60. Maria, S., Bonneau, L., Fould, B., Ferry, G., Boutin, J.A., Cabanne, C., Santarelli, X., Joucla, G., 2023. Perfusion process for CHO cell producing monoclonal antibody: Comparison of methods to determine optimum cell specific perfusion rate. Biochem. Eng. J. 191, 108779. https://doi.org/10.1016/j.bej.2022.108779

61. Murdoch, C., Finn, A., n.d. Chemokine receptors and their role in inflammation and infectious diseases.

62. National Institutes of Health, 2019, n.d. Class II Type B2 Laminar Flow Biological Safety Cabinets at Ordering Criteria for the National Institutes of Health.

63. Nelson, A.L., Dhimolea, E., Reichert, J.M., 2010. Development trends for human monoclonal antibody therapeutics. Nat. Rev. Drug Discov. 9, 767–774. https://doi.org/10.1038/nrd3229

64. Nelson, P.N., Reynolds, G.M., Waldron, E.E., Ward, E., Giannopoulos, K., Murray, P.G., 2000. Demystified …. Mol. Pathol. 53, 111–117.

65. Neuss, A., Steimann, T., Tomas Borges, J.S., Dinger, R., Magnus, J.B., 2025. Scale-up of CHO cell cultures: from 96-well-microtiter plates to stirred tank reactors across three orders of magnitude. J. Biol. Eng. 19, 5. https://doi.org/10.1186/s13036-024-00475-8

66. Nienow, A.W., Isailovic, B., Barrett, T.A., 2016. Design and Performance of Single-Use, Stirred-Tank Bioreactors.

67. Ning, Y., Manegold, P.C., Hong, Y.K., Zhang, W., Pohl, A., Lurje, G., Winder, T., Yang, D., LaBonte, M.J., Wilson, P.M., Ladner, R.D., Lenz, H.-J., 2011. Interleukin-8 is associated with proliferation, migration, angiogenesis and chemosensitivity in vitro and in vivo in colon cancer cell line models. Int. J. Cancer 128, 2038–2049. https://doi.org/10.1002/ijc.25562

68. Pérez-Rodriguez, S., Ramírez-Lira, M. de J., Trujillo-Roldán, M.A., Valdez-Cruz, N.A., 2020. Nutrient supplementation strategy improves cell concentration and longevity, monoclonal antibody production and lactate metabolism of Chinese hamster ovary cells. Bioengineered 11, 463–471. https://doi.org/10.1080/21655979.2020.1744266

69. Pradeep, R., 2024. Development of an End-to-End Monoclonal Antibody Production Process. University College Cork.

70. Pradeep, R., Zhdanov, A., Allen, E., 2026. Comparative analysis of common potency assays for assessing human TNF-alpha neutralising antibodies. Anal. Biochem. 709, 116011. https://doi.org/10.1016/j.ab.2025.116011

71. Qin, V., n.d. Size Exclusion Chromatography Analysis of a Monoclonal Antibody and Antibody Drug Conjugate Using an Agilent AdvanceBio SEC 200 Å 1.9 µm column.

72. Rawat, R.S., Kumar, S., 2023. Antibodies as Therapeutic Agents, in: Singh, D.B., Tripathi, T. (Eds.), Protein-Based Therapeutics. Springer Nature Singapore, Singapore, pp. 131–161. https://doi.org/10.1007/978-981-19-8249-1_5

73. Ritacco, F.V., Wu, Y., Khetan, A., 2018. Cell culture media for recombinant protein expression in Chinese hamster ovary (CHO) cells: History, key components, and optimization strategies. Biotechnol. Prog. 34, 1407–1426. https://doi.org/10.1002/btpr.2706

74. Rustandi, R.R., Washabaugh, M.W., Wang, Y., 2008. Applications of CE SDS gel in development of biopharmaceutical antibody-based products. ELECTROPHORESIS 29, 3612–3620. https://doi.org/10.1002/elps.200700958

75. Sahoo, A., Devenney, K., Nicolas, M.-A., Zill, N., Gupta, B., Madabhushi, S.R., 2024. Beyond viability: Advancing CHO cell culture process strategies to modulate host cell protein levels. New Biotechnol. 84, 128–139. https://doi.org/10.1016/j.nbt.2024.10.003

76. Salmikangas, P., Carlsson, B., Klumb, C., Reimer, T., Thirstrup, S., 2023. Potency testing of cell and gene therapy products. Front. Med. 10, 1190016. https://doi.org/10.3389/fmed.2023.1190016

77. Schroeder, H.W., Cavacini, L., 2010a. Structure and function of immunoglobulins. J. Allergy Clin. Immunol. 125, S41–S52. https://doi.org/10.1016/j.jaci.2009.09.046

78. Schroeder, H.W., Cavacini, L., 2010b. Structure and function of immunoglobulins. J. Allergy Clin. Immunol. 125, S41–S52. https://doi.org/10.1016/j.jaci.2009.09.046

79. Scott, A.M., Wolchok, J.D., Old, L.J., 2012. Antibody therapy of cancer. Nat. Rev. Cancer 12, 278–287. https://doi.org/10.1038/nrc3236

80. Shukla, A.A., Gottschalk, U., 2013. Single-use disposable technologies for biopharmaceutical manufacturing. Trends Biotechnol. 31, 147–154. https://doi.org/10.1016/j.tibtech.2012.10.004

81. Singh, R., Chandley, P., Rohatgi, S., 2023. Recent Advances in the Development of Monoclonal Antibodies and Next-Generation Antibodies. ImmunoHorizons 7, 886–897. https://doi.org/10.4049/immunohorizons.2300102

82. Singh, V., 2002. Disposable Bioreactor for Cell Culture Using Wave-Induced Agitation, in: Merten, O.-W., Perrin, P., Griffiths, B. (Eds.), New Developments and New Applications in Animal Cell Technology. Kluwer Academic Publishers, Dordrecht, pp. 399–407. https://doi.org/10.1007/0-306-46860-3_74

83. Streefland, M., Martens, D.E., Beuvery, E.C., Wijffels, R.H., 2013. Process analytical technology (PAT) tools for the cultivation step in biopharmaceutical production. Eng. Life Sci. 13, 212–223. https://doi.org/10.1002/elsc.201200025

84. Supermodics, n.d. Guide To Detecting Proteins: ELISA [WWW Document]. URL https://shop.surmodics.com/guide-to-detecting-proteins-elisa (accessed 10.14.25).

85. Teixeira, A.P., Oliveira, R., Alves, P.M., Carrondo, M.J.T., 2009. Advances in on-line monitoring and control of mammalian cell cultures: Supporting the PAT initiative. Biotechnol. Adv. 27, 726–732. https://doi.org/10.1016/j.biotechadv.2009.05.003

86. The Antibody Society, n.d. Antibody therapeutics approved or in regulatory review in the EU or US. Antib. Soc. URL https://www.antibodysociety.org/resources/approved-antibodies/ (accessed 10.4.25).

87. van der Valk, J., Brunner, D., De Smet, K., Fex Svenningsen, Å., Honegger, P., Knudsen, L.E., Lindl, T., Noraberg, J., Price, A., Scarino, M.L., Gstraunthaler, G., 2010. Optimization of chemically defined cell culture media – Replacing fetal bovine serum in mammalian in vitro methods. Toxicol. In Vitro 24, 1053–1063. https://doi.org/10.1016/j.tiv.2010.03.016

88. Verma, R., Boleti, E., George, A.J.T., 1998. Antibody engineering: Comparison of bacterial, yeast, insect and mammalian expression systems. J. Immunol. Methods 216, 165–181. https://doi.org/10.1016/S0022-1759(98)00077-5

89. Vidarsson, G., Dekkers, G., Rispens, T., 2014. IgG Subclasses and Allotypes: From Structure to Effector Functions. Front. Immunol. 5. https://doi.org/10.3389/fimmu.2014.00520

90. Walsh, G., 2018. Biopharmaceutical benchmarks 2018. Nat. Biotechnol. 36, 1136–1145. https://doi.org/10.1038/nbt.4305

91. Waugh, D.J.J., Wilson, C., 2008. The Interleukin-8 Pathway in Cancer. Clin. Cancer Res. 14, 6735–6741. https://doi.org/10.1158/1078-0432.CCR-07-4843

92. Weiner, G.J., 2007. Monoclonal antibody mechanisms of action in cancer. Immunol. Res. 39, 271–278. https://doi.org/10.1007/s12026-007-0073-4

93. Whaley, D., Damyar, K., Witek, R.P., Mendoza, A., Alexander, M., Lakey, J.R., 2021. Cryopreservation: An Overview of Principles and Cell-Specific Considerations. Cell Transplant. 30, 0963689721999617. https://doi.org/10.1177/0963689721999617

94. Wigmore, S.J., Maingay, J.P., Fearon, K.C., Ross, J.A., 2001. Endogenous production of IL-8 by human colorectal cancer cells and its regulation by cytokines. Int. J. Oncol. 18, 467–473. https://doi.org/10.3892/ijo.18.3.467

95. Wilde, D.D., Noack, U., Kahlert, W., Barbaroux, M., Greller, G., n.d. Bridging the Gap from Reusable to Single-Use Manufacturing with Stirred, Single-Use Bioreactors.

96. Wilman, W., Wróbel, S., Bielska, W., Deszynski, P., Dudzic, P., Jaszczyszyn, I., Kaniewski, J., Młokosiewicz, J., Rouyan, A., Satławа, T., Kumar, S., Greiff, V., Krawczyk, K., 2022. Machine-designed biotherapeutics: opportunities, feasibility and advantages of deep learning in computational antibody discovery. Brief. Bioinform. 23, bbac267. https://doi.org/10.1093/bib/bbac267

97. Wurm, F.M., 2004. Production of recombinant protein therapeutics in cultivated mammalian cells. Nat. Biotechnol. 22, 1393–1398. https://doi.org/10.1038/nbt1026

98. Xu, W.-J., Lin, Y., Mi, C.-L., Pang, J.-Y., Wang, T.-Y., 2023. Progress in fed-batch culture for recombinant protein production in CHO cells. Appl. Microbiol. Biotechnol. 107, 1063–1075. https://doi.org/10.1007/s00253-022-12342-x

99. Zhang, M., Zhao, X., Li, Y., Ye, Q., Wu, Y., Niu, Q., Zhang, Y., Fan, G., Chen, T., Xia, J., Wu, Q., 2024. Advances in serum-free media for CHO cells: From traditional

serum substitutes to microbial-derived substances. Biotechnol. J. 19, 2400251. https://doi.org/10.1002/biot.202400251